Abstract

WILLIAMSON, BRANDON ROBERT. Processing Polymers with Cyclodextrins. (Under the direction of Alan E. Tonelli.)

Cyclodextrins (CD's) are cyclic starch molecules that have the unique ability to include a variety of small molecules and polymers inside their cavities, forming "Inclusion Complexes" (IC's). While much work has been done to understand the formation and behavior of these ICs, far less is known about the fundamental property changes that can occur when CD is used to alter polymer chain morphology. The goal of my graduate research has been to discover different ways to improve upon existing polymer properties through CD processing, as well as explore the possibility of creating a novel type of IC using non-traditional forms of cyclodextrin.

Poly(ε-caprolactone) (PCL) was processed with α-CD to form an IC. The cyclodextrin was then stripped away to yield a PCL with elongated, unentangled, and constrained polymer chains, a process referred to as coalescence. The physical and rheological property changes resulting from this coalescence were then examined. It was found that reorganizing PCL in this manner resulted in an increase in the melt crystallization temperature of up to 25˚C. Coalescence also decreased the tan δ of the material and increased the average hardness and Young's modulus by 33 and 53%, respectively.

Non-stoichiometric IC's (NS-IC's), or IC's with at least parts of some polymer chains uncovered, were formed between poly (methyl methacrylate) (PMMA) and γ-CD as well as a synthesized poly(ε-caprolactone)-poly(prolpylene glycol)- poly(ε-caprolactone) (PCL-PPG-PCL) triblock copolymer and β-CD. The property changes of the non-complexed polymer chains were then studied. The PMMA/γ-CD NS-IC samples were determined to be extremely

heterogeneous, however glass transition temperature increases of up to 27˚ C above that of as-received PMMA were observed. Diffraction data for the PMMA NS-IC's suggests slight crystallinity at partial coverage, with a similar crystal structure to that of the fully covered IC. XRD, DSC and FTIR data revealed an almost total disruption of the PCL crystallinity upon complexation of the PCL-PPG-PCL triblock, suggesting possible miscibility of PCL blocks and PPG blocks threaded with β-CD or partial coverage of the PCL blocks by the β-CD.

A non-crystalline and unreactive modified CD, diethylamine-terminated monochloro-triazinyl-β-CD (DEAMCT), was synthesized from an industrially available β-CD derivative. DEAMCT was complexed with poly(propylene glycol) (PPG) as well as a poly(ethylene glycol)- poly(propylene glycol)- poly(ethylene glycol) (PEG-PPG-PEG) triblock copolymer (trade name Pluronic). The IC's formed between these polymers and the non-crystalline cyclodextrin derivative were studied with a variety of techniques. Two-dimensional ROESY ^{1}H-NMR demonstrated through-space spin coupling interactions between backbone protons of the PPG and two of the inward-facing cavity protons in the β-CD cavity, strong evidence for IC formation between these materials. Unexpectedly, these IC's displayed clear X-ray observed crystalline behavior, with long-range order that was comparable for both the DEAMTC- and β-CD-ICs formed with guest Pluronics. The IC formation with the Pluronic material resulted in the complete disruption of the PEG block crystallinity in a fashion similar to the PCL-PPG-PCL triblock copolymer. Unexpectedly, the aqueous solubility for both the Pluronic and PPG homopolymer decreased upon low-coverage DEAMCT inclusion.

Processing Polymers with Cyclodextrins

by
Brandon Robert Williamson

A dissertation submitted to the Graduate Faculty of
North Carolina State University
in partial fulfillment of the
requirements for the Degree of
Doctor of Philosophy

Fiber and Polymer Science

Raleigh, North Carolina

2010

APPROVED BY:

_____	_____
Alan E. Tonelli Chair of Advisory Committee	C. Maurice Balik
_____	_____
Samuel Hudson	Wendy Krause

Dedication

This work is dedicated to my supportive and loving wife, my family, and my friends. Thank you for everything you have given me. I could not have done this without you.

Biography

Brandon Williamson was born in Charlotte, NC and raised in nearby Gastonia, NC. He has lived in both North Carolina and Texas, but decided to attend North Carolina State University in 2001. Originally coming to NCSU with the intent to major in Mechanical Engineering, Brandon attended an information session for the Materials Science and Engineering department and was fascinated by the various demonstrations and explanations of the field. After changing degree programs, he obtained his Bachelor of Science degree in Materials Science and Engineering in 2005. With the compliments of some of his MSE professors, Brandon planned to pursue a graduate degree in polymer science. He eventually decided to pursue a Doctorate degree in Fiber and Polymer Science at North Carolina State University under the direction of Dr. Alan Tonelli.

Acknowledgements

I would like to first and foremost thank my advisor, Dr. Alan E. Tonelli, for his invaluable guidance in my time as a graduate student at NC State. Without his assistance, I would never have come this far or achieved so much. I would also like to extend my gratitude to the rest of my graduate committee as well, Drs. Maury Balik, Sam Hudson, and Wendy Krause. I know that the life of a professor is a busy one, and the time and assistance you've offered have been so important to my success.

Thank you to all of my past and current group members: Drs. Brad Busche, Marcus Hunt, Anushree Mohan, Hyun Suk Whang, as well as Manisha Agrawal, Gerry Antony, Alper Gurarslan, Ashwin Krishnaswamy, and Abhay Jiojode. Also, thank you to Carrie Cornelius, Rebecca Klossner, Mangesh Champhekar, and Nagarajan Muthuraman. You have all provided great conversation, great laughs, and great friendship. A special thanks to Drs. Dan Shin, Sabapathy Sankar, and Hanna Gracz for assisting in many NMR experiments as well as Dr. Keith Beck for his assistance with SEC testing. Finally, I must offer a special thank you to Birgit Andersen for helping me in countless ways during my graduate career. Her training, advice, encouragement, and friendship will always be remembered.

Table of Contents

List of Tables

List of Figures

Chapter 1: An Introduction to Cyclodextrin and Cyclodextrin Inclusion Complexes

History of Cyclodextrin Research

Cyclodextrins were first discovered in 1891, but were originally named cellulosine.[1] Schardinger later discovered products resulting from starch digestion with the microbe *Bacillus macerans* that seemed to match Villeirs' cellulosine. [2,3] Schardinger continued work with what would eventually be named cyclodextrins, including distinguishing and naming α- and β-dextrins based on the color of an iodine reaction.[4] Pringsheim followed Schardinger's work with many years of cyclodextrin study. Much of the work has been deemed unreliable due to poor methods, but one major contribution is the discovery that the crystalline cyclodextrins tend to form complexes with a range of organic compounds.[5,6]

Between the 1930's and the 1970's, many studies led to better understanding and characterization of cyclodextrins. Freudenberg and colleagues' work in the 1930's led to the discovery that these crystalline "dextrins" are formed from maltose units and contain nothing but α-1,4-glycosidic linkages.[7-9] They were also the first to suggest the cyclic nature of the cyclodextrins.[10] The presence of γ-CD was discovered and its structure was determined during this period.[11] Additional work carried out included enzymatic production[12] and inclusion complexation[13] studies. French's review also incorrectly reported on the toxicity of CD on laboratory rats, reporting that even small doses of "purified" CD killed all the subjects within a week. With the information available today, it is evident that the deaths were more likely caused by the presence of some toxic impurity, perhaps an organic solvent.

From the 1970's onward, industrial production of cyclodextrin skyrocketed and research into the practical uses of cyclodextrin became prominent. The price of 1 kg of CD dropped dramatically, and many variations including methylated and acetylated cyclodextrins were developed and marketed. The number of cumulative CD publications, which include patents, published patent applications, and conference abstracts, have also risen with CD development. Figure 1 demonstrates the trend in CD publication since its initial discovery.

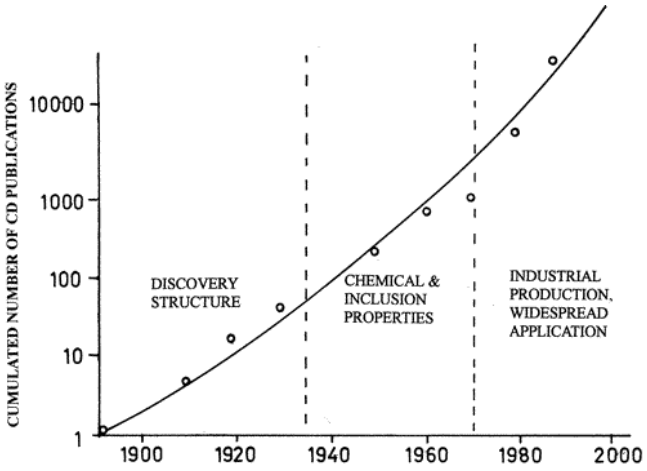

Figure 1: Number of cyclodextrin publications over the past 120 years[14]

Currently, cyclodextrins are used heavily in the pharmaceutical and industrial processing areas. They have become affordable and are valuable for their ability to aid in pharmaceutical delivery and polymer processing, and their ability to provide new production and processing techniques.

Cyclodextrin Properties and Behaviors, and their Characterization

Structural Properties

Cyclodextrins (CD) are a group of cyclic oligosaccharides, the most common varieties being α-, β-, and γ-CD, containing 6, 7, and 8 glucopyranose units respectively. Cyclodextrins are formed by a simple enzymatic conversion of starch, produced with environmentally friendly techniques, and in large enough quantities and easily enough to reduce prices to industrially feasible levels.[14] Figure 2 shows the basic structures of the commonly used types of cyclodextrin.

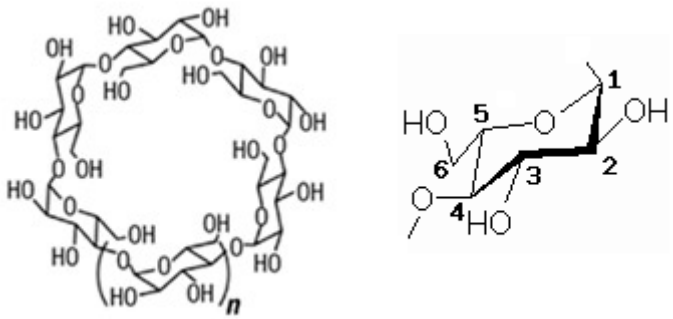

Figure 2: Chemical structure and numbering of α-, β-, and γ-cyclodextrin (n=1 for of α, n=2 for β, and n=3 for γ)[15]

The majority of cyclodextrin work today uses α, β, and γ-CD. Table 1 provides some basic properties for each of these three main varieties.[16]

Table 1: Basic properties of α-, β-, and γ-cyclodextrin[16]

Property	*α-CD*	*β-CD*	*γ-CD*
Number of glucopyranose units	6	7	8
Molecular weight (g/mol)	972	1135	1297
Solubility (% w/v in water, 25 C)	14.5	1.85	23.2
Outer diameter (Å)*	14.6	15.4	17.5
Cavity diameter (Å)	4.7-5.3	6.0-6.5	7.5-8.3
Height of torus (Å)	7.9	7.9	7.9
Cavity volume (Å)	174	262	427

* Values vary slightly depending on source

The geometrical structure of cyclodextrins is a truncated conical cylinder shape, which places all the primary hydroxyl groups on one side of the cylinder and all the secondary hydroxyl groups on the other side.[14] The aliphatic ring hydrogen atoms are directed inwards, as are the glycosidic oxygen bridges that connect the glucopyranose rings. This structure creates a hydrophilic outer surface and a hydrophobic inner cavity. A simple schematic representation of this can be seen in Figure 3 below.

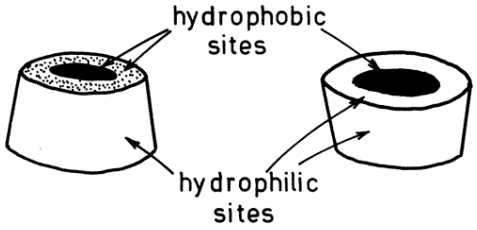

Figure 3: Location of the hydrophobic and hydrophilic interactions for cyclodextrin[14]

The hydroxyl group from the second carbon can interact with the hydroxyl group from the third carbon on the adjacent glucopyranose unit (numbering scheme shown in Figure 1). This occurs completely in β-CD creating a "secondary ring" of hydrogen bonding that provides rigidity to the structure. Ring distortion in α-CD prevents complete hydrogen bonding around the molecule, while the ring bonding in γ-CD is hindered by a non-coplanar, collapsed ring structure.

Solubility

Generally speaking, cyclodextrins are soluble in hydrophilic-compatible solvents, such as water and DMSO. It has also been suggested that the previously discussed secondary ring formed by the hydrogen bonding is responsible for the lowered solubility of β-CD in water. As seen in Table 1, the solubilities of α- and γ-CD are 14.5 and 23.2 % w/v respectively in water at 25 C. The solubility of β-CD under the same conditions, however, is only 1.85 % w/v.

Linert et al. have also calculated the free energy of mixing for α, β, and γ-CD with water to be 4.72, 10.21, and 4.26 kJ mol^{-1} respectively.[17] The driving force for solution formation decreases as the free energy of mixing increases, also explaining why β-CD has the lowest solubility, even though all cyclodextrin chemistries are, essentially, the same.

Crystalline Structures

Cyclodextrin forms multiple types of crystalline structures depending on the environment and the type of molecule included inside the cavity. Schematics of three common types of cyclodextrin crystal structures can be seen below in Figure 4.

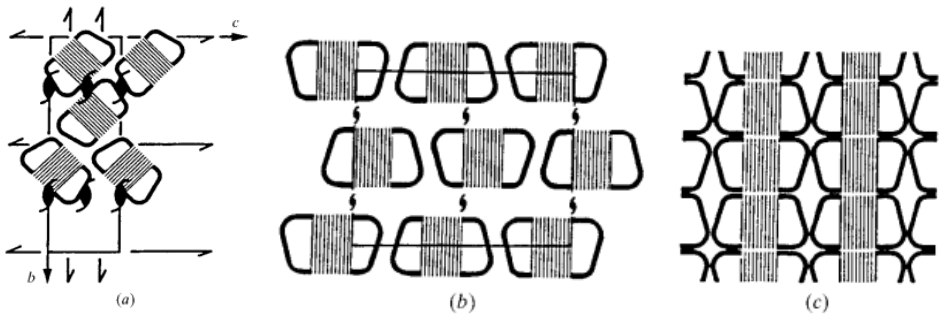

Figure 4: Three common types of CD crystalline structures: herringbone-type cage (a), brick-type cage (b), and channel (c)[18]

The herringbone-type cage structure is generally formed when α, β, and γ-CD are crystallized as hydrates (crystallized in water with no other included molecule present).[18] α- and γ-CD can be dissolved and recrystallized into the channel form as hydrates under certain conditions.[19] The crystal structures of cyclodextrin with included guests comprise the brick-type cage, channel, and other structures, and will be discussed in the inclusion complex section.

DSC and TGA

The thermal properties of cyclodextrin remain largely unchanged among the different varieties. Most of the differences arise in the method of water loss in the hydrated forms. Outside of this change, the three main types of cyclodextrins all begin to degrade just above 250˚ C[20] before undergoing any melting. Figures 5-7 are the thermoanalytical profiles of α-, β-, and γ-cyclodextrin. They each contain the thermogravimetric analysis (TG), differential scanning calorimetry analysis (DSC), and derivative thermogravimetry analysis (DTG), which is the slope of the TG curve showing the degradation/weight loss rate of the material.

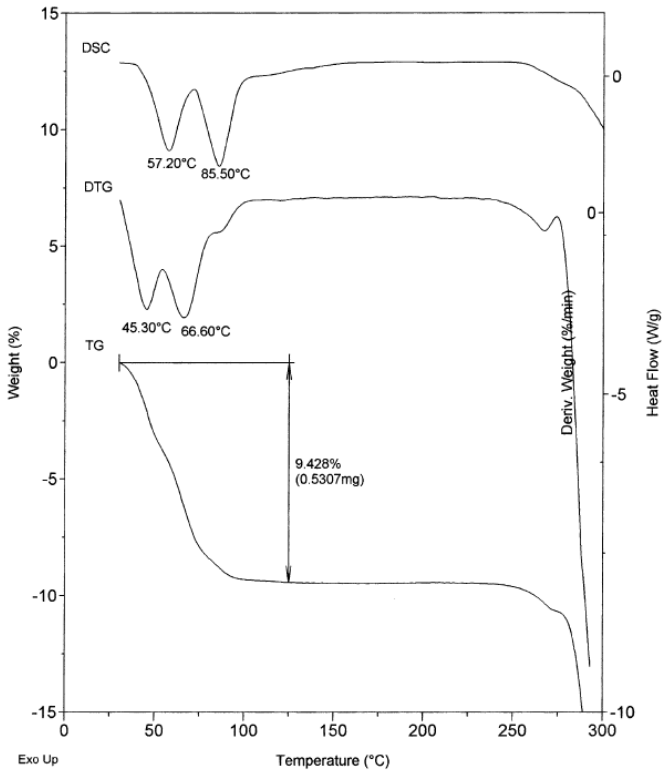

Figure 5: Thermoanalytical Profile of α-CD[20]

α-CD forms hydrates containing either 6 or 7.5 water molecules. The six-molecule hydrate has two forms, one demonstrating a two-step water loss pattern and the other a three-step water loss pattern. The three-step pattern contains a slight endothermic peak after the water loss due to a phase change of the anhydrous α-CD (see Figure 5).

In Figure 6, β-CD shows generally the same thermal properties as α-CD, but can crystallize with either 11 or 12 water molecules. It has been reported that the undecahydrate form of β-CD undergoes a two-step dehydration mechanism, losing seven and four water molecules in each step. This dehydration is followed by a period of no degradation up to around 255°C.

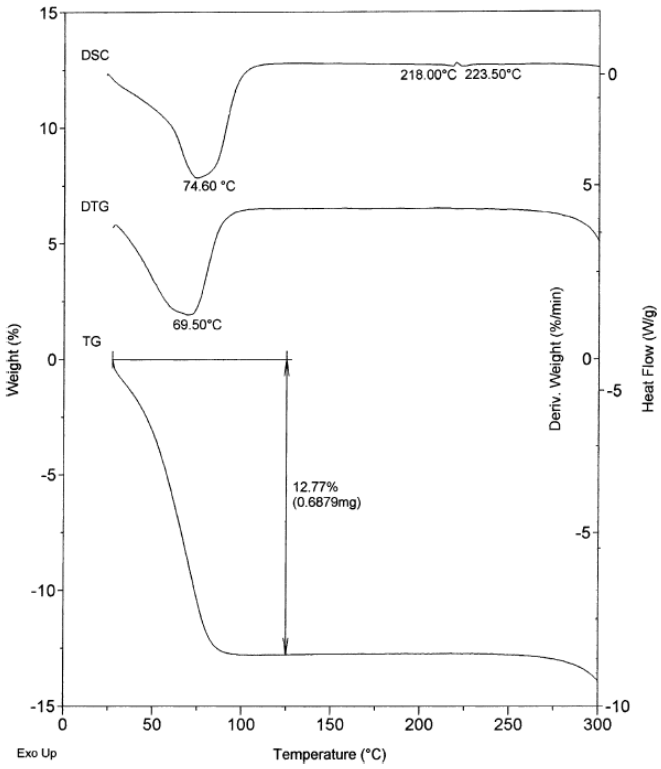

Figure 6: Thermoanalytical Profile of β-CD[20]

Often, small modulations are observed in the DSC data as seen above. There is no consensus as to what creates these minor modulations, though it is hypothesized that perhaps it is a minor phase transition from one crystallographic form of β-CD to another.

In Figure 7, γ-CD also exhibits the common behavior of water loss and then degradation slightly above 250° C. The water loss occurs in two steps. A fully saturated hydrate stored at 93.6% RH contains 17 water molecules,[21] while intermediate hydrates containing 7 water molecules have been observed during dehydration and rehydration.

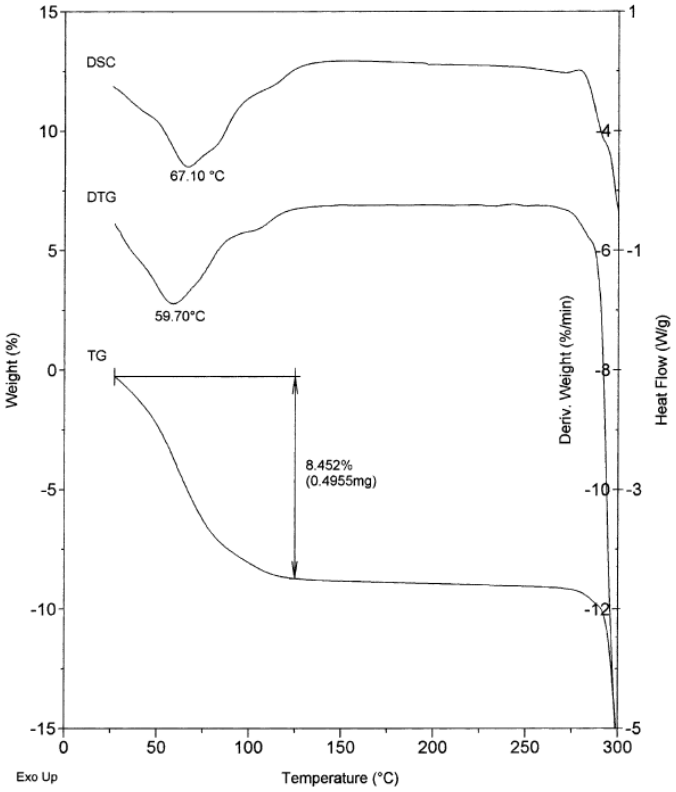

Figure 7: Thermoanalytical Profile of γ-CD[20]

NMR

NMR provides a valuable tool for the study of natural and modified cyclodextrins. Proton NMR allows us to observe specific resonances of the various protons located on the cyclodextrin and detects which of these protons are changed upon complexation. The ^{13}C-NMR resonance frequencies (chemical shifts vs. TMS) of unsubstituted cyclodextrins are presented in Table 2 and Figure 8 shows the proton NMR spectra of as-received of β-CD in

D_2O and d_6-DMSO. The resonance frequencies for α- and γ-CD do not deviate with any significance from β-CD.

Table 2: ^{13}C NMR chemical shifts for unmodified cyclodextrins in D_2O[22]

Carbon	δ value (ppm)			
	α-CD	β-CD	γ-CD	δ-CD
1	102.19	102.58	102.42	100.96
2	72.61	72.67	73.19	73.08
3	74.21	73.89	73.82	73.74
4	82.07	81.94	81.33	79.26
5	72.91	72.89	72.69	72.34
6	61.37	61.17	61.21	61.29

ppm downfield from external tetramethylsilane at 50 °C in D_2O soln.

Solvent has a profound effect on the NMR spectra, especially the proton spectra. Figure 8 below shows that the difference in spectra for the same material in D_2O versus d_6-DMSO is significant. A phenomenon called proton exchange can occur between the hydroxyl groups on the cyclodextrin and the solvent. This event is prominent in D_2O, where rapid exchange between the hydroxyl protons and the deuterium occurs. The proton spectra of β-CD in D_2O shown above contains no hydroxyl peaks because the –OH protons have all exchanged with the deuterium and become invisible to the proton-tuned probe. Instead, we find that a large HDO peak is present.

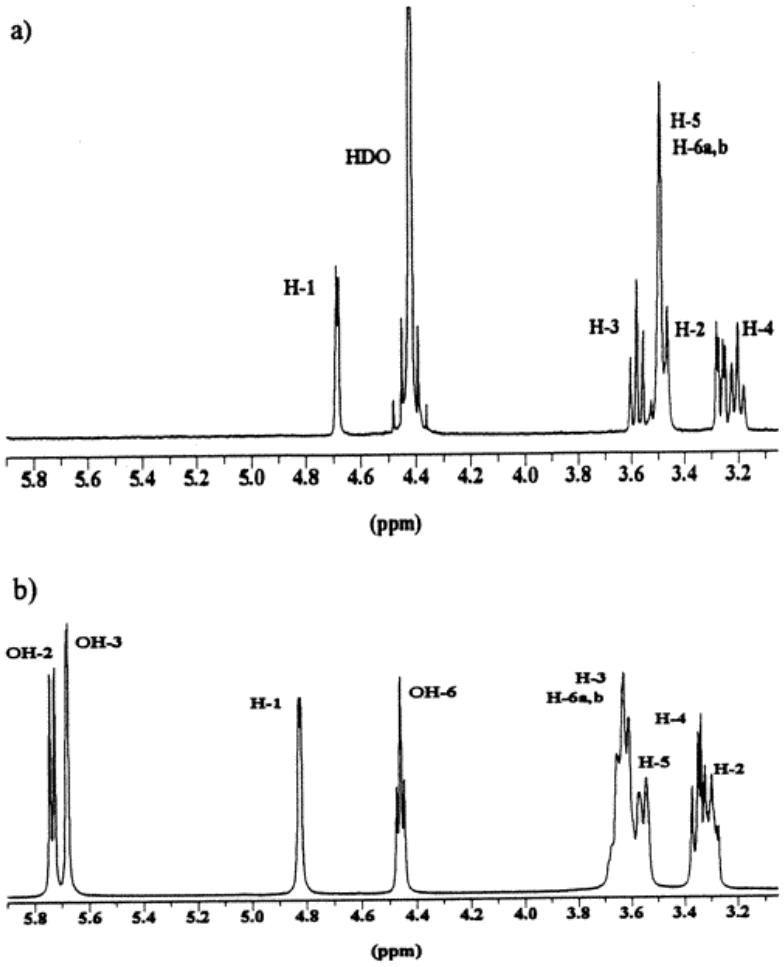

Figure 8: Proton NMR spectra (400 MHz) of unmodified β-cyclodextrin in D2O (a) and d-DMSO (b)[23]

FTIR

Fourier Transform Infrared Spectroscopy (FTIR) provides an opportunity to help study cyclodextrin and cyclodextrin IC's, especially in cases where the presence of certain materials needs to be quickly verified (for example, the presence of CD threaded on a

polymer). The kinetic vibrations of specific bonds and groups cause infrared light absorption at specific frequencies. By detecting these signal reductions over a range of frequencies, we can assign a peak or group of peaks to a particular bond or group, much like NMR. Figure 9 below is an example of the FTIR spectrum of γ-CD in the hydrate form.

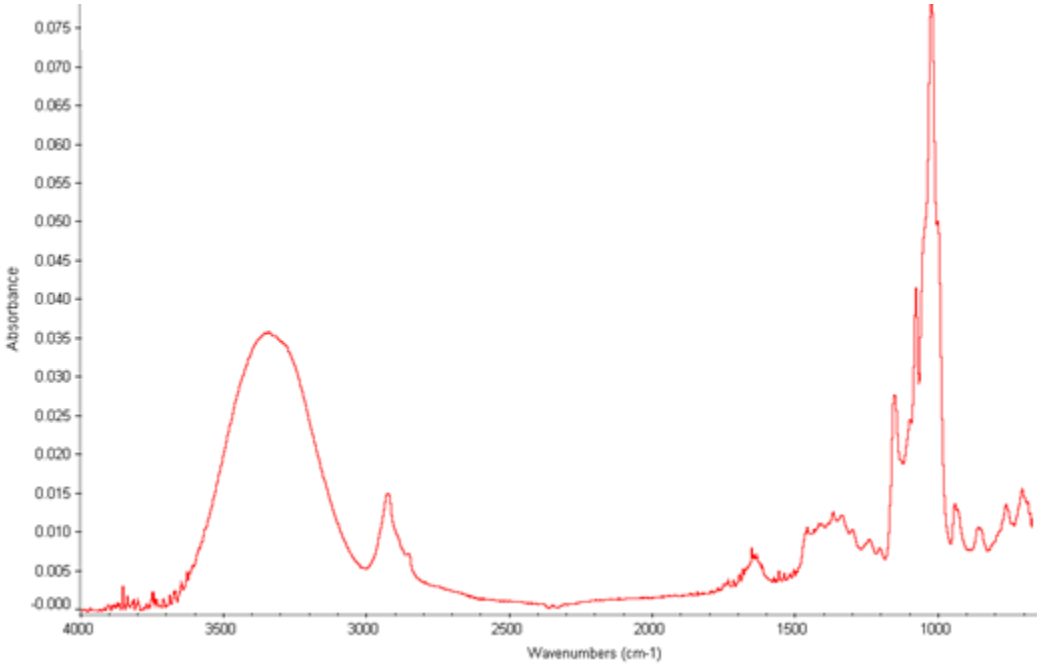

Figure 9: FTIR spectrum for as-received γ-cyclodextrin

Cyclodextrin Inclusion Complexes

One of the most commonly used features of cyclodextrin is the cavity created by the 1-4 linked glucopyranose units. The hydroxyl groups on both ends of the cyclodextrin molecule create a hydrophilic external environment, while the cavity interior is relatively hydrophobic

in character. The cavity formed with these specific properties allows many different molecules, many of which are hydrophobic in nature, to position themselves inside the cyclodextrin cavity. This inclusion of secondary molecules inside the cyclodextrin cavity forms what is called an "inclusion compound" or "inclusion complex" (IC). These IC's can be formed by the inclusion of small molecules, such as organic molecules[24], monomers[25], and dyes[26], or even oligomers and polymers[27-30] inside the CD cavity.

The properties of an IC can be drastically different from those of the CD host from which it was formed, and it is these property changes we must use to help determine whether or not an IC has been formed in the first place. The solubility, crystal structure, NMR peak locations, and DSC observations are some examples of the data that can help us to determine whether or not inclusion has taken place.

Solubility Changes

Sometimes, small hydrophobic guest molecules included inside the CD cavity can be dissolved into an aqueous solution, though the pharmaceutical industry has found that modified cyclodextrins often do a better job of creating a soluble IC than the unmodified versions.[31] The preference of unmodified CD-IC's for the crystalline state tends to result in an insoluble material. Polymer guests also often have different solubility properties than their CD-ICs. IC formation can lead to precipitation out of solution even when the unincluded polymer was soluble to begin with. This is an important step in common IC production methods like the precipitation method.[25] One would think that covering a hydrophobic polymer with CD might drive the solubility of the polymer in aqueous solution up; however, the same aggregation that occurs in small-molecule ICs occurs in polymer ICs. Because of this, polymer IC's made with unmodified cyclodextrins are generally crystalline

by nature. The cyclodextrin does not thread and spread evenly across the entire polymer, but instead aggregates together and forms the previously discussed channel structure.[32-34]

Sometimes, a polymer can be partly covered by cyclodextrin, but still be soluble in a solvent that is good for the polymer. Zhao and Beckham made a series of rotaxanes with poly(ethylene glycol) (PEG) and α-CD (partially covered PEG/α-CD IC's with bulky end-groups on PEG to prevent dethreading) with coverage ranging from 19 to 70%. Using diffusion ordered 2D ^{1}H-NMR, the diffusion constants were studied and it was revealed that the PEG and α-CD protons have the same self-diffusion characteristics, distinct from those of unthreaded PEG and α-CD.[35] This observation proves PEG/α-CD rotaxanation and suggests that end-capped polymer-CD-IC's (polymer-CD-rotaxanes not fully covered and not able to dethread) take on random coil conformations in solution as do their non-complexed counterparts.

Kildemark et al. also observed soluble polymer inclusion complexes while studying the competitive inclusion of poly (propylene glycol) (PPG) , PEG, and poly(N-vinylpyrrolidone) with cyclodextrin/methyl orange complexes.[36] They observed that having a low concentration of cyclodextrin may not form enough of a crystalline IC to precipitate out of solution. Though the results are legitimate and logical, Kildemark and colleagues incorrectly stated of the polymer-CD-IC, "At one point, most of the water shell will be displaced and the solubility will be lost." It is true that the polymer/water contact is lost, but this contact is not what keeps the polymer in solution. It is the ability of the polymer to remain a flexible random coil that prevents the polymer from precipitating out of solution. Once the polymer is covered with enough cyclodextrin, crystallization and aggregation will take place until precipitation occurs.

CD-IC Crystal Structures

As previously mentioned, the crystal structures of cyclodextrin hydrates for the three main types of cyclodextrin exist mainly as the herringbone-type cage structure. This crystal structure is also found when α-CD includes small molecules (iodine, methanol, and krypton).[18] The brick-type crystal structure can arise when slightly larger small molecules are included into the cyclodextrin and distort it enough to change the crystalline structure. An example of this would be the inclusion of small aromatic guests into α-CD that distort the macrocycle into an elliptical shape. γ-CD can only be found in the herringbone-type cage structure as a hydrate. Any other inclusion type generally leads to a tetragonally-arranged channel or slightly distorted channel structure.

β-CD also has some crystalline forms slightly modified from the three previously listed. It does form the herringbone structure for the hydrate and inclusion with small alcohols, but any "larger" small molecules will result in a "basket" type structure that can take many different, yet similar, forms as illustrated in Figures 10-13. The "baskets" are essentially cyclodextrin dimers that form via hydrogen bonding. These baskets then act independently to form a modified structure resembling something between the brick-type cage structure and the channel structure. Mentzafos and colleagues helped organize these slightly varied crystal structures into the channel (CH), chessboard (CB), intermediate (IM), and screw channel (SC) types, seen below.[37]

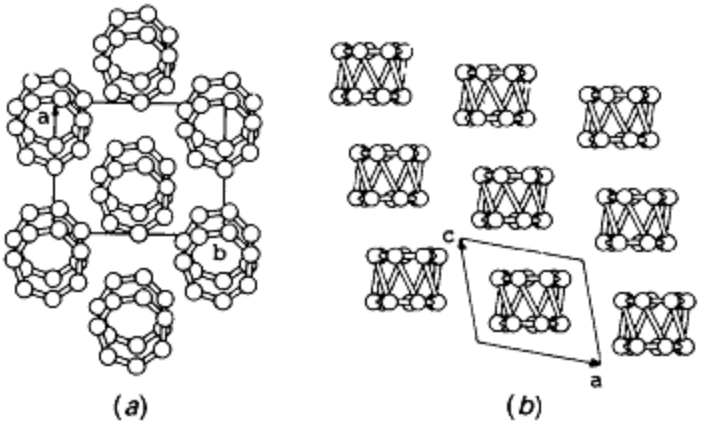

Figure 10: Channel (CH) packing mode in β-cyclodextrin as seen along the c axis (a) and the b axis (b)[37]

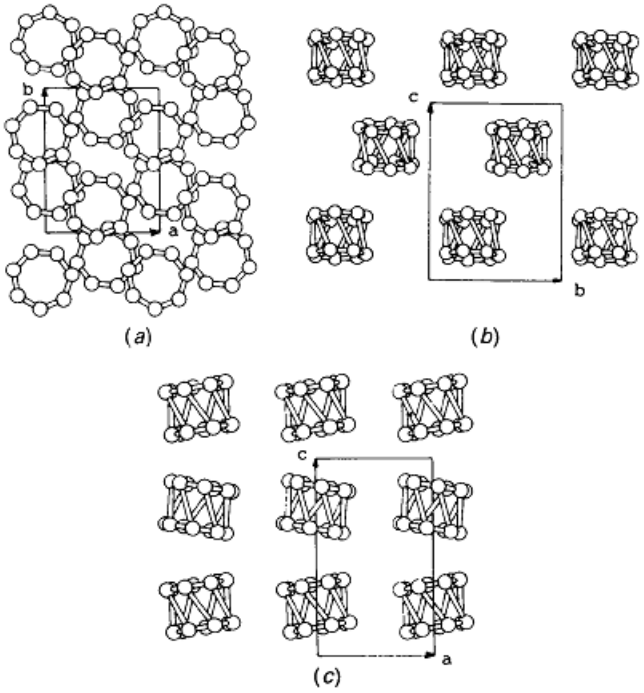

Figure 11: Chessboard (CB) packing mode in β-cyclodextrin as seen along the c axis (a), the a axis (b), and the b axis (c)[37]

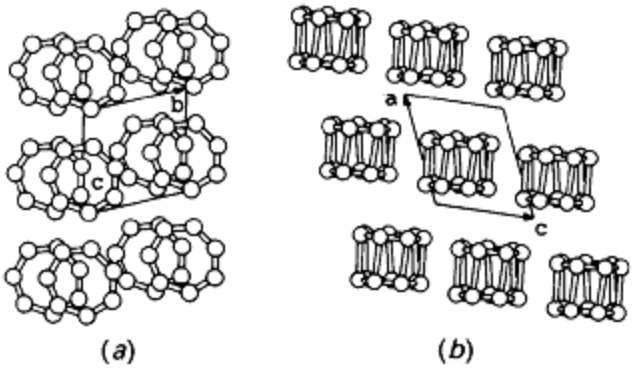

Figure 12: Intermediate (IM) packing mode in β-cyclodextrin as seen along the a axis (a) and the b axis (b)[37]

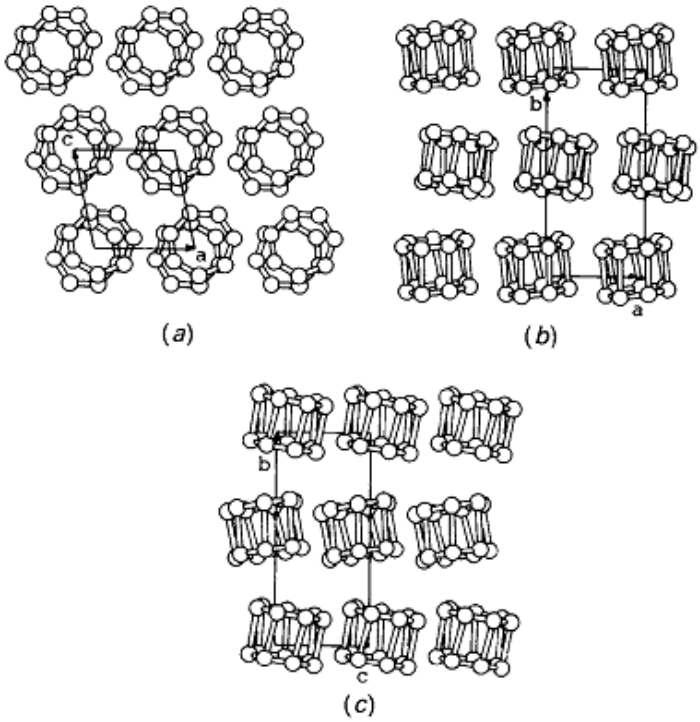

Figure 13: Screw channel (SC) packing mode in β-cyclodextrin as seen along the b axis (a), the c axis (b), and the a axis (c)[37]

The inclusion of longer, polymeric molecules leads to a channel structure in all three main cyclodextrin types. In this form, the cavities of the cyclodextrins line up and form long channels that house all or part of the included polymer. This structure was shown in Figure 4 in the pure CD crystal structures section. In addition to XRD changes, polymers trapped inside CD channels show distinctly different properties when analyzed by DSC and FTIR.

DSC Behavioral Changes

Inclusion of a polymer inside cyclodextrin channels can lead to drastic changes in the DSC behavior. Adding a small amount of cyclodextrin can change the amount of crystallinity in a polymer, resulting in changes in the size and/or location of thermal transition peaks. It is also possible that, with enough inclusion, the entire polymer is trapped within the channel structure created by the cyclodextrin and the melting peak will disappear completely. Below is an example of the suppression of polymer melting peaks upon IC formation.

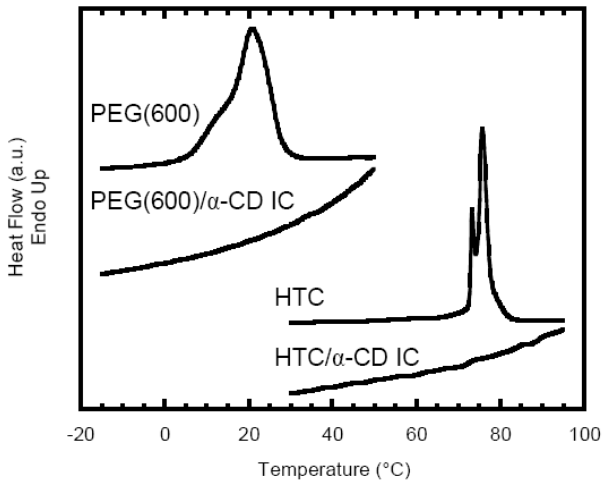

Figure 14: DSC Thermograms of PEG, hexatriacontane (HTC), and their IC's[38]

FTIR Changes

Since the FTIR profile of a material is based upon the vibrational properties of its molecular structure and its environment, inclusion of a molecule inside cyclodextrin can have a visible effect on the spectra. Not only are both sets of peaks visible in the spectra, but a slight change or shift in some of the peaks may also be observed due to steric or secondary interactions.

Inclusion of a polymer inside regular cyclodextrin channels results in a more regular structure. Because the FTIR data is sensitive to slight structural changes, straightening a random coil into a linear, regular arrangement will "clean up" the FTIR data by improving peak resolution.

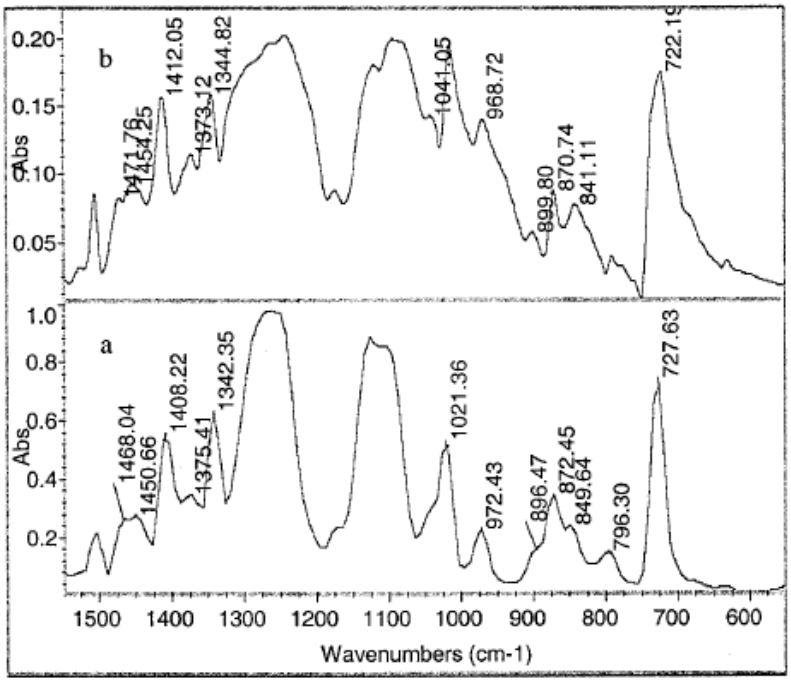

Figure 15: FTIR spectra of coalesced (a) and solution-cast polyethylene terephthalate (b)[39]

Some peaks, sensitive to slight changes in the conformation in the coiled state, will become better resolved as the entire polymer adopts, essentially, a single extended conformation. Figure 15 above demonstrates the difference between a less-ordered solution-cast polymer and a coalesced (straightened) polymer. Note that the coalesced polymer is no longer included inside the cyclodextrin channel, as the cyclodextrin has been washed away, but the mostly extended conformations of its unentangled chains remain and narrower better resolved peaks can be seen.

NMR Changes

Inclusion can also change NMR spectra. In fact, these NMR spectral changes are one of the most reliable methods of detecting IC formation. Upon complexation, shifts can be seen in both proton (solution) and carbon (solution and solid-state) NMR spectra. ^{13}C NMR shifts, however, are much more commonly used to explore the complexation phenomenon than proton shifts, because of their greater sensitivity to the inclusion phenomenon. According to Schneider et al., the ^{13}C NMR shifts ($\delta\ ^{13}C$) observed during complexation are now thought to be more the result of intramolecular conformational changes than intermolecular shielding effects.[40] Some examples of approximate values of proton complexation shifts can be seen below in Table 3, though the actual chemical shifts observed on complexation with CDs are specific to each guest molecule and can have a range of values.

Table 3: Proton chemical shift values for α-CD IC's with various aromatic guests[40]

proton	7	8	9	10	11
1 (CyD)	−0.04	−0.03	−0.02	−0.01	−0.03
2 (CyD)	−0.08	−0.04	−0.05	−0.03	−0.06
3 (CyD)	−0.25	−0.35	−0.25	−0.26	−0.13
4 (CyD)	0.00	0.01	0.00	0.01	−0.01
5 (CyD)	0.02	−0.05	0.35	0.36	0.14
6 (CyD)	0.00	0.00	0.03	0.03	0.01

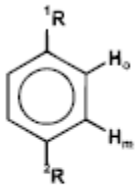

7	$^1R = O^-$	$;^2R = NO_2$
8	$^1R = OH$	$;^2R = NO_2$
9	$^1R = O^-$	$;^2R = I$
10	$^1R = OH$	$;^2R = I$
11	$^1R = CH_2COOH$	$;^2R = I$

Aromatic guest compounds for α-CyD.

When a guest molecule is included inside a CD cavity, the nuclear spin polarization of a guest proton can interact with the nuclear spin of the CD protons. This non-bonded, through-space interaction is called the Nuclear Overhauser Effect (NOE) and can be examined using one of several types of 2-dimensional NMR analyses. One of these techniques is called Nuclear Overhauser Effect Spectroscopy, or NOESY. This form of 2D NMR allows us to detect the presence of these through-space interactions, which only exist over a few tenths of a nanometer. An example of an IC NOESY spectrum can be seen in Figure 16 below. Cross peaks appear off the diagonal when the NOE is present. In this case, polystyrene is included inside γ-CD. The detection of NOESY interaction means that the two molecules are close enough together for the Overhauser Effect to occur, which in the case of CDs can only happen upon complexation. There are also other more complex techniques

that detect NOE presence. ROESY 2D NMR, for example, can actually do a slightly better job detecting the presence of these interactions when NOESY NMR is not sufficiently sensitive.

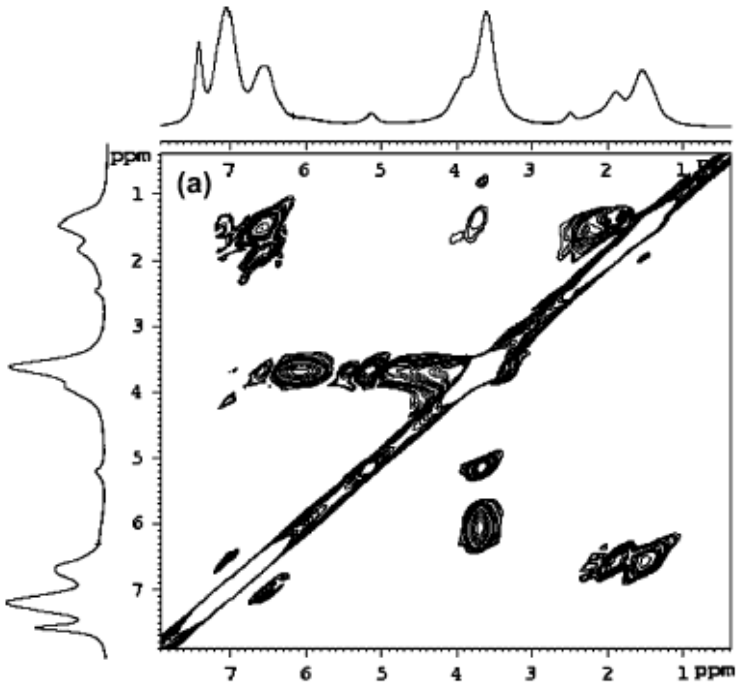

Figure 16: Example 2D NOESY ^{1}H NMR spectrum[41]

Cyclodextrin IC Formation Techniques

Hedges describes many of the IC formation techniques in his Industrial Applications review.[42] According to his review, the most commonly used methods of IC formation are the coprecipitation, slurry, paste, and dry mixing methods.

The coprecipitation method is often used in the laboratory in small scale experimentation. A solution of cyclodextrin (the solvent often being water) is made and the guest is added. As the IC forms, it precipitates out of solution and can be collected and dried. Since the solubility of β-CD is lower than that of α-CD and γ-CD, solutions of β-CD are often heated to form the initial cyclodextrin solution.

The slurry and paste method use less water, 20-30% w/w for the paste method and 40-45% w/w for the slurry method. The guest molecule is then mixed in with the cyclodextrin slurry or paste until inclusion takes place.

The dry mixing method is often slower and therefore not preferred. The cyclodextrin and guest molecule are mixed without added water or solvent. Inclusion times can range from hours to days. One reported guest that does include quickly by the dry mixing method is lemon oil. For fast inclusion to occur, it is said that the guest molecule should act as a solvent for the cyclodextrin.

Thermodynamics and Kinetics of IC formation

The kinetics, thermodynamics, and yield of polymer IC formation depend on the type of host cyclodextrin and the guest polymer and its molecular weight, temperature, and solvent.[43] It has been suggested that the driving force for inclusion is enthalpic rather than entropic, mainly because the water molecule displacement that occurs upon polymer threading balances out the lowered entropy of the included polymer configurations. More recent investigation has found that there is also a “hydrophobic” effect on the inclusion of guest polymers.

In the general case, polymer inclusion is governed by the basic thermodynamic equation:

$$\Delta G = \Delta H - T\Delta S = - RT \ln K_{eq}$$

Becheri and colleagues had previously visualized the threading equilibrium process as

$$\text{polymer} + m\text{CD} \leftrightarrows \text{D}\ \sigma^* \rightarrow \text{polypseudorotaxane}$$

and then used a derivation based on transition-state theory to arrive at the governing equations for the rate and equilibrium extent of polypseudorotaxane formation:

$$\frac{1}{t_{th}} = \frac{3k_B T}{2h}[CD]^m \exp\left(-\frac{\Delta G^{\neq}}{RT}\right)$$

$$\left[\frac{\partial(\Delta G^{\neq}/T)}{\partial T}\right] = -\frac{\Delta H^{\neq}}{T^2}$$

$$\Delta S^{\neq} = \frac{\Delta H^{\neq} - \Delta G^{\neq}}{T}$$

$$\Delta C^{\neq}_{P} = \left(\frac{\partial \Delta H^{\neq}}{\partial T}\right)_P$$

$$\ln K^{\neq}(T) = -\frac{\Delta G^{\neq}(T_0)}{RT_0} + \frac{\Delta H^{\neq}}{R}\left(\frac{1}{T_0} - \frac{1}{T}\right) - \frac{\Delta C_P^{\neq}}{R}\left[\left(1 - \frac{T}{T_0}\right) - \ln\left(\frac{T}{T_0}\right)\right]$$

In the above equations, m, t_{th}, k_B, h, [CD], and $K^{\neq}$ are the number of cyclodextrins on the polymer chain, the threading time, Boltzmann's constant, Planck's constant, cyclodextrin concentration, and equilibrium constant, respectively. σ* is meant to represent some intermediate rate-controlling step between the two components and the pseudorotaxane. Also, T_0 is generally chosen to be room temperature.

These equations permit the calculation of various thermodynamic parameters associated with cyclodextrin formation based on observations of the inclusion process at different temperatures. What the authors find from studying a variety of pseudorotaxanes is that the complexation is, in fact, driven by enthalpic interactions. They also observed that initial cyclodextrin concentration is of importance. The authors' observations led them to conclude that the formation of a channel cyclodextrin structure precedes the threading of

polymer guests. They state that this hypothesis supports previous observations that the inclusion process occurs faster at lower temperatures, that there seems to be some sort of concentration threshold necessary for inclusion to take place (in other words, enough CD must be present to aggregate in this manner), that the threading kinetics do not depend on solvent viscosity, and that the threading is either enhanced or crippled to a high degree by the addition of secondary solutes that assist or degrade the hydrogen bonding network of the dissolved cyclodextrin.

Peet et al. examined the solid-state inclusion of low molecular weight PEO with α-CD using much simpler and more practical 1st order kinetics analysis.[44] By measuring the change in the intensity of the 2θ = 12˚ XRD peak (I) and assuming the intensity was proportional to the amount of cage structure remaining, they arrived at the kinetic data for the inclusion under an array of variables. Table 4 below provides the kinetic equation along with the different variables examined in their experiments.

Table 4: First order kinetic parameters for PEO-α-CD inclusion[44]

$$I = I_{\infty}(1 - e^{-kt})$$

sample[a]	k (s^{-1})	I_{∞} (%)
PEG200, AR 2:1, 20 °C	0.30 ± 0.03[b]	98 ± 4[b]
PEG200, AR 3:1, 20 °C	0.31 ± 0.03	94 ± 3
PEG200, AR 3:1, 40 °C	0.71 ± 0.10	92 ± 3
PEG200, AR 3:1, 60 °C	1.7 ± 0.1	97 ± 1
PEG200, VD 3:1, 20 °C	0.31 ± 0.03	97 ± 3
PEG200, VD 5:1, 20 °C	0.47 ± 0.04	100 ± 2
PEG400, AR 2:1, 20 °C	0.077 ± 0.019	120 ± 20

[a] AR = as received; VD = vacuum-dried; 3:1 = PEG repeat unit/α−CD molar ratio. [b] Uncertainties in the parameters from the curve-fitting process.

The authors found that increasing the temperature or the amount of PEO in the mixture increases the complexation rate and that increasing the molecular weight of the PEO causes the rate to decrease. These results are attributed to the changes in the mobility of the polymer in the sample, which logically would play an important role during solid-state inclusion.

Altered Structures/Properties as a Result of Processing with Cyclodextrins

Cyclodextrin can produce a variety of changes in the properties of a polymer when incorporated into polymer processing techniques. Polymerization of a variety of hydrophobic monomers in aqueous solution may become possible when the monomers are included in CD and thus made soluble in water.[45] This reduces the amount of organic solvent necessary in polymer production, reducing costs and negative environmental effects.

Uyar et al. demonstrated that by including a polymer inside the cyclodextrin channel crystal structure and then washing away the cyclodextrin, the polymer can be coalesced into a highly aligned form, as indicated in Figure 17.[46] As previously mentioned, the FTIR spectra of the coalesced polymers demonstrate better resolution, with narrower and more distinct peaks. The coalesced polymer also demonstrates slightly higher thermal stability and a significantly higher glass transition temperature (shown in Figure 18).

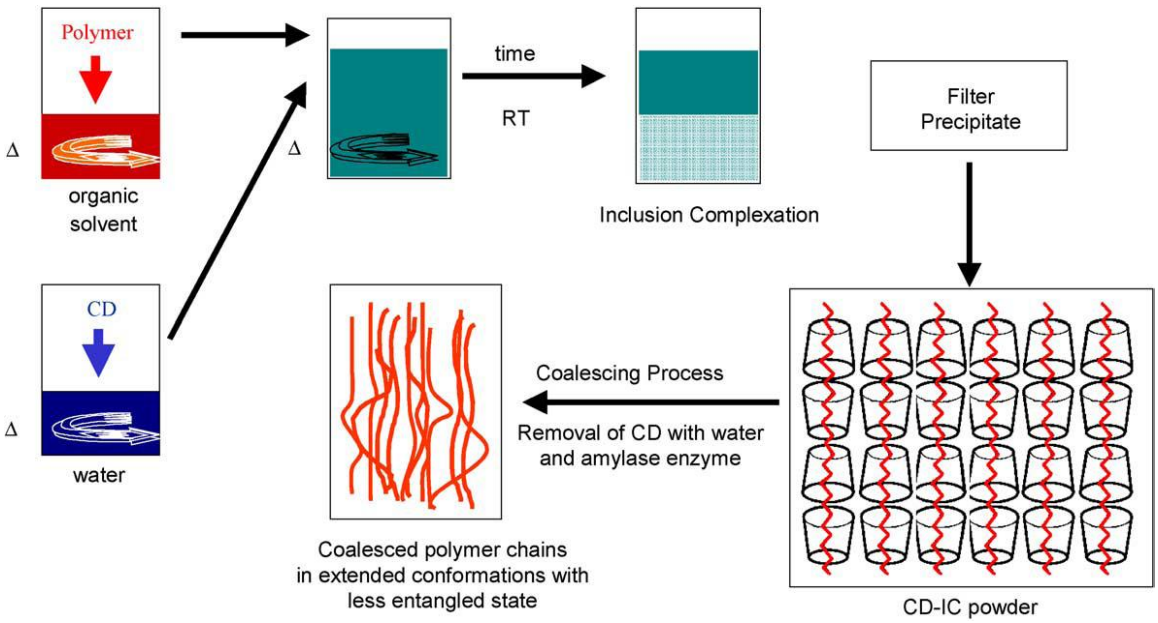

Figure 17: Restructuring polymers by processing with CD's[46]

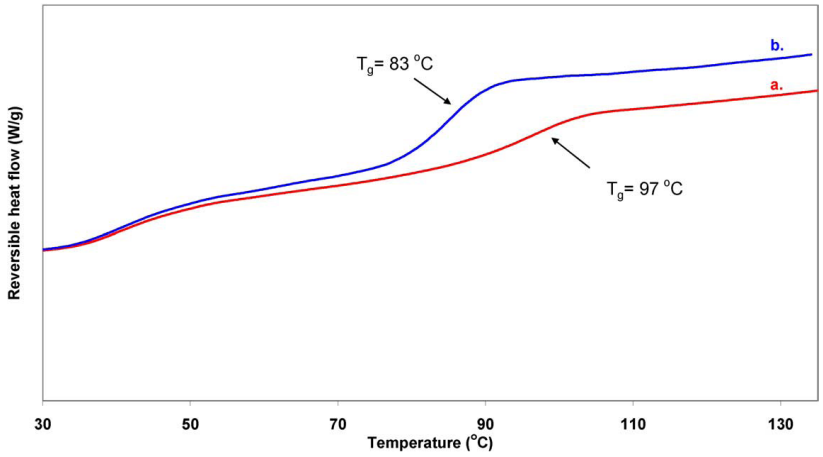

Figure 18: Modulated DSC thermograms of the second heating scan of coalesced PMMA (a) and as-received PMMA (b)[46]

It is also possible to intimately mix two polymers that are thermodynamically incompatible by way of common inclusion and coalescence.[28] The same authors that formed the coalesced polymers also blended two different types of polymers by forming common IC's containing both polymers before washing the CD away. Blends of PC/PMMA, PC/PVA, and PMMA/PVA [PC = polycarbonate, PMMA = poly (methyl methacrylate), PVAc = poly (vinyl acetate)] were all made in this fashion. These blends displayed thermal stability and degradation mechanisms different than those of the individual components. The intimate polymer blends displayed a single glass transition temperature as compared to a physical mixture of the two (see Figure 19).

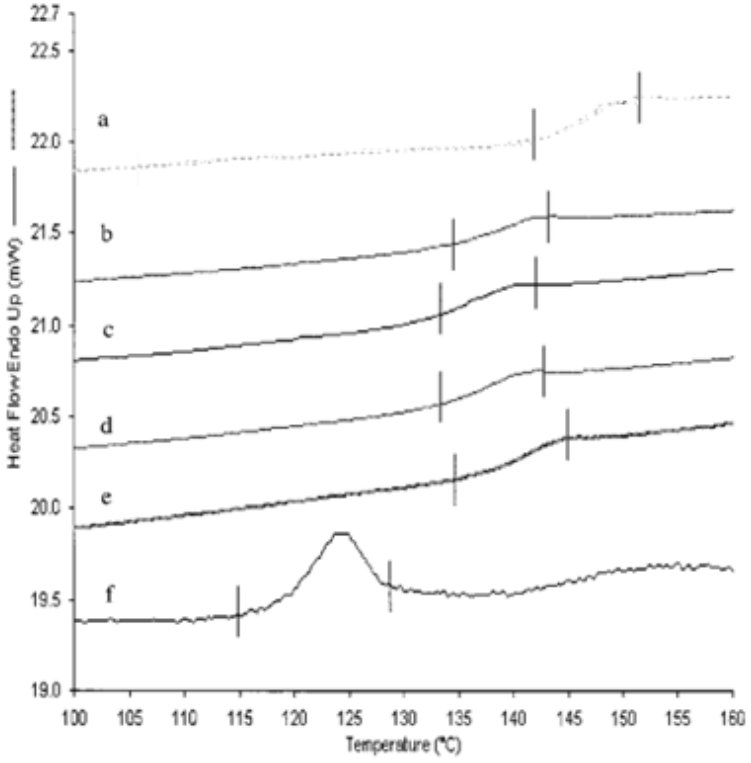

Figure 19**:** DSC heating scans of PC (a), the 2nd, 3rd, 4th, and 5th heating scans of a coalesced PC/PMMA/γ-CD IC (b, c, d, and e, respectively), and PMMA (f)[28]

Star polymers may also be formed using cyclodextrin as a core.[47,48] Modified or unmodified cyclodextrins create starting points for controlled polymerization of "arms" off of the cyclodextrin. Rusa and Tonelli demonstrated the use of cyclodextrin as a tool to purify polymer mixtures.[49] They used cyclodextrin and urea to separate a mixture of PEG of two different molecular weights, 600 g/mol and 20,000 g/mol. The urea showed a definitive selectivity for the higher molecular weight PEG while the cyclodextrin showed a strong preference for the high molecular weight PEG, but did include both. Rusa, Luca, and Tonelli also tested the selected preference of a polymer versus a small molecular model of the repeat unit.[50] They verified that the CD-ICs for PCL underwent nucleation and growth at a faster rate than the hexanoic acid CD-IC. It was suggested that the difference in solubility may have been the key factor in the higher molecular weight preference, which could explain the preference of high molecular weight PEG as well.

Xue et al. also demonstrated the possibility of using cyclodextrin to purify a polymer blend.[51] They took a mixture of PEG's, some terminated with methyl groups and other terminated with a carboxyl group, and added α-CD to the mixture to form an IC. Since the IC of PEG-COOH forms at a much faster rate than the PEG-CH_3, the exposure time of the materials was limited to allow for inclusion of only one polymer. The IC was then separated from the polymer mixture and the mostly carboxyl-terminated polymer isolated. This purification step was repeated again on the remaining polymer mixture and tests were done to confirm that most of the –COOH IR signal was gone. This demonstrates that end group functionality can play an important part in the IC formation kinetics as well.

Other uses for cyclodextrin in polymer processing do not involve polymer inclusion at all. A common practice is to attach the cyclodextrin to or blend cyclodextrin-ICs with pure polymer for the purpose of incorporating small molecules in the mixture. Blending a small amount of a non-stoichiometric polymer/CD IC (with portions of unincluded polymer dangling from the CD crystals) with the same bulk polymer has been shown to greatly

improve the nucleation kinetics in polymer crystallization,[52,53] allowing for an environmentally friendly and biocompatible approach. Hydrogels with cyclodextrin pendant groups were also formed and the controlled drug release from these hydrogels was measured.[54] Using cyclodextrin to assist in synthetic fiber dyeing has also been topic of study in recent years. Savarino et al. demonstrated that the addition of free or dye-complexed β-CD to nylon fibers helped improve the dye uniformity and brightness.[55] However, the authors also observed that the tendency of dyes to complex with cyclodextrin hinders the covalent dyeing of cellulosic fabrics.[56] This would indicate that cyclodextrin is useful in fabric dyeing only when the cyclodextrin does not hinder any normal covalent attachment, as is the case for a lot of cellulosic dyeing techniques.

Another use of polymer-CD-ICs is to use cyclodextrins as crosslinks. Crosslinking two mobile cyclodextrins together creates a flexible network with mobile crosslink points. Okumura and Ito prepared a hydrogel by crosslinking a sparsely covered and end-capped PEG.[57] Okumura and colleagues then went on to prove that the sliding only occurs in the sparsely rotaxanated polymer gels.[58] Sliding-ring hydrogels continue to be studied and provide another unique perspective on polymer-IC processing.

As evidenced by its many practical applications, cyclodextrin-based polymer processing plays an important role in the current development of new techniques and materials in the world of polymer science. Cyclodextrins offer us the ability to change the behavior of a polymer post-synthesis that would not otherwise be available. Regular cyclodextrin, however, is not the only valuable processing tool. Modified cyclodextrins may also play an important role in polymer processing, and the research opportunities in this field are far less explored.

Motivation for Research

Cyclodextrins and modified cyclodextrins provide a great opportunity to alter the behavior and properties of many materials, including polymers.

Coalescing a polymer material from its CD-IC should theoretically have a great impact on the physical properties of the material; however, the coalescence process often leaves so little yield that physical testing cannot be performed. If we scale up the IC production so that we obtain a large enough polymer sample post-coalescence, we should be able to observe the direct physical effects of the change in chain morphology in the coalesced sample in a way not previously achieved.

How much would this elongated and restricted chain structure change the physical and rheological properties of the material? How would the materials behave? What practical applications would exist for a coalesced material if enough could be made? But these are not the only questions we hope to answer.

Though there has been much research on the marriage of unmodified cyclodextrin and polymers, there has been very little published on the property changes available by the use of modified cyclodextrin during polymer formation/processing.

The crystallinity and aggregation of cyclodextrin seems to be interrupted when random modifications are made to the CD structure. Certain studies suggest that threading these kinds of modified cyclodextrins onto a polymer chain does not result in an aggregated, channel structure, but no hard evidence has been published to support these observations.

If it is possible to form non-crystalline, non-aggregated polymer-CD-ICs, what kind of property changes could this afford? Would bulk properties and solution properties be affected as much if the normal aggregation did not occur? If non-aggregated polymer-CD-

ICs remain soluble, then rheological studies of these interactions could be made much easier. Could specially selected modified cyclodextrins be used to give polymers additional properties that would otherwise have to be built into the polymerization process? These are all questions that we can answer by better understanding the inclusion behavior and property changes of polymer-modified CD-ICs.

One particular modified cyclodextrin presents itself as an interesting candidate for modified polymer processing. Monochlorotriazinyl-β-CD (MCT-β-CD) is a randomly modified, reactive β-CD produced in commercial quantities. The reactivity of the monochlorotriazinyl group, along with the fact that no publications involving the threading of this material onto a polymer chain exist, make it an extremely interesting candidate to begin the modified CD research.

Analytical Techniques Overview

DSC

DSC thermograms were collected on a TA Instruments Q1000 Differential Scanning Calorimeter with an attached LNCS liquid nitrogen cooling system. Various heating and cooling rates were used, depending on the sample, and will be noted where appropriate. Hermetically sealed aluminum pans were used in all instances.

DSC data were analyzed using Universal Analysis, part of TA's Thermal Advantage software. Glass transition temperatures and melting and crystallization temperatures and enthalpies were all determined automatically by the software based on the collected data.

TGA

TGA was performed using a Perkin Elmer Pyris1 Thermogravimetric Analyzer. Nitrogen was used as the furnace purge gas. Samples were generally heated at a rate of 20° C per minute.

FTIR

FTIR analysis was performed on a Nicolet Nexus 470 Spectrometer. The sampling head was a Nicolet OMNI Germanium Crystal ATR. The software's built in ATR correction was applied to all collected data.

XRD

X-ray diffraction data was collected on a Philips XLF, ATPS x-ray diffractometer with an OMNI Instruments customized automount and copper tube, producing an x-ray wavelength of 1.54Å.

NMR

^{1}H-NMR spectra were collected on one of two instruments. A Bruker 500 MHz NMR was used for many of the 1D proton and all of the 2D testing. In some cases where the Bruker 500 was unavailable, a Mercury 400 MHz NMR was used. NMR spectra taken by the Mercury 400 will be noted as such.

One-dimensional analysis was typically performed using ACD SpecManager (software version 10.02). Zero filling was used to bring the data count up to 65536 and an apodization of 0.3 was used during Fourier transformation. The HDO peak was used as a reference at 4.75 ppm *vs* TMS. Generally, autophase was used with good results, though on rare occasions, manual phasing was necessary. Peak selection and integration were also performed manually. Two-dimensional analysis was performed using Bruker's Topspin Analysis Software (Version 2.1). Many of the processing characteristics were handled automatically by the software, though manual identification of the reference peak was occasionally necessary. Due to proton peak overlap, HSQC and HMBC 2D NMR (^{1}H to ^{13}C correlation) were used for proton peak assignment for all samples in Chapter 4.

DMA

DMA was performed using a TA Instruments Q800 Dynamic Mechanical Analyzer with an attached film tension clamp and LNCS liquid nitrogen cooling system. Samples were quickly cooled to -100˚C and then a strain-mode test at a frequency of 1Hz was performed while the sample heated at 3˚C per minute to 50˚C.

Similar to DSC, data was analyzed using TA's Universal Analysis software. Glass transition temperatures were determined automatically by the software based on the Storage modulus data.

Melt Rheology

Melt rheology was performed on a Stresstech HR melt rheometer at 120° C with 25mm stainless steel parallel plates. This testing temperature was used to encourage complete

melting of both PCL types tested with this instrument. A stress sweep was first performed to determine the linear viscoelastic regime (LVE). Then, using a stress in the LVE, oscillatory shear testing was performed across a range of frequencies. As-received samples were held for one minute at temperature, while the coalesced samples were held for longer times to ensure complete melting of the material before testing began. Data interpretation was performed using RheoExplorer software, version 5.0.

Nanoindentation

Nanoindentation was performed using a Hysitron TriboIndenter hardware and TriboScan software. All tests were performed at room temperature (approximately 22˚C). Each sample, a small 5mm by 5mm square of melt pressed material approximately 1mm thick, was indented 9 times using a Berkovich tip in a 3x3 square pattern set 15 µm apart. Young's modulus and hardness values were all determined automatically by the software.

Topographic visualization of the indented material was also collected using the Hysitron hardware and software. The software allows for the automatic scanning of the surface of the film, adjusting the tip height based on the force feedback and mapping surface topography.

Chapter 2: Physical Properties of Coalesced Poly(ε-caprolactone)

Abstract

Poly(ε-caprolactone) (PCL) is a biodegradable/bioabsorbable polyester used in such biomedical applications as drug delivery and suture manufacturing. PCL has relatively poor physical properties, however, limiting the materials load-bearing applications. In this work, PCL was processed with α-CD to form an inclusion complex (IC). The cyclodextrin was then stripped away to yield a PCL with a reorganized morphology of elongated, unentangled, and constrained polymer chains, a process referred to as coalescence. The physical and rheological property changes resulting from this coalescence process were then examined. It was found that the coalesced polymer had an increased melt crystallization temperature of up to 25˚C. Coalescence also decreased the tan δ of the material and increased the average hardness and Young's modulus by 33 and 53%, respectively.

Introduction

Poly(ε-caprolactone) (PCL) is a biodegradable/bioabsorbable polyester that was first synthesized in the 1930's by ring-opening polymerization of ε-caprolactone. Today, PCL is well established in the biomedical field, often acting as the main component for bone and cartilage tissue scaffolding. Medical-grade PCL is a higher density, slower degrading version of PCL often used in place of research-grade PCL in these applications. Due to its relatively low melting temperature, PCL can be melt processed using very simple techniques and is often strengthened using secondary fillers, such as fibers or particulates.[59] Often, PCL is used in combination with another biodegradable polyester, poly (lactic acid) (PLA). Blends of PLA and PCL have been shown to have good gas barrier properties.[60]

For all PCL's unique and valuable properties, it is not a very strong material. Due to its low melting temperature and relatively poor physical properties (compared to other current implantable materials), PCL has not made great headway as a load bearing implantable material. If it is possible to strengthen PCL in some fashion, then a biomedical application such as a load bearing implantables, may be added. However, if a nucleating agent is used to improve PCL's semi-crystalline morphology and resultant physical properties, it must also be non-toxic and bioabsorbable to preserve PCL's use as an implantable material.

Though coalescing PCL from its IC with α-CD should have a great effect on the material, it is unlikely that the mass production of a coalesced polymer would be feasible or profitable. Production on the laboratory scale, however, is quite feasible and could provide great insight into the importance of the role played by polymer chain organization on the physical properties of a material. Due to the extremely small polymer product yield of the IC formation and coalescence processes, no publications exist that examine the physical property changes that occur when PCL is coalesced; the goal of previously completed work has been to understand the change in thermal transition behavior[61] and behavior of a

partially included PCL IC.[62,63] In this work, our interest lies in determining a way to produce in high yield, completely coalesced PCL polymer, with virtually no remnant α-CD, for the purpose of examining physical and rheological property changes. However, before we can begin to observe the physical property changes that occur in coalesced PCL, we must first examine the properties of PCL in its traditional form.

Physical and Chemical Properties of PCL and PCL IC's

PCL is a semicrystalline aliphatic polyester with a melting point (T_m) around 59-64˚C and a glass transition temperature (T_g) around -60˚C.[64] It has a reported tensile strength of 20-42 MPa and a tensile modulus of 0.2-0.44 GPa.[65] Sigma-Aldrich reports a Shore D hardness value for PCL of 55; however, no conversion tables can be found to understand what this value would be in units of MPa. PCL is formed by the ring-opening polymerization of ε-caprolactone (Figure 20 below).

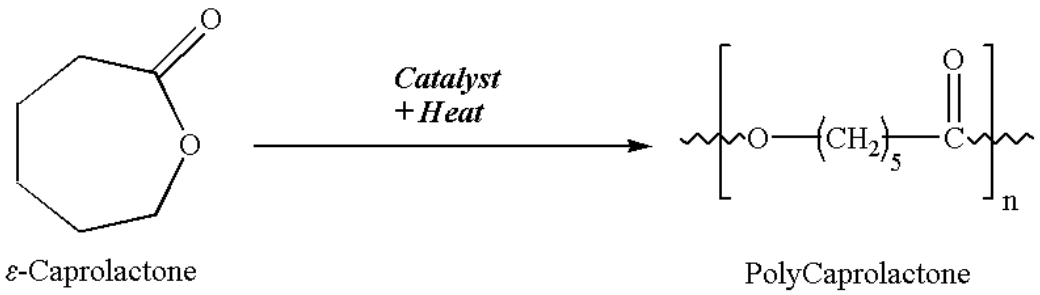

Figure 20: Schematic of PCL ring opening polymerization

As the degradation of PCL involves the hydrolytic chain scission of the ester linkages, PCL's hydrophobicity contributes to its longer degradation time when compared to PLA (2 to 5 years).[66] The degradation properties of the material are not of concern in this particular work, although we would theoretically expect an increase in degradation time as the level of coalescence and thus the expected density of the material increases.

PCL is widely known to form an inclusion complex with α-CD, and the properties of these inclusion complexes have been studied at great length.[30,67,68] The IC has been shown to adopt the channel crystalline structure common to polymer-CD IC's. Other common polymer IC behaviors are observed as well, including a suppression of the melting/crystallization peaks and changes in the FTIR (in the case of PCL, the expansion of the carbonyl stretching band of PCL in FTIR and elimination of the crystalline peak component).[67] The effect of the molecular weight on the formation and stability of PCL-α-CD IC's was also studied.[68] It was found that the IC yield decreased with increasing molecular weight and lower molecular weights resulted in a more highly covered IC sample.

PCL Nucleated with Non-stoichiometric PCL IC's

What practical applications exist for PCL IC formation? There exists a small collection of work examining the nucleation effects of non-stiochiometric (n-s) PCL-α-CD-IC's on bulk PCL. Dong et al. from Tokyo Institute of Technology have spent the last few years exploring (n-s)-PCL-α-CD-IC nucleation of bulk PCL.[69-71] The group found the uncovered though constrained PCL chains emerging from the (n-s) PCL-α-CD-IC crystals to be an effective nucleant for the melt-crystallization of bulk PCL, providing a strong increase in the crystallization rate and thermal stability of the bulk material. They observed that the storage modulus (G') increases with nucleation as well as a higher loss component peak

(G'') during glass transition. They also observed an increase in the Young's modulus and yield stress of the material by about 200 and 130%, respectively.[69]

Luo et al. also formed a (n-s) PCL-α-CD-IC with partially covered chains and tested the physical properties of this material by itself. With a relatively high percentage of uncovered polymer chains (~70% remained uncovered) interconnecting many smaller channel IC crystals, the IC acts as a type of cross-linked, shape-memory material. The non-stoichiometric PCL/α-CD IC had a recovery ratio of approximately 90-95% depending on the degree of coverage and a significantly higher storage modulus. Its degradation, however, was actually quicker than the as-received PCL.[62,63]

There are even fewer examples of studies being done on completely coalesced materials. This is likely due to the fact that it takes a large amount of IC to get a very small amount of coalesced polymer. To our knowledge, the only known work performed on a completely coalesced PCL polymer sample was published in 2003. Wei et al. performed melt and crystallization studies on a PCL enzymatically coalesced from its α-CD IC. After the coalescence process, the removal of the α-CD was confirmed by the absence of FTIR bands characteristic for α-CD. The coalesced PCL melted and crystallized at slightly higher temperatures, but no other properties were observed.[61]

This leads us to the work done in this project. Until now, a majority of the small number of relevant studies had been limited to nucleated bulk PCL, non-stoichiometric IC's, or DSC measurements of small amounts of coalesced material that suggested little change between the two components. Obviously, a coalesced PCL, with its elongated chain structure, should demonstrate drastically different physical and rheological properties. To achieve the ability to perform these types of tests, scaling up of the IC formation and coalescence processes have to be performed, as well as refining the coalescence process to ensure that no

remnant CD remains. In doing so, we may be able to understand the property differences produced in PCL by the IC formation and coalescence processes.

Materials and Methods

PCL with a molecular weight of 80,000 g/mol was obtained from Sigma-Aldrich. The material was used without further treatment in the "as-received" samples. Cyclodextrin was obtained from Cerestar USA and used without further modification or treatment. All non-aqueous solvents, chemicals, and enzymes were also obtained from Sigma-Aldrich and used without further purification or treatment.

IC Formation Technique

The α-CD-PCL IC formation technique was adopted from the procedure used by Wei et al.[61] The technique was scaled up from the original and slightly different solvent ratios were used as a result. A short period of sonication was also added to help with the inclusion. There is no evidence that these differences negatively affected the procedure.

To produce the IC, 4.0 grams of PCL were dissolved in approximately 500 ml of acetone. PCL pellets were added to the solvent and the mixture was heated at 60˚C and stirred until the PCL pellets were completely dissolved. During this time, 37.0 grams of α-CD were dissolved in 250 ml of deionized water. This mixture was heated for a short time at 60˚C to aid in CD dissolution. Once both materials were dissolved (or as dissolved as possible in the case of the CD), the CD solution was dripped into the polymer solution while stirring. Immediately, a white precipitate was formed (presumably the CD). After adding all the CD solution, the mixture was then sonicated for 5 minutes and stirred overnight (approximately 36 hours) at

room temperature. The resulting precipitate was filtered, washed with deionized water to remove any non-complexed CD, and dried overnight under vacuum. Approximately 20g of IC were collected, a yield of ~ 50%. A schematic of the IC formation technique can be seen in Figure 21.

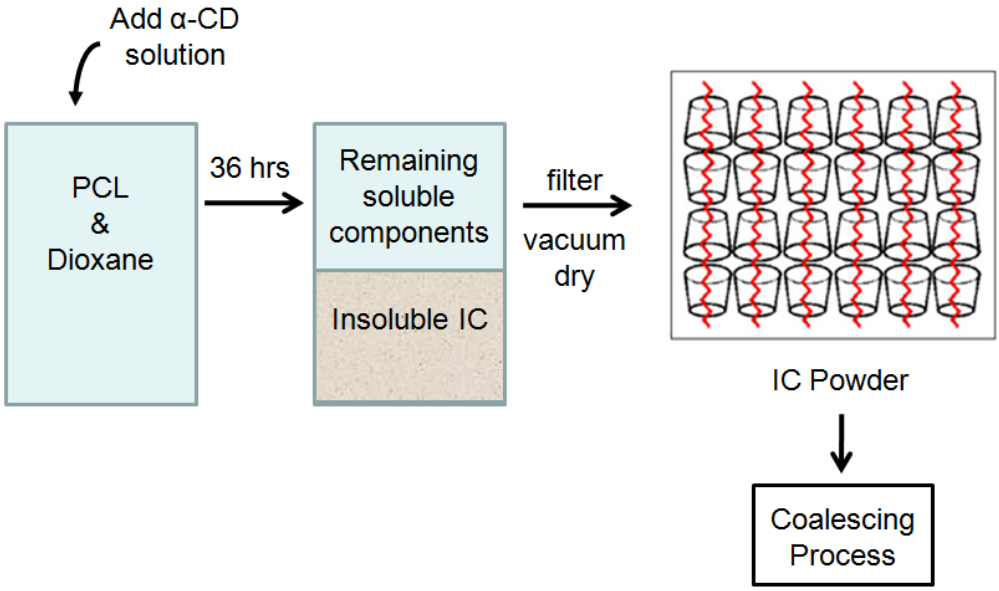

Figure 21: Schematic of the α-CD-PCL IC formation process

The product was then examined using XRD to look for the channel crystalline structure, as evidence of IC formation. The XRD pattern can be seen in Figure 22. The standard α-CD-PCL IC peaks can be observed in our sample (as compared to the IC diffraction pattern of Dong et al.[69]), suggesting we have successful IC formation.

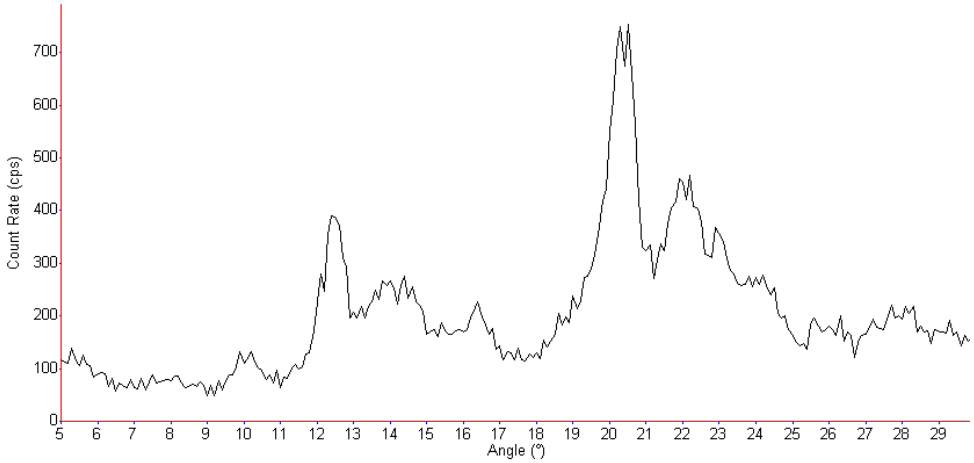

Figure 22: X-Ray diffraction pattern of our α-CD-PCL IC sample

Coalescence Techniques

We knew that to accurately measure the physical properties of the coalesced PCL, we needed to completely remove all traces of the cyclodextrin. If we have even a small percentage of threaded cyclodextrin remaining in the material, the potential "crosslinks" created by this threaded PCL and crystalline α-CD would interfere with our physical testing results.

To coalesce our material, we first turned to the literature to find an existing method that we could easily adopt for our system. The two common methods for IC coalescence were hot water washing and washing with an α-Amylase enzyme. Soxhlet extraction was also a purification method used in the past, so this technique was tried as well. After much experimentation with these methods, it was determined that too little CD was removed to

meet our specifications. Acid washing had been used in other recorded cases to coalesce Nylon, so this was also attempted and appeared successful.

The techniques for each washing method will be described below, but it is important to note that many of the methods were performed over a variety of temperatures and/or time periods to get as much of the α-CD removed as possible.

Hot Water Washing - The hot water washing method was a very simple one. The IC material was added to a high volume of water (generally at least 100 ml for every 2.5g of IC) and stirred overnight at 90˚C. This washing was performed with and without sonication, and washing for longer periods of time at 60˚C and room temperature were also attempted. The material was dried under vacuum before measuring.

Enzyme Washing - Washing with the α-Amylase enzyme was fairly similar to washing with water, except with the addition of 2 ml of α-Amylase enzyme solution (31k Units of enzyme) per 300 ml of water. The mixture was stirred at 35˚C overnight (again, procedure outlined by Wei et al.[61]), or for longer periods of time as determined. The material was dried under vacuum before measuring.

Soxhlet Extraction - Soxhlet extraction is a technique similar to hot water washing, but the device allows for the constant recycling of the solvent to prevent solute saturation and encourage continued purification/extraction. The IC powder was added to a cellulose filter and placed in a soxhlet extraction setup. The IC was left to wash for a period of up to two weeks. The material was dried under vacuum before measuring.

Washing with HCl - After IC production, the material was first stirred in room temperature deionized (DI) water for 4 hours to reduce the amount of CD removal necessary by acid degradation. Then the material was filtered and stirred in stock 37% HCl solution at relatively low concentration (0.5 g of washed IC per 100 ml 37% HCl solution) for no more

than 1 minute, after which the coalescence process was “quenched” by the addition of the acid/IC mixture to a relative large volume of DI water. It was determined that any dilution of the HCl solution resulted in no CD removal and any HCl exposure time beyond two or three minutes seemed to damage the polymer. The solution was then filtered to collect whatever solid remained and washed with water to remove any degraded starch material. The collected polymer was dried under vacuum before measuring.

Determination of the effectiveness of the “unsuccessful” coalescence techniques was done by weighing the dried IC sample and the dried coalesced sample to determine how much material was removed. Two assumptions were made in the CD% removal calculations; first, that all the weight loss corresponds to the removal of cyclodextrin, and second, that the beginning IC material was 100% covered polymer with a PCL repeat unit to α-CD molecule ratio of 1:1. With these assumptions in place, we observe α-CD removal on the order of the values listed in Table 5. Apparent complete removal of α-CD from the IC by acid washing was verified by FTIR measurements and proton NMR. The FTIR spectra can be seen in Figure 23. It is observed that the acid-washed material displays no characteristic α-CD peaks (1029 and 3050 cm^{-1}) and a strong carbonyl stretch band at 1724 cm^{-1} characteristic of PCL (a band that quickly disappears as α-CD inclusion percentage increases).

Proton NMR spectra (not shown) were collected by dissolving the coalesced PCL in a 2:1 ratio solvent mixture of deuterated chloroform and deuterated DMSO. The sample dissolved completely in this solvent mixture and no trace of α-CD was observed. It was determined by adding a small amount of α-CD to this solvent mixture that OH(2) and OH(3) resonances appear at 5.4 ppm. This resonance was not observed in the dissolved coalesced sample, confirming the FTIR results.

Table 5: Percentage of remaining cyclodextrin after various coalescence techniques

Coalescence Technique	*Estimated Remaining CD (%)*
Hot Water Washing	17.8
Enzyme Washing	12.7
Soxhlet Extraction	12.6
Acid Washing	No trace

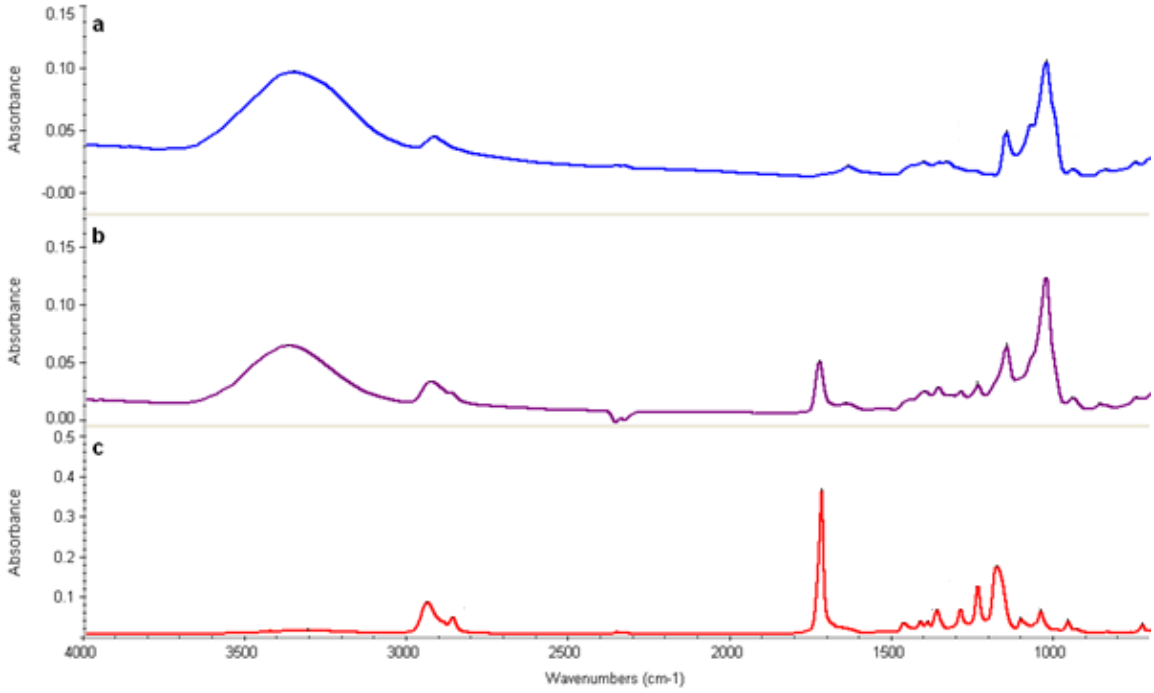

Figure 23: FTIR spectra of α-CD (a), enzymatically washed PCL (b), and HCl-coalesced PCL (c)

Now we address the validity of these assumptions and their relatively small effects on the results. The first assumption that all the weight loss comes only from the cyclodextrin is most likely not accurate, as some small percentage of the weight loss is certainly tied to sample remaining on the filter or in the glassware. However, making this assumption would likely only slightly overestimate the amount of CD removed. The second assumption that

the PCL was 100% covered is most likely incorrect as well. There was likely some portion of uncovered PCL, as it is generally uncommon to have every single repeat unit covered by α- CD. This assumption would probably result in a slight underestimation of the amount of CD removed.

These assumptions and their resulting effects on the values provided probably work to partially cancel out each other; however, since the percentage of α-CD removed needs to be as close to 100% as possible, the measurements for each of the "unsuccessful" techniques are of little concern. The "successful" acid washing method removed almost all traces of α-CD as measured by the FTIR, which is the end result necessary for further testing. For comparison, a film was cast of a physical mixture of PCL and 2 wt% α-CD. This film was measured by transmission FTIR to see if the CD peaks would show through the PCL signal, and surprisingly they did not. This would suggest that there could be a small trace of α-CD remaining in the system, though significantly less than the other coalescence methods. NMR experiments were performed on our coalesced PCL using a 2:1 solvent mixture of $CDCl_3$ and d_6-DMSO. These experiments showed no remaining α-CD, but α-CD resonances did appear after a trace amount of pure α-CD was added to the NMR tube. It appears that solution ^1H NMR is superior to solid state FTIR for the assessment of remnant CD in coalesced polymer samples.

Hot water washing, enzymatic washing, or soxhlet extraction would serve as excellent methods for arriving at non-stoichiometric IC's. This would make another interesting project, as the free PCL in these materials likely remains coalesced compared to starting with a smaller stoichiometric ratio of α-CD:PCL.

To examine whether or not our acid washing technique has any detrimental effects on the molecular weight of the polymer, viscometer flow times of an as-received PCL/acetone solution and an HCl-treated PCL/acetone solution were recorded. The treated PCL was

washed alone (no α-CD) in full stock concentration HCl for the same amount of time and then added to water similar to the acid coalescence technique. 0.3 g/dL solutions were prepared and three flow separate flow times were measured and averaged. The flow times for the as-received and the HCl treated solutions were 96.66 and 96.33 seconds, respectively. Any chain scission (molecular weight reduction) would significantly reduce the flow time, so we can say with good confidence that our particular HCl treatment did not damage our polymer.

Our measurements indicate we have nearly completely coalesced the polymer and have not damaged the PCL in the process. The next step is to explore the physical and rheological properties of coalesced PCL.

Physical Properties of Coalesced PCL

DSC

Thermal transitions observed in a material can provide a large amount of information about its physical structure. We suspect the coalesced PCL chains are more extended and less entangled. If this were the case, we would expect to observe a strong difference in the crystallization behavior of the material, especially if the material remains extended and at least partially structured above the melting temperature. Figures 24 and 25 show the melting and crystallization behavior of coalesced and as-received PCL. We can see that coalescence results in little to no effect on the melting behavior of PCL when compared to the as-received material; however, a very large change in the melt-crystallization temperature is observed.

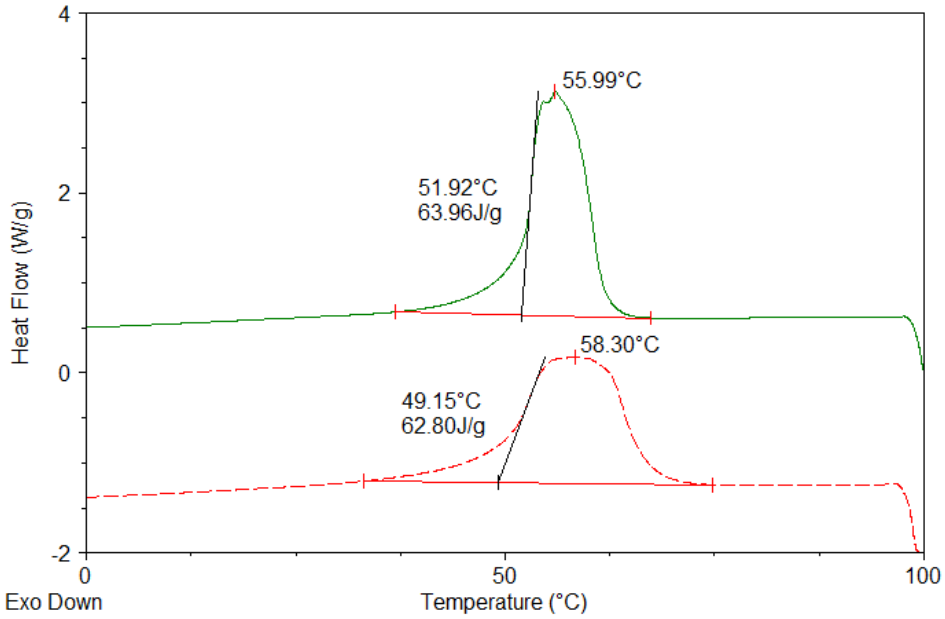

Figure 24: Melting curves of as-received PCL (lower) and coalesced PCL (upper) at 20˚C/minute

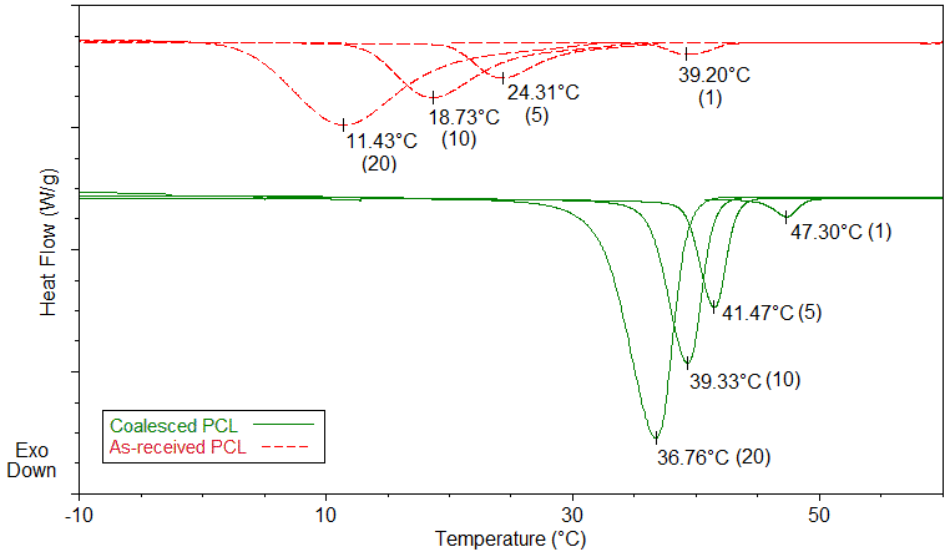

Figure 25: Crystallization Curves of as-received PCL (upper) and coalesced PCL (lower) at 20˚, 10˚, 5˚, and 1˚C/minute cooling rates (left to right for each sample)

Because the change in crystallization temperature (T_c) is so drastic at 20˚C, we examined the effect of changing the cooling rate. It is well known that a polymer's T_c varies with cooling rate. For this reason, it is helpful to provide the crystallization temperatures across a span of cooling rates. Figure 26 is a plot of the crystallization temperature of as-received and coalesced PCLs for 20, 10, 5, and 1˚C/minute cooling rates. We can see this relationship is non-linear and the crystallization temperatures for the two PCL varieties begin to converge as the cooling rate is reduced. This is not to say, however, that at a zero cooling rate the two materials will crystallize at the same temperature.

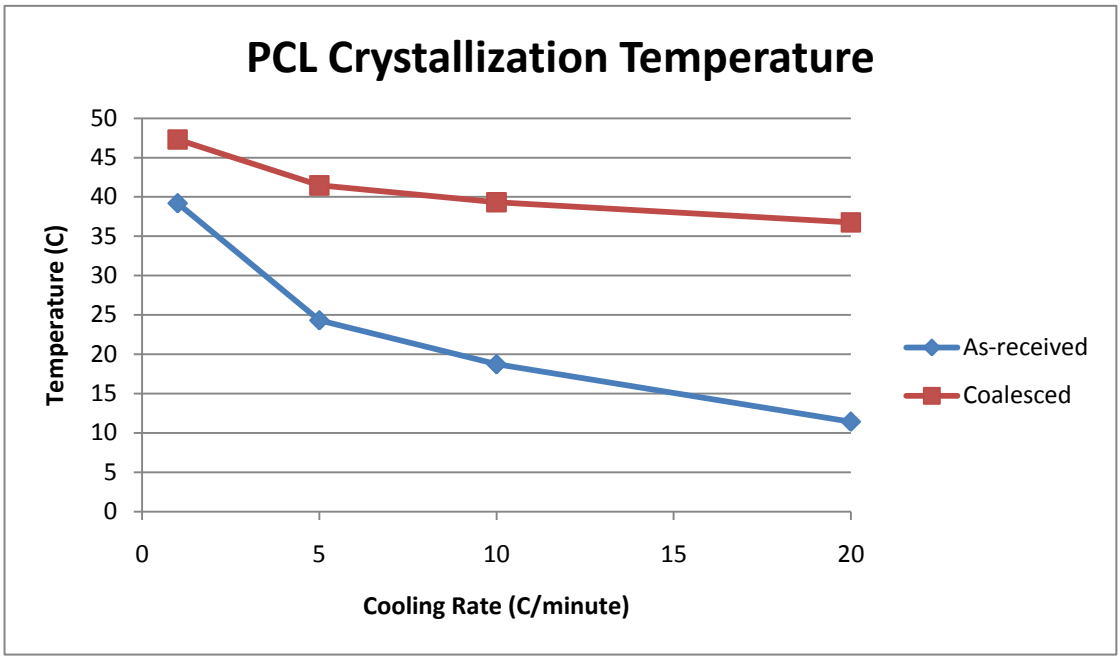

Figure 26: Crystallization temperature as a function of cooling rate for as-received and coalesced PCL

We can also examine the slopes of these two lines and qualitatively, at least, make a determination about the sensitivity of the material to the cooling rate, a behavior

corresponding to how quickly the material can crystallize. We can see that as the cooling rate is increased from 1 to 20˚C per minute, the as-received material's crystallization temperature changes from 39 to 11˚C. The coalesced material's T_c only changes about 10˚C for the same change in cooling rates. This information suggests that the as-received material is less easily able to transition from the more randomly coiled melt structure to the aligned crystalline structure. Considering that the coalesced PCL should theoretically already have extended chain conformations, with little entanglement, this behavior is as expected.

As previously mentioned, Wei et al. examined the crystallization properties of coalesced PCL, finding that the difference in crystallization temperature between the synthesized and coalesced material was only 6˚C.[61] In their work, the synthesized PCL only had a molecular weight of 10kg/mol, possibly causing the coalescence process to have less of an overall effect. The T_c of the coalesced material also showed a higher sensitivity to cooling rate than the synthesized material, the opposite observation from our own. It is likely that the molecular weight difference played some role in creating the varying results. Further study of molecular weight variations and their effects on coalescence behavior should help develop our understanding of what exactly is taking place and in what manner the restricted chains are behaving.

The percent crystallinity in the material for the as-received and coalesced samples is approximately the same. Ong and Price reported the melting enthalpy for 100% crystalline PCL to be 135.56 J/g.[72] Our observed melting enthalpies were 62.8 and 64.0 J/g for as-received and coalesced PCL, respectively (Figure 24). These values correspond to percent crystallinity values of 46.3% for as-received PCL and 47.2% for coalesced PCL.

To examine the stability of the coalesced PCL, the material was annealed at 90˚C for a period of 1 hour and the crystallization temperature reexamined. After this annealing, the T_c (at 20˚C per minute) was 35.3˚ C, representing a very slight drop. To determine if this

slight drop was a trend that would continue with more annealing, the material was then held at 90˚C again, but for 48 hours, well beyond the diffusion time of PCL chains in the molten state. The T_c was then measured to be 35.9˚ C. The annealing process did not change the crystallization temperature of the coalesced PCL, confirming the long-time stability of the material's unique morphology in the melt. This melt stability is likely due to the extremely slow diffusion and entanglement of the tightly packed, coalesced polymer chains, as suggested by Tonelli.[73] For comparison, the as-received PCL was also held for 48 hours at 90˚C to test for any T_c variation. The annealed PCL had a T_c of 14.2˚ C, not significantly changed from the original value of 11.4˚ C.

If we briefly jump ahead and consider potential applications of our material, we realize that production of coalesced PCL on an industrial scale may not be cost effective. However, just like coalesced nylon-6 can effectively nucleate the melt-crystallization of bulk nylon-6,[74] coalesced PCL may act as a great bioabsorbable, chemically compatible nucleating agent for bulk PCL. To demonstrate feasibility of potential PCL nucleation applications of this material, we can examine the DSC thermogram of a bulk PCL sample nucleated with 2.5 wt% of our coalesced PCL. Figure 27 demonstrates the increased crystallization temperature of bulk PCL when nucleated with coalesced PCL, 26.3˚C *vs* 11.4˚C. The enthalpy of melting also increased by 4.2 J/g, suggested a slightly increased overall crystallinity.

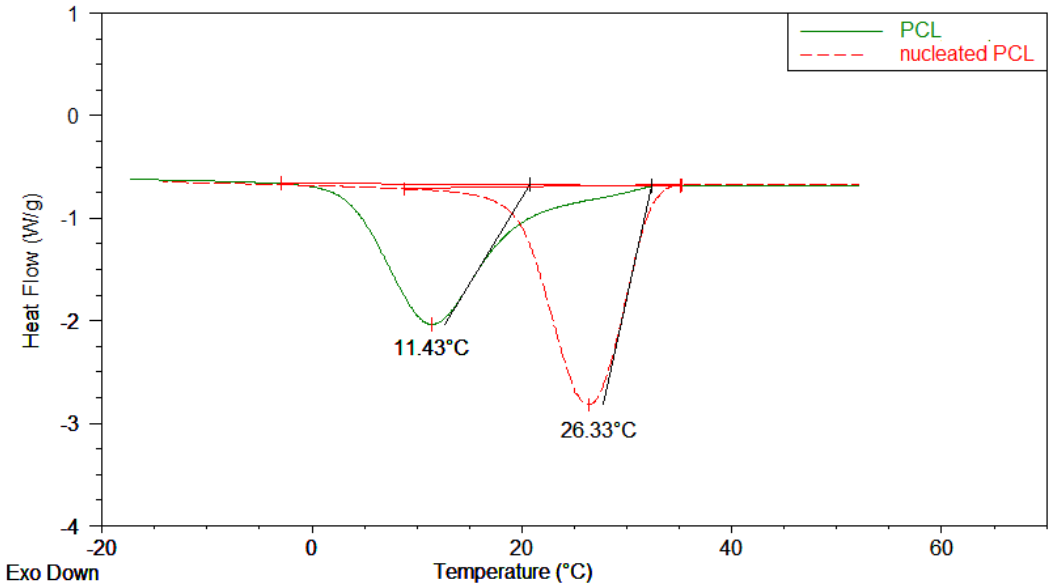

Figure 27: DSC cooling thermograms of as-received PCL nucleated with 2.5 wt% coaled PCL

For comparison, we can also look at a bulk PCL sample nucleated with 2 wt% α-CD. Performing DSC on this sample resulted in a T_c of 28.9˚C and a melting enthalpy of 45.9 J/g, suggesting drastically reduced crystallinity despite a slightly increased crystallization temperature. It is possible that this reduced crystallinity would likely impair our material's physical properties, a phenomenon that would not be of concern when nucleating with coalesced PCL.

DMA

Dynamic Mechanical Analysis allows us to determine the viscoelastic behaviors of solid materials across a wide temperature range as well as the glass transition temperature. When an external force is applied, polymers often react with both an elastic and viscous

response. The elastic and viscous behaviors can be considered as being on opposite ends of a spectrum, with almost all polymeric materials falling somewhere in between the two extremes.

The extent of the elastic behavior is given by a parameter called the storage modulus (G'). A high G' indicates that the material behaves in a more elastic manner, storing the energy applied by the external force, often through the structural limits put in place by crosslinking or molecular restriction. The viscous flow of a material is quantized by a parameter called the loss modulus (G''). A high G'' indicates the energy imparted to a material by external forces is lost through heat and friction cause by molecular flow. The ratio of G''/G' is referred to as tan δ. This term is often used to indicate the relative values of both moduli. A high tan δ is indicative of a material with a large amount of viscous molecular motion/flow.

Below are the plots of G' and G'' for our as-received and coalesced PCL samples. An across the board increase in elastic response (G') is observed for the coalesced material, suggesting the material has increased elastic, reversible responses. This behavior may possibly be tied to the increased density of the unentangled PCL chains in the amorphous regions of the coalesced material (Seen in the Density of Coalesced PCL section). The as-received material has higher G'' in the vicinity of the glass transition temperature (the peak around -50˚C), indicative of a larger amount of viscous molecular motion. From this, we can suggest that the restricted chains of the coalesced material do not have as much irreversible viscous molecular motion in this temperature regime.

Unexpectedly, the loss modulus is actually higher above the Tg for our coalesced material. One possible explanation of this behavior is that the non-crystalline regions of the coalesced PCL do not have the molecular entanglements present in the as-received polymer. Without these entanglements, the polymer chains may move more freely above the T_g, increasing the G''.

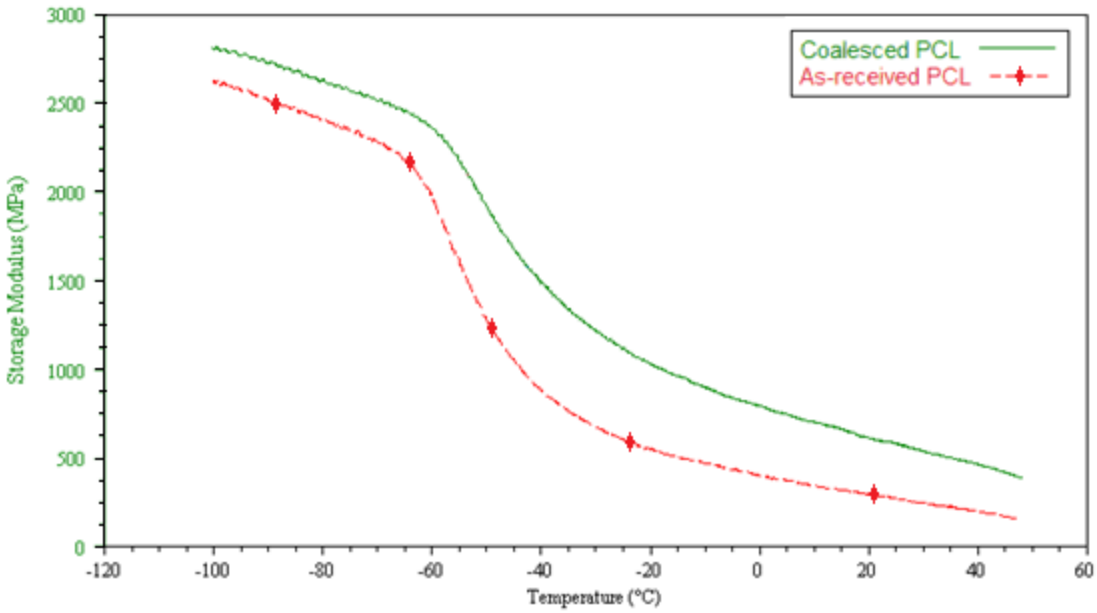

Figure 28: Storage Modulus (G') of as-received and coalesced PCL

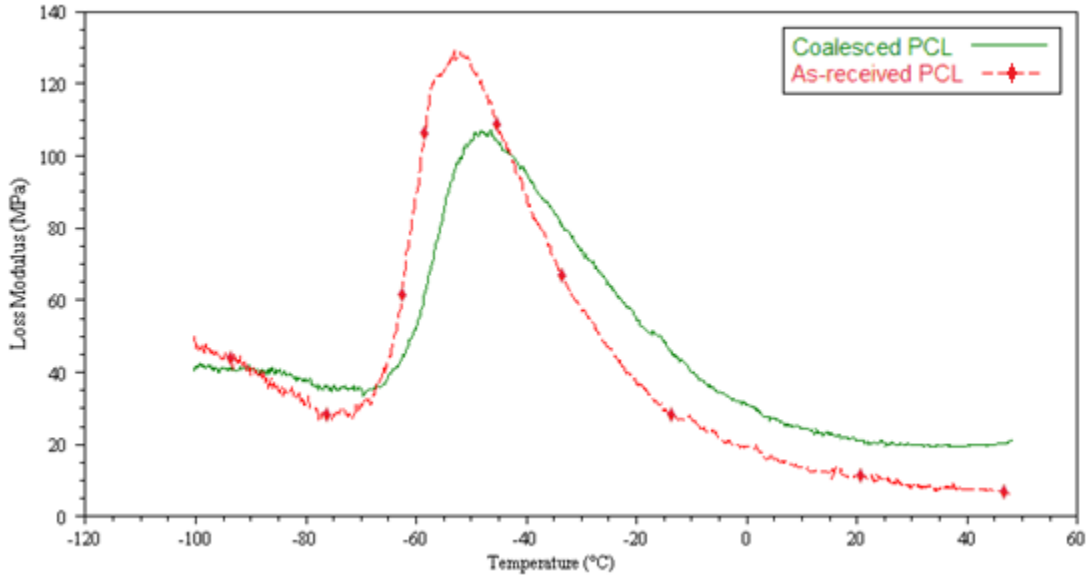

Figure 29: Loss modulus (G'') of as-received and coalesced PCL

The glass transition temperature of a material can be determined by the location of the drop off in storage modulus. In Figure 28, the drop off for both materials is clearly observed, and a quick software analysis to determine the inflection point (not shown) allows us to determine that the T_g's for the as-received and coalesced material are -56.8˚C and -50.9˚C, respectively. With a restricted chain conformation, the glass transition temperature would likely increase, so this behavior is as expected. The slight increase in Tg can be observed in the shifting of the loss modulus peak as well.

If we take a look at a plot of the tan δ (Figure 30), the change in the "lossy" behavior resulting from the coalescence process can be readily observed. Below room temperature, the as-received PCL acts as a more viscous material than the coalesced PCL, with the largest difference present in the vicinity of the glass transition temperature. Above room temperature, the coalesced PCL seems to display increased loss properties. It is possible that this behavior could also be explained by a lack of molecular entanglement. While the elongated chains of the coalesced material are generally more restricted at temperatures well below the melting point, it is possible that molecular entanglement helps to keep the loss modulus of the as-received material lower at temperatures closer to the melting point.

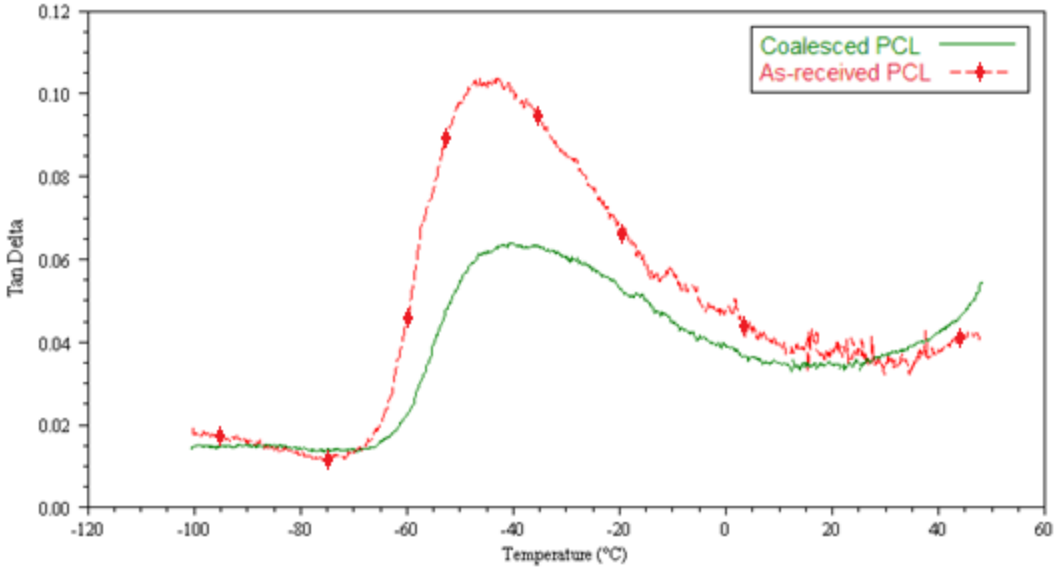

Figure 30: Tanδ as a function of temperature for as-received and coalesced PCL

No previous studies of the mechanical/rheological properties of a completely coalesced PCL have been published; however, Dong et al. have performed studies of bulk PCL nucleated with (n-s) PCL-α-CD-ICs.[69] The most interesting observation in this work is the tan δ behavior of the nucleated material. A higher tan δ measured above T_g for their materials indicated an increase in the G'' (not shown). This behavior is similar to the unexpected observations for our coalesced material.

Perhaps, then, the simple expectation that coalescence or nucleation of a polymer sample simply results in higher reversible elastic properties and reduced viscous flow may not actually be correct. Dong et al. demonstrated that Young's modulus and the yield stress of nucleated PCL increase while the elongation at break decreases. Our coalesced PCL results indicate that we would be able to observe a similar increase in tensile properties if we had enough coalesced PCL and were able to perform tensile property testing.

Luo et al. also performed DMA on a (n-s) PCL-α-CD-IC that they were able to press into a film. Like our coalesced material and the nucleated PCL, an increase in storage modulus was observed. However, no information about the loss modulus was given.

Nanoindentation

Nanoscale indentation is a relatively easy test requiring little material that can at least give us an indication of the physical property changes resulting from our coalescence procedure. It is worth noting up front that nanoindentation is actually a micro-scale test method that performs indents approximately 18µm wide and just under 1µm deep. The depth of the indention is worth noting here. This sub-micrometer scale (thus the terminology nanoindentation) really only allows us to examine the properties near the surfaces of our material, not the entire cross-section like traditional tensile testing. Theoretically, the material properties should be roughly the same, but to be accurate, we need to be aware that we are actually measuring close-to-surface properties.

With that said, we can begin by looking at a sample indent provided in the nanoindenter user manual. Figure 31 is a plot of force as a function of displacement for the indenter tip as presented inside the software's data analysis panel. This plot shows the loading and unloading of the tip from the material. Figure 32 is a topographical scan of our as-received PCL sample surface after indention has taken place. The purpose of this scan is to provide an idea of the size scale of a typical indent. This indent, produced by a 2000 µN force, is approximately 12µm across the center and just under 1µm deep.

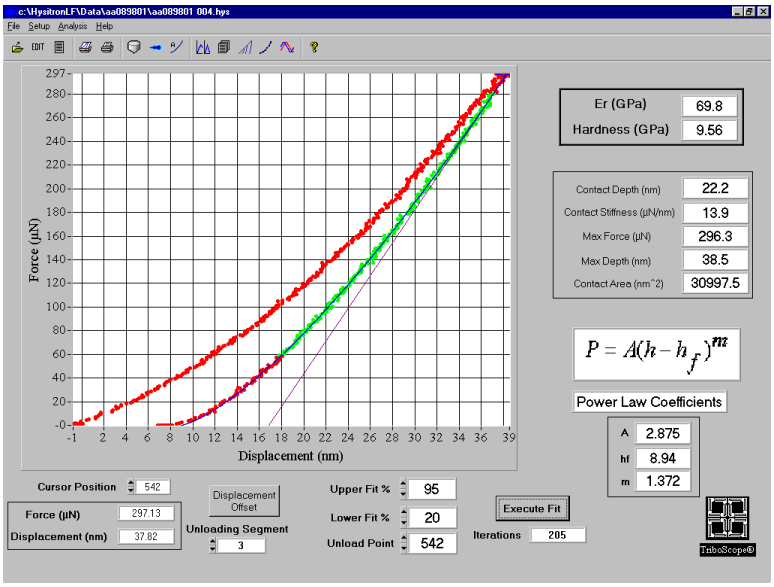

Figure 31: Example of a nanoindentation loading and unloading curve

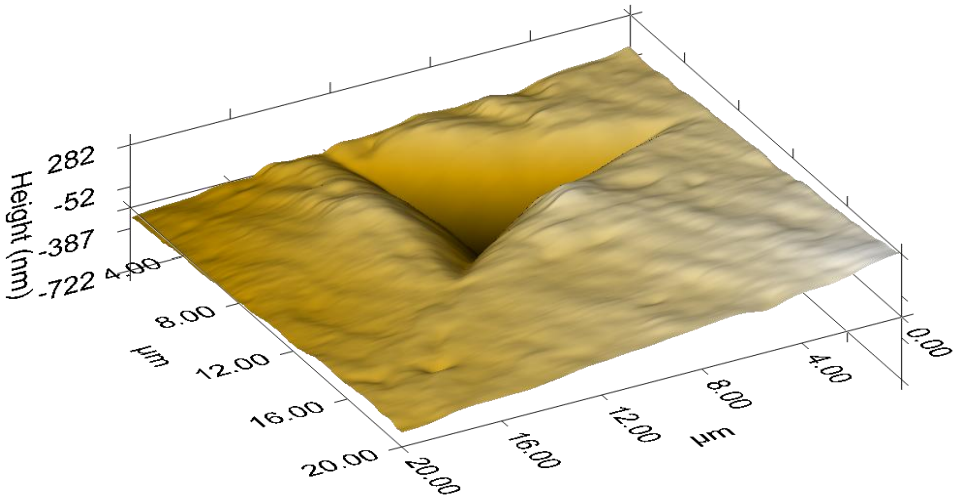

Figure 32: Topographical scan of the as-received PCL sample surface post-indent

The reduced Young's modulus (E_r) and hardness are calculated automatically by the software; however, to understand where these values come from, we can outline the method by which the software determines these values. The chosen portion of the unloading curve (green section in Figure 31) is fit to the Power law where P is the loading force, h is the displacement, and A is the area function:

$$P = A\left(h - h_f\right)^2$$

The derivative with respect to depth (h) (also the slope of the curve) is used to arrive at the material stiffness (S). The contact depth (h_c) is then calculated as:

$$h_c = h_{max} - \ 0.75\frac{P_{max}}{S}$$

The hardness (H) is then calculated as:

$$H = \frac{P_{max}}{A(h_c)}$$

The reduced Young's modulus (E_r) is calculated from the following equation using the predetermined area function ($A(h_c)$) for the current tip:

$$E_r = \frac{\sqrt{\pi}}{2\sqrt{A(h_c)}} S$$

Using the above set of equations, the software can automatically be set to determine the hardness values and Young's modulus values for each individual indentation.

Because this particular method is so small-scale, it is fairly susceptible to defects in the sample such as cracks or bubbles. To allow for the accurate determination of physical properties, a 3x3 test pattern was set up and nine separate indentations were taken approximately 15 µm from any adjacent test. This test pattern was also performed at four different max force inputs, 500, 1000, 1500, and 2000 µN. Theoretically, the max force input (which changes the depth of the indentation) should not change the calculated values, but by performing the tests across a range of forces, any depth related trends can be observed.

The reported modulus and hardness values were then averaged and any errant data points were removed based upon the application of one round of Dixon's Q-test to a confidence of 95%, though most errant data points were easily distinguishable. Only a very small number of obviously errant data points were removed.

Figure 33 is a plot of average hardness for both the as-received and coalesced PCLs as a function of testing force. Vertical error bars indicate the standard deviation of the multiple valid values obtained. Hardness values for the as-received PCL ranged from approximately 32.5 to 37 MPa, while hardness values for the coalesced PCL range from approximately 43 to 51 MPa. On average, a hardness increase of 33% is observed as a result of the coalescence process. It is important to note here that the DSC data suggested that both the as-received and coalesced PCL had approximately the same crystallinity. Because of this, we

are able to determine that any increase in the sample hardness is not due to any increase in overall material crystallinity.

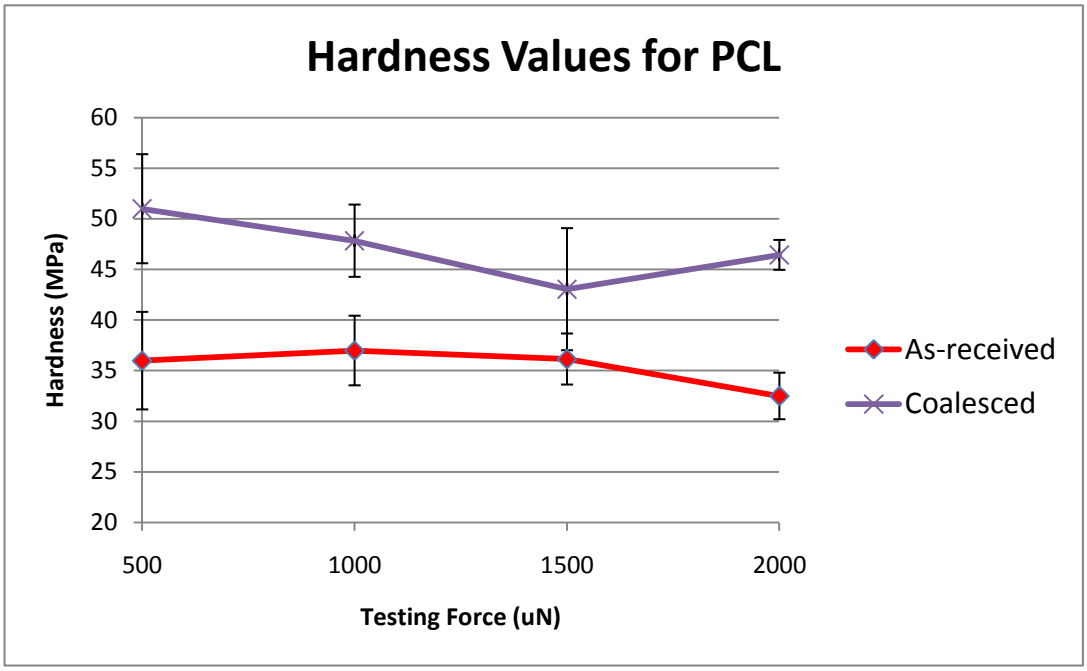

Figure 33: Hardness as a function of force for as-received and coalesced PCL

Figure 34 is a plot of the Young's modulus as a function of testing force for our materials. Again, vertical error bars indicate the standard deviation for each point's data set. The as-received PCL shows Young's modulus values ranging from 0.44 GPa to 0.5 GPa. We can see that as we increase the testing force (thus going deeper in the material), the measured Young's modulus begins to approach the values for PCL determined by traditional tensile testing (values reported on page 37). The coalesced material has values ranging from 0.68 GPa to 0.77 GPa. Overall, we observe an average increase in the Young's modulus of 53%, an even more significant increase than observed in the hardness measurement.

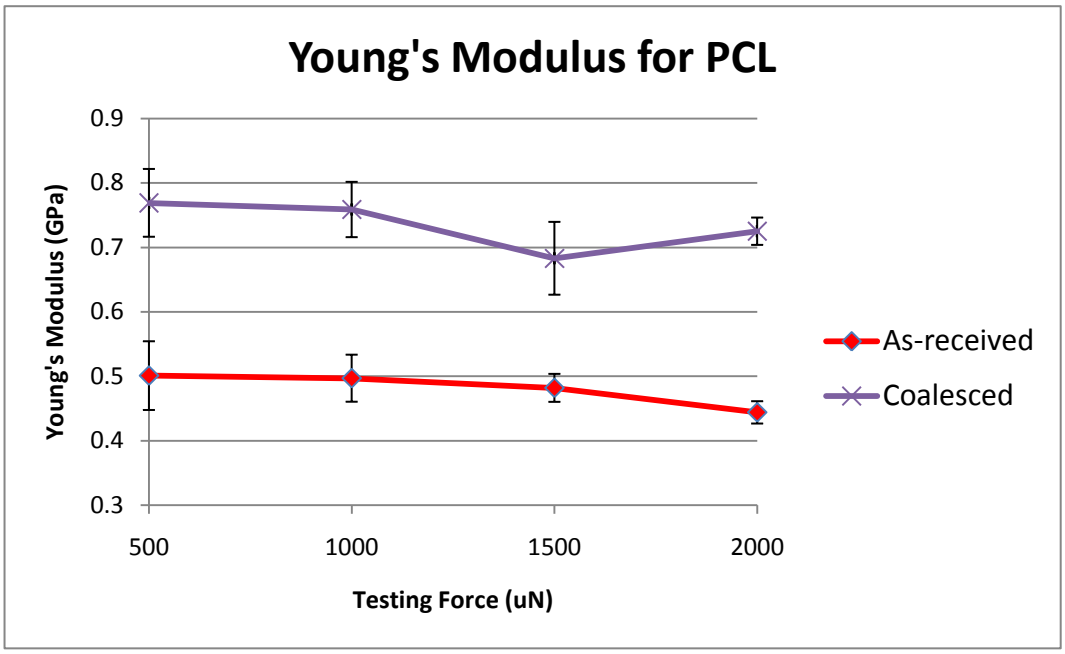

Figure 34: Young's modulus as a function of force for as-received and coalesced PCL

While nanoindentation only realistically allows for close-to-surface measurements of the hardness and Young's modulus, it seems reasonable that we could extend these observed property changes to the bulk material as well. While we do not currently have enough sample to produce a standard-size tensile testing bar for comparison, it would be interesting to eventually scale up our IC formation and coalescence process even further to be able to test these properties at the larger scale. Would the bulk properties display such a large increase? How would other mechanical properties be affected by the coalescence process? These are all questions that remain to be answered.

Melt Rheology of Coalesced PCL

Melt rheology experiments were performed on as-received and coalesced PCLs. Melt rheology allows us to examine the differences in the behavior of the two materials above the melting temperature. Stress sweeps were performed prior to the oscillatory tests to confirm that our tests were in the linear viscoelastic regime (LVR). This allows for slight variations in the testing stress (a testing constant) without any significant change of the measured values. Testing in the LVR allows for direct comparison between multiple samples, even though the testing stresses may be different.

If the coalesced polymer chains were to stay in an elongated, unentangled conformation above the melt temperature, we would expect to observe stark differences in the melt rheology of the material. An immediate difference became apparent when the coalesced material did not obtain the same melt-like behavior after the 1 minute hold time. During testing of our coalesced material at 1 minute hold time, the parallel plates did not obtain a good grip on the material (more suggestive of solid-like behavior), instead slipping at frequencies of 1 Hz and higher. This rendered testing at that hold time invalid. Holding the material for 30 minutes at the testing temperature prior to testing provided much more meaningful data. Holding the material for longer demonstrated no difference in melt rheology behavior.

Figure 35 is the graph of the storage and loss modulus and the apparent viscosity (G', G'', and n*, respectively) as a function of frequency obtained by oscillatory melt rheology testing for as-received PCL. Figure 36 is the same graph but for our coalesced PCL sample. The most obvious and noteworthy difference between the two materials is the reduction of apparent viscosity by two orders of magnitude for the coalesced PCL sample. A viscosity reduction such as this could normally be explained by a reduction in molecular weight between the two samples; however, we have shown through viscometer flow times that

the molecular weight has likely not changed as a result of the coalescence procedure. The other possible interpretation of the data is that the polymer chains in the coalesced PCL are unentangled and, therefore, able to slide easily past one another. This behavior would lead to the observed drastic viscosity reduction and supports the theory that we have elongated, unentangled polymer chains in our coalesced PCL sample.

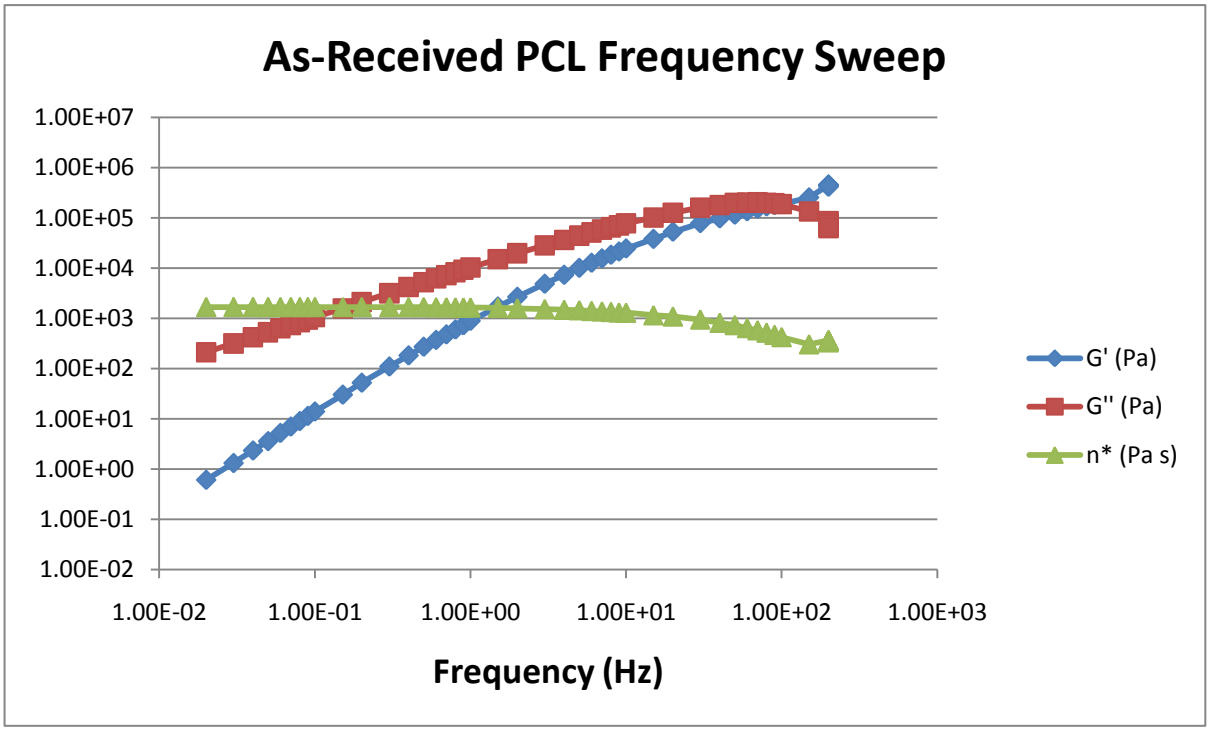

Figure 35: Storage modulus, loss modulus, and apparent viscosity (G', G'', and n*, respectively) for as-received PCL as obtained through oscillatory melt rheology (testing stress = 750 Pa; pre-test hold time = 1 minute)

While Figure 35 is a typical rheology plot of a high molecular weight, entangled polymer melt[75], Figure 36 is somewhat different. The relatively low frequencies used in our tests were well into the terminal zone, the region where the polymer chain rearrangement

becomes possible in the oscillatory period. Generally, polymers with molecular weights lower than the critical entanglement molecular weight undergo a direct transition to glassy behavior as frequency increases, while entangled polymers often demonstrate a rubbery plateau before arriving at the glassy state. It is possible that with further melt rheology testing at higher frequencies, we would be able to observe the presence or absence of a plateau region in our coalesced samples, offering further information regarding individual chain morphology and entanglement.

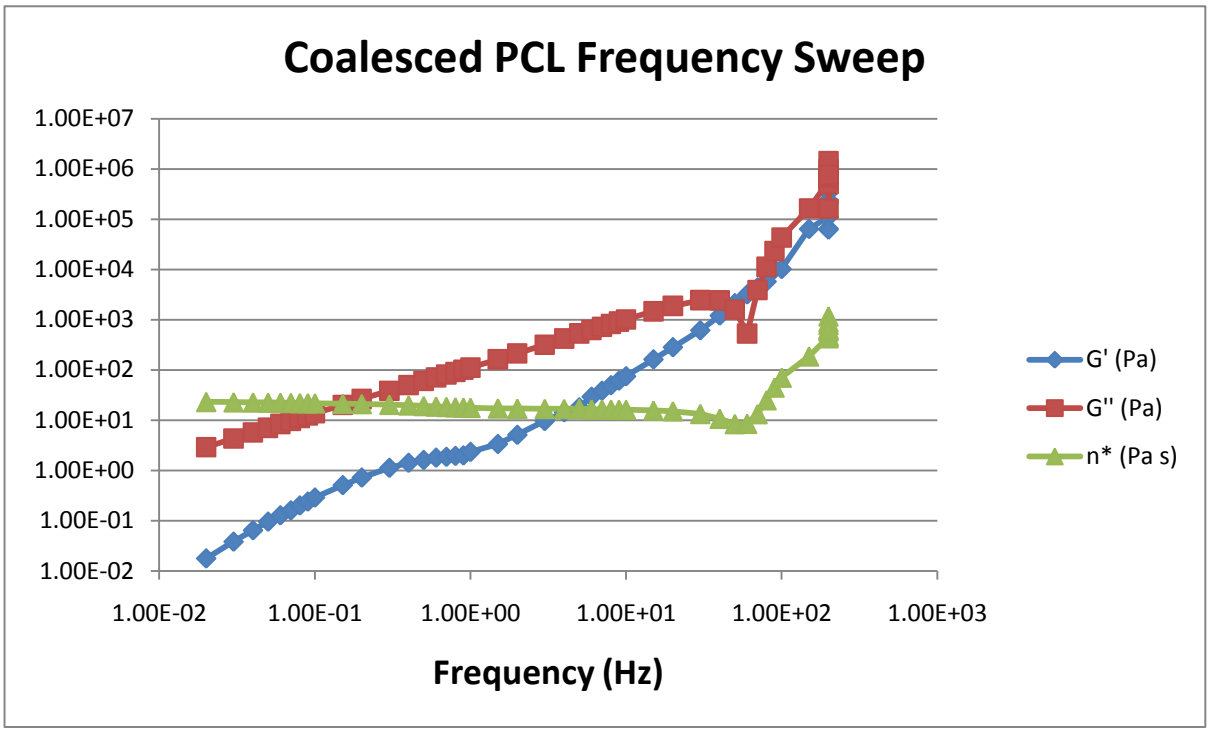

Figure 36: Storage modulus, loss modulus, and apparent viscosity (G', G'', and n*, respectively) for coalesced PCL as obtained through oscillatory melt rheology (testing stress = 300 Pa; pre-test hold time = 30 minute)

Density of Coalesced PCL

Bittiger and Marchessault reported that the PCL crystal structure had a density of 1.17 g/cm^3.[76] We know that our PCL samples, containing ~50% crystallinity, should have a density less than the value for the pure crystal. We measured the density of the as-received and coalesced PCL samples by floatation using a combination of deionized water and an aqueous NaBr solution of measured density 1.184 g/ml. The high density salt solution was added to the deionized water containing both PCL samples until the density of the each sample matched the density of the aqueous salt solution and the samples reached neutral buoyancy.

The measured density of the as-received PCL was 1.137 g/cm^3. The measured density for the coalesced PCL was 1.152 g/cm^3, 1.3% higher than the as-received sample. Knowing the crystallinity of each sample, we can use the equation below to calculate the density of the non-crystalline regions in each sample (ρ and X represent density and fractional crystalline content, respectively; subscripts c and nc represents the crystalline and non-crystalline components, respectively).

$$(\rho_c \times X_c) + (\rho_{nc} \times X_{nc}) = \rho_{sample}$$

Using this equation, we can determine our the as-received and coalesced non-crystalline densities to be 1.11 g/cm^3 and 1.136 g/cm^3, respectively, an increase of 2.4%. Similar density measurements were performed on a solvent-coalesced PET and an increase in amorphous chain packing and orientation were tied to the increased observed density.[77] Similar behavior is mirrored in our coalesced PCL.

Conclusions

Our mechanical and rheological measurements demonstrate that by processing a polymer with cyclodextrin, we are able to significantly change its solid-state organization and resulting physical properties. PCL coalesced from its α-CD-IC, while chemically equivalent to as-received PCL, has drastically different properties, only reinforcing the importance of the role of polymer chain morphology when determining the performance of a polymer.

We were able to scale up the PCL IC formation process approximately 10-fold in order to obtain enough coalesced PCL to perform rheological measurements. A survey of different coalescence techniques demonstrated that common literature techniques, such as hot water washing or enzyme washing, removed a majority of the CD, but not enough to meet our particular needs. We observed that washing our IC with stock concentrated HCl for a short time was an appropriate method to achieve nearly complete coalescence of PCL and we were able to obtain enough sample to perform our measurements.

Upon coalescence, increases in melt crystallization temperatures of up to 25˚ C were observed, depending on the cooling rate. This change, most likely resulting from the change in polymer chain morphology, proved to be stable even after annealing above the melting temperature for long periods of time. Below the melting temperature, an increase in the elastic modulus was observed, as well as unique changes in the loss modulus similar to the effects of nucleating bulk PCL. It was also determined that the glass transition temperature increased by roughly 6˚C. In the melt, coalesced PCL exhibited an apparent viscosity two orders of magnitude lower than as-received PCL. Through nanoindentation, we were also able to observe a 33% increase in the hardness of the material as well as a 53% increase in the Young's modulus. Additionally, though the extent of crystallinity did not change, the coalescence process seemed to increase the density of the material by roughly 1.3% overall,

likely a result of the alignment and closer packing of polymer chains in the non-crystalline regions.

These observations are just part of the story necessary to understand how coalesced polymers behave and what potential applications exist for these materials. Suggestions for further exploration and some possible applications for coalesced PCL can be found in the following section.

Suggestions for Future Work

Opportunities for future work geared toward understanding the properties and behaviors of coalesced PCL are many. One of the more immediate and interesting studies would be to examine more thoroughly the rheological behavior of as-received and coalesced PCL melts. These studies may be able to shed light on the structure of coalesced PCL above the melting temperature, which seems to remain constant even after long periods of annealing.

If the process could be scaled up even further, it should be possible to arrive at enough sample that tensile property testing could be performed to arrive at an idea of how all of the bulk mechanical properties change. While we know from nanoindentation that the bulk Young's modulus likely changes, it would be interesting to observe the elongation at yield and yield modulus values and see if they also behave in a similar fashion to PCL nucleated with (n-s) PCL-α-CD-ICs.

The other potential avenue for research is tied directly into the potential applications for this material. While much work has been done to examine the nucleation effects of (n-s) PCL-α-CD-IC's on bulk PCL, no studies have yet been published on the nucleating effects of the coalesced polymer. It is possible that the nucleating effects would be similar; however it is reasonable to expect better dispersion of the coalesced PCL within the bulk, because

there are no α-CD crystals tying the polymer chains together. All these are potential routes of study, leading to a better understanding of coalesced PCL and possible further improved understanding of the behavior of polymers processed with cyclodextrins.

Potential Applications

A promising potential application for coalesced PCL is as nucleating agents for bulk PCL. It has been previously shown that (n-s) PCL-α-CD-ICs make acceptable nucleating agents for bulk PCL[70,71] and the same has been observed for(n-s) nylon-6-CD-IC nucleation of bulk nylon-6.[74] Coalesced PCL should have similar biodegradability and bioabsorbability and be able to act as a nucleating agent in any role where PCL is an acceptable material. Figure 37 is a general schematic of how coalesced PCL could act as a nucleating agent for bulk PCL. It is conceivable that the coalesced material may act as a better nucleating agent, leading to better physical properties and the potential for stronger PCL sutures, scaffolding, and possibly the development of load-bearing PCL implants.

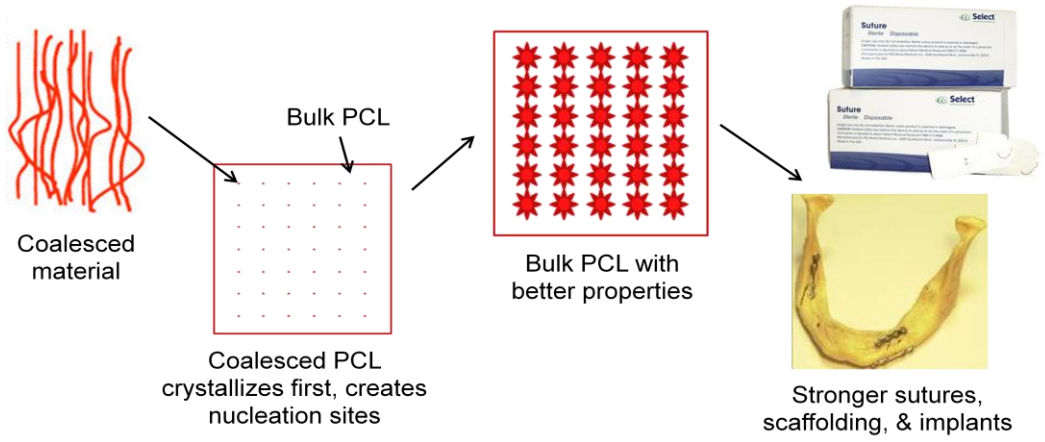

Figure 37: Schematic of coalesced PCL nucleation of bulk PCL and potential applications

Chapter 3: Constrained Polymer Chain Behavior in Non-Stoichiometric Inclusion Complexes

Abstract

Much has been learned by examining polymer properties after CD removal or by studying the physical properties of fully covered polymer IC's, but what scientific knowledge do we stand to gain from the studying the properties of restrained "dangling" polymer chains that remain when we form partially covered, "non-stoichiometric" IC's (NS-IC's)?

Non-stoichiometric IC's (NS-IC's), or IC's with at least part of the polymer chain uncovered, were formed between atactic poly(methyl methacrylate) (PMMA) and γ-CD, as well as a synthesized poly(ε-caprolactone)-poly(propylene glycol)- poly(ε-caprolactone) (PCL-PPG-PCL) triblock copolymer and β-CD. The property changes of the non-complexed polymer chain portions were then studied. The PMMA/γ-CD NS-IC samples were determined to be extremely heterogeneous by nature. However, glass transition temperature increases of up to 27˚ C were observed. X-ray diffraction data for the PMMA NS-IC's suggest slight crystallinity at partial coverage, with a similar crystal structure to that of the fully covered stoichiometric PMMA/γ-CD-IC. XRD, DSC and FTIR data revealed an almost total disruption of the PCL crystallinity upon PCL-PPG-PCL complexation, suggesting possible coverage of the PCL blocks by β-CD, or some compatibilization and mixing of PEG and β-CD threaded PPG blocks.

Introduction

Much has been learned by examining polymer properties after CD removal or by studying the physical properties of fully covered polymer IC's, but what scientific knowledge do we stand to gain from observing the properties of the restrained "dangling" polymers that remain when we form partially covered, "non-stoichiometric" IC's (NS-IC's)?

Non-stoichiometric IC's are inclusion complexes that contain a CD:polymer repeat unit ratio lower than that necessary to completely cover the polymer. The theory behind these materials is that the free polymer chains dangling out of the channel CD structure are restricted and closely packed, similar to a polymer brush. Constrained polymer chains like these are likely to display significant property differences.

Recent work in our group by Anushree Mohan has shown that NS-IC's of nylon-6 result in increased physical properties of the dangling polymer segments such as increased melt crystallization temperatures. This behavior allows Nnylon-6 NS-IC's to act as efficient nucleating agents for bulk Nylon samples.[74] As mentioned in the coalesced PCL chapter, Luo et al. also reported that a PCL NS-IC of roughly 30% coverage demonstrated significantly increased physical properties compared to the as-received PCL.[63]

The current view is that the partially covered chains in an NS-IC are included in more than one CD crystal. The uncovered chain length (and subsequently, the measured properties) should vary depending on many factors, including coverage stoichiometry, polymer crystallinity, molecular weight, and degree of CD aggregation. In this work, we attempt to form NS-IC's of different stoichiometric ratios with atactic poly (methyl methacrylate) (PMMA) and γ-CD and study the property changes in the uncovered polymer chains. In an attempt to control the location of the CD molecules on the polymer chains, a PCL-PPG-PCL triblock copolymer was also synthesized. An IC was formed with β-CD, in anticipation that

the host β-CDs would thread over and include only the guest PPG blocks. The change in behavior of the PCL chains upon IC formation was studied. In performing this research, we may be able to further our scientific understanding of the behavior of polymer chains in physically constrained environments.

Materials & Methods

PMMA (M_w=15,000 g/mol), PPG (M_w=3,000 g/mol), and ε-caprolactone were obtained from Sigma-Aldrich.

PCL-PPG-PCL Triblock Copolymer Synthesis

Polymerization of the PCL-PPG-PCL was based on the technique Shuai used to produce a similar polymer.[78] 1.0 g of PPG (M_w = 3,000 g/mol, dried in vacuum oven overnight), 3.0 g of ε-caprolactone (twice distilled and dried with CaH_2), and 16 mg of Tin(II) 2-ethylhexanoate (SnOct2) were placed in a vial together, capped with dry argon, and heated at 110°C for 3 days. The sample was dissolved in dichloromethane and then precipitated out in cold methanol. The precipitate was filtered and dried. 2.08 g were collected, a yield of 52%.

Proton NMR of the triblock copolymer suggested that the PCL:PPG repeat unit ratio was 1.79:1. Knowing that our center block consists of 3,000g/mol PPG (approximately 52 repeat units) and assuming even PCl polymerization from both ends of each PPG block, we can suggest that our PCL end-blocks are approximately 46 repeat units long (or ~ 4,700 g/mol).

IC Formation Technique

For a majority of the PMMA NS-IC's and fully covered IC samples, a method similar to that of Uyar and Tonelli's has been implemented.[46] PMMA (varying molar amounts) was dissolved in 50 ml dioxane and stirred in an oil bath at 50˚ C. An appropriate amount of γ-CD (depending on the stoichiometric ratio of the sample) was dissolved in 5ml of deionized water and then added drop wise to the polymer solution. Upon addition of the γ-CD solution to the dioxane (a non-solvent), a white precipitate was formed. Presumably, this precipitate was mostly γ-CD, but a PMMA/γ-CD IC is believed to form over time. The samples were stirred in the heated oil bath for 1 hour then allowed to cool for three days while stirring. The samples were then filtered through Watman #6 cellulose filters and dried at elevated temperature in a vacuum oven to remove any excess solvent. Some inconclusive experiments on the formation of PMMA/γ-CD NS-IC's in both solid state and solution can be found in the Appendix.

To form the PCL-PPG-PCL/β-CD IC, 0.251 g of the synthesized triblock was dissolved in 25ml of dichloromethane. 0.87 g of β-CD was dissolved in 4ml DMSO and added dropwise to the polymer solution. The sample was sonicated for 10 minutes and allowed to stir for 3 days at room temperature. Material was filtered and dried overnight under vacuum. Unfortunately, the sample weight was not recorded, leaving us unable to provide the yield.

It is important to note that any coverage values provided are the starting stoichiometric ratios, not the measured coverage values. While a sample may be labeled as an 80% NS-IC, the true coverage values are likely less than 80% as it is unlikely that all cyclodextrins thread onto the polymer.

PMMA and PCL-PPG-PCL Copolymer NS-IC Analysis

X-Ray Diffraction

X-ray diffraction of various PMMA NS-IC samples as well as as-received PMMA and a precipitated γ-CD were collected. Figure 38 presents their stacked diffractograms. We can see that the PMMA in its as-received form is completely amorphous. The 60 and 80% NS-IC samples begin to show some channel crystalline characteristics, though the structure is largely ill-defined. As we increase the coverage ratio to 100%, there is a large increase in long range crystalline order as demonstrated by the well-defined diffraction peaks that are characteristic of the channel γ-CD structure.

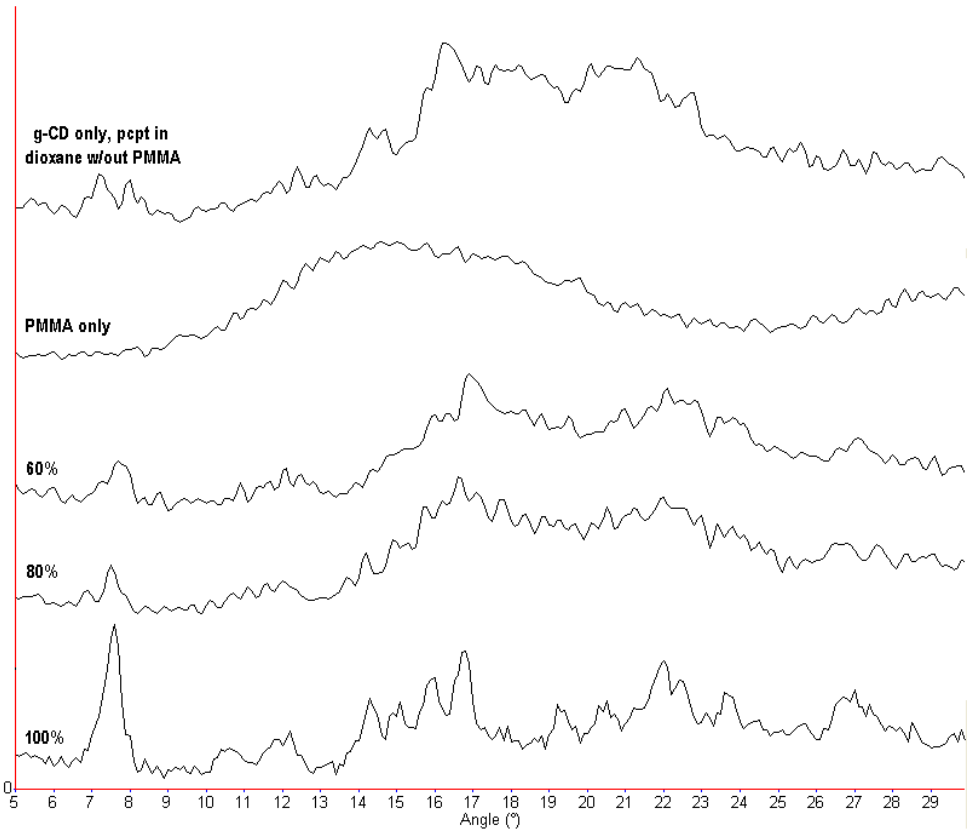

Figure 38: XRD patterns of precipitated γ-CD, as-received PMMA, and PMMA/γ-CD IC's containing 60, 80, and 100% stoichiometric coverage ratios

From this data, we can conclude that, at least for PMMA, a large degree of long range crystalline order does not develop until the CD coverage approaches 100%. The work of Zhao and Beckham on α-CD and poly(oxyethylene) (POE) supports this observation.[79] They observed that increasing molecular weight in POE results in a reduced maximum CD coverage and a smaller number of repeating CD's along the chain. This behavior may also be mirrored for other polymer NS-IC's.

DSC Analysis

DSC analysis of the PMMA NS-IC samples revealed a perplexing combination of behaviors that suggests restricted chain conformations may be present in at least one of our samples. Figure 39 shows the DSC results of a 100% PMMA/γ-CD IC, two PMMA NS-IC's (80% and 60%), and as-received PMMA. Initially, the 80% coverage sample demonstrated a very uniform and increased T_g at 102 C, an increase of 20˚. However, another DSC sample taken from the same IC batch demonstrated two separate T_g's, as seen in Figure 39. Additionally, it can be observed that the 60% covered IC sample has no glass transition, even though there is presumably a higher percentage of uncovered polymer. This behavior strongly suggests that after the filtration and washing of the IC, the samples themselves are extremely heterogeneous. Some additional observations of the heterogeneity of the PMMA NS-IC's can be found in the Appendix.

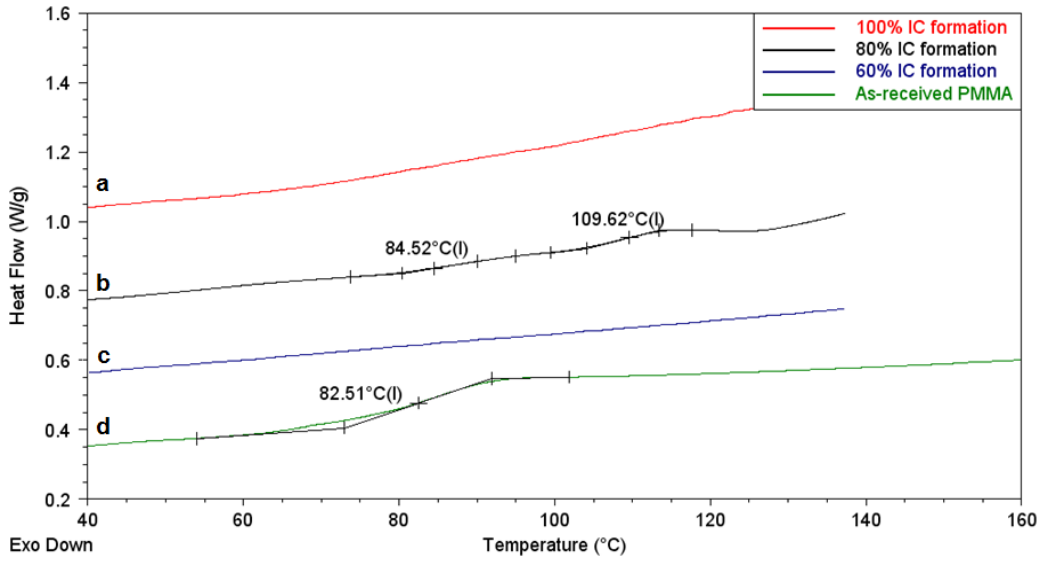

Figure 39: DSC scans of PMMA IC's with CD coverage of 100% (a), 80% (b), and 60% (c), and as-received PMMA (d)

To perform any further study of chain behavior in homopolymer NS-IC's, it would be helpful to control where on the polymer chain the IC is located. While a PMMA NS-IC could theoretically have any part of the polymer chain located in a channel CD crystal, a triblock copolymer with a compatible center block and incompatible outer blocks would make a great candidate for a location-controlled NS-IC.

A PCL-PPG-PCL triblock copolymer was synthesized from a hydroxyl-terminated 3,000 g/mol PPG and ε-caprolactone. An IC was then formed with this material and β-CD under the assumption that all the β-CD would reside on the PPG center block (synthesis and IC formation methods described in Materials & Methods section). If the IC formed was as expected, we would have created an NS-IC with well-controlled CD placement. Figure 40 and Figure 41 present DSC observations of the original triblock copolymer and the β-CD-IC formed with this material, respectively. For the as-synthesized copolymer, we can observe a single T_g at -64˚C. Low molecular weight PPG has a T_g of approximately -73˚C while PCL has a T_g of approximately -56˚. It is likely that the observed T_g is that of the PPG and the high % crystallinity of PCL precludes observation of a PCL glass transition.

Upon complexation, the T_g values undergo drastic changes and the crystallization of the PCL almost disappears. The single observed T_g now becomes two transitions, one at -68˚C and the other at -31˚C. If the β-CD were to have only covered the PPG portion, it seems likely that we would no longer see a T_g for the PPG and crystallization of the PCL would still be present. Based on the observations below, it seems likely that the β-CD has in some way mixed with or included the PCL blocks enough to eliminate any chain crystallization, resulting in a PPG T_g of -68˚C. The T_g present at -31˚C is likely the PCL glass transition, now visible due to the higher amorphous PCL content.

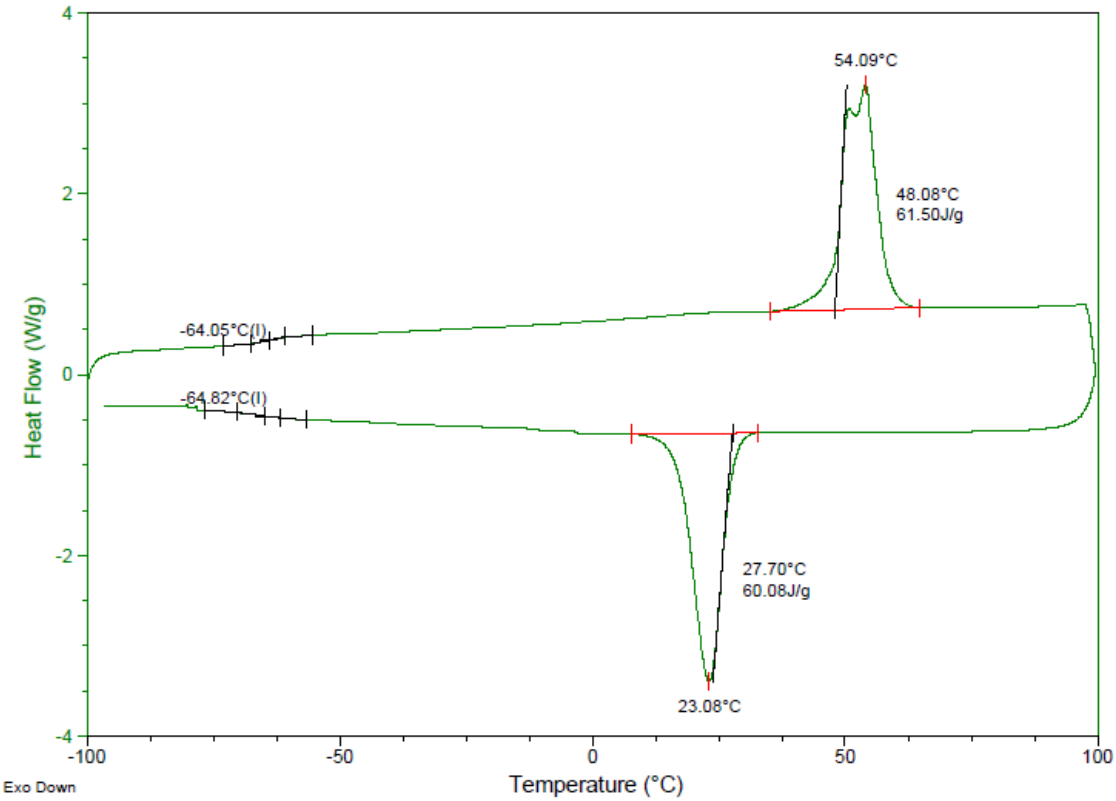

Figure 40: DSC heating and cooling cycle of a PCL-PPG-PCL triblock copolymer

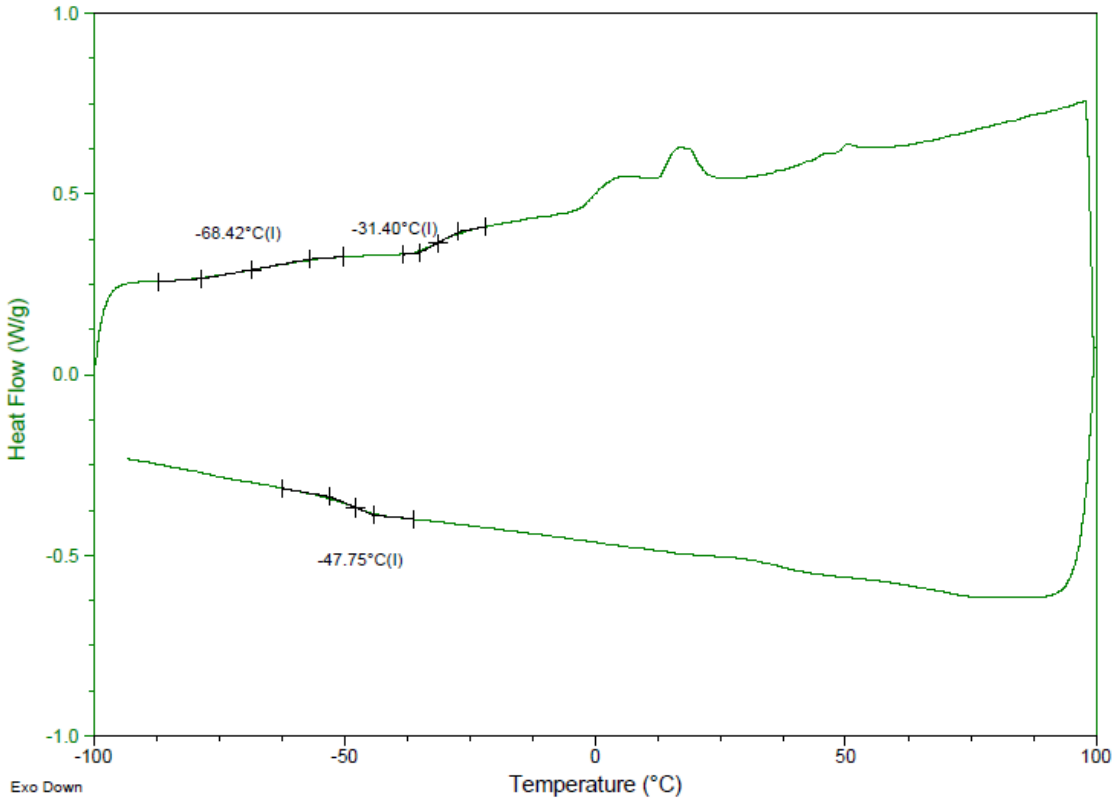

Figure 41: DSC heating and cooling cycle of a PCL-PPG-PCL/β-CD IC

FTIR Observations

Shuai's studies of PCL-PPG-PCL block copolymers also contained some FTIR analysis of the PCL carbonyl peak. It was observed that a carbonyl peak at 1726 cm^{-1} corresponded to that of crystalline PCL, while a slightly shifted peak at 1736 cm^{-1} corresponded to the carbonyl of amorphous PCL.[78]

Figure 42 is the FTIR spectra of both the as-synthesized PCL-PPG-PCL triblock and "subtracted" spectrum of the IC formed between this material and β-CD. The "subtracted"

spectrum was created by subtracting the FTIR data of as-received β-CD from the PCL-PPG-PCL IC spectrum in an attempt to accentuate the PCL carbonyl peak. Both spectra are expansions of the 1650 to 1800 cm^{-1} region.

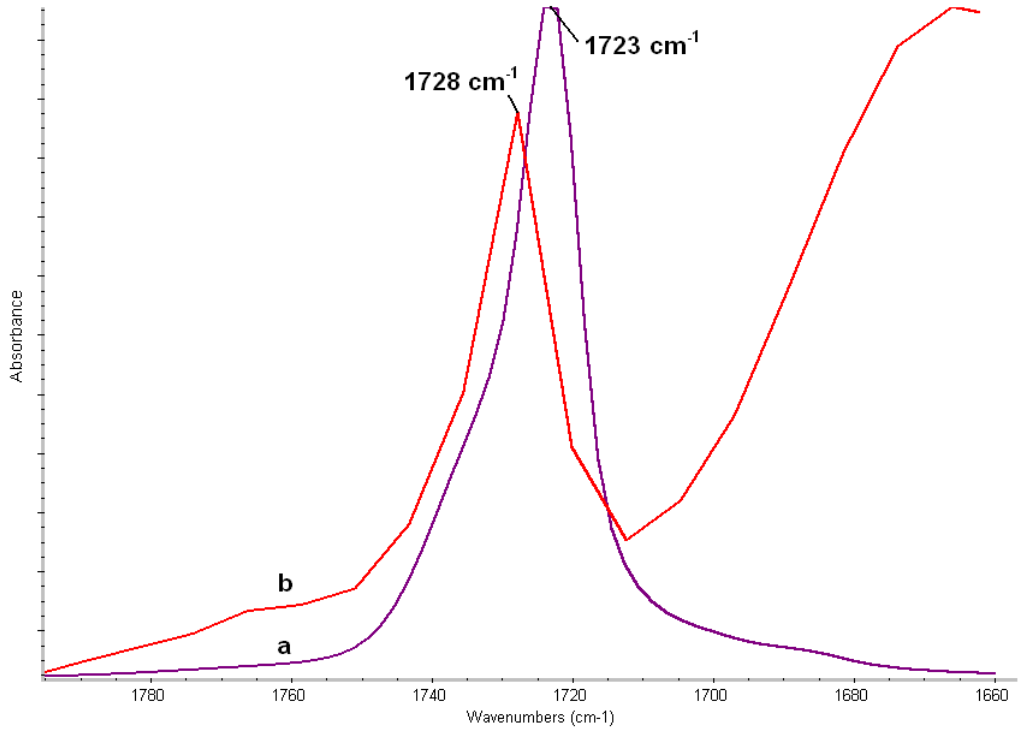

Figure 42: FTIR Spectra (PCL carbonyl region) of as-synthesized PCL-PPG-PCL triblock copolymer (a) and PCL-PPG-PCL/β-CD IC (b)

When comparing the two samples, it is clear that there is a distinct carbonyl peak shift. The as-synthesized sample has a carbonyl peak of ~1723 cm^{-1} with only a slight shoulder. The triblock IC has a carbonyl peak at ~1728 cm^{-1}. This information suggests that the as-synthesized sample contains a very high percentage of crystallized PCL while the IC contains

very little crystallized PCL, agreeing with our DSC observations and suggesting at least partial inclusion of the PCL blocks.

Conclusions

DSC studies of PMMA/γ-CD NS-IC's suggested a strongly heterogeneous material that could perhaps be made more homogeneous upon annealing. The presence of an increased T_g in some of the DSC samples (transition increases as high as 27˚C) suggest that in certain environments, restriction of dangling PMMA chains may result in a drastic increase in the glass transition temperature. Calculations published by Tonelli suggest that, at least for an end-capped, soluble PEG/α-CD NS-IC in DMSO, the cyclodextrin molecules likely aggregate in small groups of 3-4 CD's.[80] If these small groups remain separate from each other in solution, it is possible that only small crystallites dispersed along the entire length of the polymer chain might exist in the solid state. If this is the case, then the behavior of the free polymer chains in this IC structure would vary drastically from that of our triblock IC. This also may explain the extreme heterogeneity of our PMMA/γ-CD NS-IC sample.

Attempts at concentrating the location of CD molecules on an IC were made by complexing a PCL-PPG-PCL triblock copolymer with β-CD. Initially, it was thought that the β-CD would only complex with the PPG center block, creating a type of "forced" NS-IC, allowing for property examination of the restricted PCL block. However, DSC and FTIR observations show that the β-CD also interacted with the PCL in such a way as to prevent crystallization almost entirely. Whether this is due to threading of the PCL blocks by β-CD or some other type of interaction between the two block types is unknown. Either way, the continued development of these particular polymer/CD systems and further study of NS-IC's with different coverage ratios could eventually allow for the understanding of the property

differences of constrained “dangling” uncovered polymer chains in non-stoichiometric polymer IC systems.

Future Work

To better understand the behaviors observed in this chapter, further study of non-stoichiometric PMMA IC’s would be useful. It is likely that beginning with a higher PMMA repeat unit:γ-CD ratio as well as taking extra steps to wash the material would allow for a more homogeneous IC structure. A study of this type of NS-IC that does not limit the location of the cyclodextrin would perhaps provide some useful information when compared to a CD-location-controlled IC like our PCL-PPG-PCL-β-CD- IC. The difference in behavior between NS-IC’s formed with crystalline and non-crystalline polymers may be an interesting study as well.

For the purpose of specifically understanding the behavior of restricted, dangling polymer chains, diblock or triblock copolymers would be a more ideal sample type than a traditional polymer NS-IC. If the β-CD does, in fact, thread the PCL with some small percentage or cause some other type of block to block interaction, then perhaps a different type of copolymer could be developed. Once an appropriate copolymer system is defined, highly controlled diblock or triblock samples with well defined molecular weights could be produced. Varying the size scales of the center and outer blocks should allow for the understanding of the effects of dangling chain length on the polymer properties. The behavior of such a system could be compared to other NS-IC’s as well as polymer brush systems.

Chapter 4: Inclusion Complex Formation between Modified β-Cyclodextrin and Polypropylene Glycol Homopolymers and Block Copolymers

Abstract

A non-crystalline modified CD, diethylamine-terminated monochlorotriazinyl-β-CD (DEAMCT), was synthesized from an industrially available β-CD derivative. DEAMCT was complexed with poly(propylene glycol) (PPG) as well as a poly(ethylene glycol)-poly(propylene glycol)- poly(ethylene glycol) (PEG-PPG-PEG) triblock copolymers (trade name Pluronics). The inclusion compounds (IC's) formed between these polymers and non-crystalline cyclodextrin were studied with a variety of techniques. Two-dimensional ROESY NMR demonstrated through-space spin coupling interactions between backbone protons of the PPG and two of the inward-facing protons on DEAMCT, strong evidence for PPG threading and inclusion and IC formation with DEAMCT. Unexpectedly, these IC's displayed some weak crystalline ordering. The IC formation of DEAMCT with the Pluronic materials resulted in crystalline order comparable to ICs formed with un-modified β-CD, and in both cases complete disruption of the PEG block crystallinity in a similar fashion to the PCL-PPG-PCL triblock copolymer. Thus, DEAMCT was able to thread over and include PPG and the Pluronics forming crystalline ICs, even though neat DEAMCT does not crystallize. Also, the aqueous solubility for both the Pluronic and PPG decreased upon low-coverage DEAMCT inclusion.

Introduction

Though cyclodextrins offer a large variety of uses, modifications are sometimes necessary to improve upon or altogether change their properties. Modified cyclodextrins have become a staple component in the pharmaceutical and food industries, and have various analytical applications.[81] More often than not, these modified cyclodextrins are used for their enhanced solubility, the ability to complex with specific components, or for heightened complex stability.

Bettinetti and colleagues were observing the complexing ability of cyclodextrin with naproxen when they observed that modification of β-CD with methyl, hydroxypropyl, or hydroxyethyl groups offers a significant increase in complex stability.[82] The methyl group showed the most improvement. Modified cyclodextrins also seem to provide an opportunity for high drug solubility. Methylated β-CD's, 2-hydroxypropylated β- and γ-CD's, and sulfobutylated CD's are some examples of commercially available "highly soluble" cyclodextrins.[83] It is thought that the reason for this increased solubility is the disruption of the secondary hydrogen bonding network of the hydroxyl groups located on the edge of the cyclodextrin, especially for β-CD.

The random replacement of a hydroxyl group with the respective modification groups may also prevent the aggregation and crystallization of the cyclodextrin by producing a non-uniform structure. Methylated cyclodextrins are still crystalline; however, the hydroxylpropyl- and hydroxyethyl-β-CD's show no crystallinity.

The inclusion of small molecules in cyclodextrins has been a thoroughly studied topic. Many different types of cyclodextrin have been studied with many different types of small-molecule guests. Though seemingly an interesting research extension, the interaction between polymers and modified cyclodextrins has not been the subject of much research.

As previously discussed, unmodified cyclodextrins tend to group together when threaded on a polymer chain, forming the channel crystal structure. But as we have seen for modified cyclodextrins, the regularity and secondary hydrogen bonding network are disrupted due to the random modification of the hydroxyl group. If modified cyclodextrins lose their ability to crystallize effectively or at all, what happens once they are threaded onto a polymer?

Little work exists studying inclusion of modified cyclodextrins onto polymers. Yang et al. attempted to change the solubility of a polyimide by complexing the monomer into dimethyl-β-CD and trimethyl-β-CD and then polymerizing to form polypseudorotaxanes containing 4.2 – 11.2% cyclodextrin.[84] While the regular β-CD improved the solubility of the polyimide in THF and dioxane, the incorporation of methylated cyclodextrins also added chloroform and dichloroethane solubility. Additionally, the small amount of CD found on the polymer did not seem to disrupt the natural crystallinity of the polyimide. These pseudorotaxanes were created not by threading of the cyclodextrin onto the chain, but by polymerizing the exposed ends of an IC with a second component. Is it possible, then, to thread a modified cyclodextrin onto a preformed polymer chain?

Harada and Okada examined the complex formation of the hydrophobic polymers oligoethylene and polypropylene with methylated cyclodextrin in aqueous solution.[85] Visual observation and NMR data suggested that oligoethylene and polypropylene do form complexes with methyl-β-CD, but instead of forming a precipitate, as in the case of regular CD and polymer, the complex remained soluble. This suggests that whatever aggregation of the cyclodextrin material causes a crystalline IC to become insoluble may not be occurring in this type of system. No x-ray crystallographic data were presented, however, to confirm this hypothesis. Harada and Okada also referenced two other unreported experiments where methylated cyclodextrins were complexed with polypropylene glycol and polytetrahydrofuran.

If non-crystalline soluble inclusion complexes can be made from hydrophobic polymers and methylated cyclodextrins, which demonstrate some crystallinity in the pure hydrate state, then it seems possible to create the same kind of soluble polymer IC system using other modified cyclodextrins with less crystalline characteristics. Since there has been little work done to explore the behavior of these types of systems, it is possible that they may be able to tell us more about the inclusion process and the interactions that are occurring between the host and guest molecule. A water-soluble IC, formed by a polymer partially threaded into CD derivatives, may also have some important industrial uses, such as in paints, adhesives, or lubricants.

In the following experiments, we tried to apply existing inclusion techniques to a heavily modified non-crystalline cyclodextrin in an effort to obtain a truly non-crystalline inclusion complex. While the inclusion technique remains the same, sample isolation and analysis became even more important as our major traditional method of determining whether an IC has formed (channel CD structure evident in XRD) may no longer be applicable.

Materials and Methods

Sample Preparation Techniques

Polypropylene glycol (average M_w=1,000) was obtained from Sigma-Aldrich and used without further treatment. The Pluronic copolymer samples and cyclodextrins were generously donated by BASF and Wacker, respectively.

Sample Nomenclature

Sample nomenclature found throughout this chapter is based on a variety of information about the sample. The first percentage value of the sample name represents the weight percent concentration of polymer in water. The second value indicates the mixing stoichiometry of cyclodextrin to polymer. This number indicates the theoretical coverage percentage of the polymer if all the cyclodextrin were to thread only the polymer chain, though the actual value of polymer chain coverage is likely lower.

For certain samples, other tags exist to help indicate other changes in sample preparation. "RT" stands for room temperature, indicating the IC was formed at room temperature rather than at an elevated temperature. "R" stands for reverse. In these samples, the polymer was dissolved into the water before the cyclodextrin was added. A P before the sample name indicates a Pluronic triblock copolymer sample.

Standard and Diethylamine-terminated Monochlorotriazinyl-β-CD

We initially began by using a commercially available non-crystalline modified cyclodextrin from Wacker, monochlorotriazinyl-β-CD (referred to throughout as simply MCT). Reuscher and Hirsenkorn, researchers at Wacker in Germany, wrote a paper in 1996 about the uses of MCT.[86] Though the monochlorotriazinyl group is found frequently in dye chemistry, its random attachment to β-cyclodextrin allows for a cyclodextrin with interesting properties and the ability to form covalent bonds with various nucleophilic groups. These "built-in" reactive groups offer MCT the ability to attach to another component without the need for a third "linking agent" necessary for unmodified cyclodextrins. It may also be possible to use a single linking agent to connect the MCT together to form a sliding ring-type crosslink. Though this type of structure has been seen before, the non-aggregation of MCT could

possibly result in much different behavior or a more uniform crosslinking density. The use of a soluble polymer-MCT-IC for surface attachment may also be possible. Adhesion and wetting properties are both examples of surface characteristics that could be modified by such an easily-attached IC.

The structure of MCT can be seen below in Figure 43. The reported substitution for Wacker's commercially produced MCT is 0.4, or 2.8 monochlorotriazine substitutions per β-CD molecule.

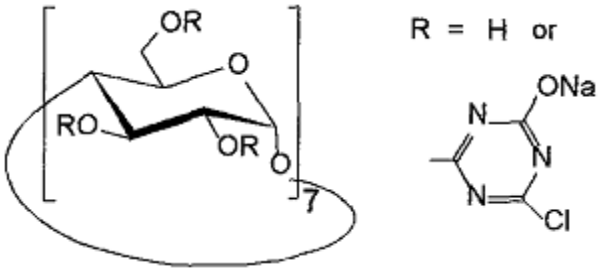

Figure 43: The structure of monochlorotriazinyl-β-cyclodextrin[86]

A majority of the previously published work utilizing the triazine-modified CD takes advantage of the material's ability to attach itself covalently to starch, paper, and surfaces containing nucleophilic attachment sites.[87-92] Hebeish et al. also attached MCT to starch to measure the material's applications as a textile sizing agent.[88] They found that the reaction of the MCT group with the starch was more prevalent at higher pH levels and that the reaction decreased with increasing temperature from 40 to 90° C. More recent work published in 2006 and 2007 explores MCT's ability to bond to cellulose in cotton fibers and filter paper.[89,90] Both papers used a curing temperature of 150° C, perhaps basing their

technique on the 2006 paper by Furuta et al. reporting that 150° C for ten minutes created the optimal reaction conditions for attaching MCT to Japanese washi paper.[92]

The purpose of many of the previously mentioned studies of MCT was to examine the ability of the modified CD to include small molecules once attached to the various surfaces.[87,90-93] Rehmann and colleagues attached MCT to starch in 2003 and monitored the inclusion behavior[87]. They observed that, upon attachment to the starch, the MCT was still able to undergo small molecule inclusion of d-limonene at the exact same molar ratio as plain β-CD. Hara and colleagues, however, reported that MCT included less of a fragrance molecule than other modified β-CDs. This indicates that the type of guest molecule included plays an important role in determining if the modified MCT includes small molecules in the same fashion as unmodified β-CD.

Little data has been published regarding the solid state behavior of MCT. As-received MCT does not demonstrate any long range crystalline order (see Figure 44). This unique feature allows MCT to be the building block for our modified cyclodextrin.

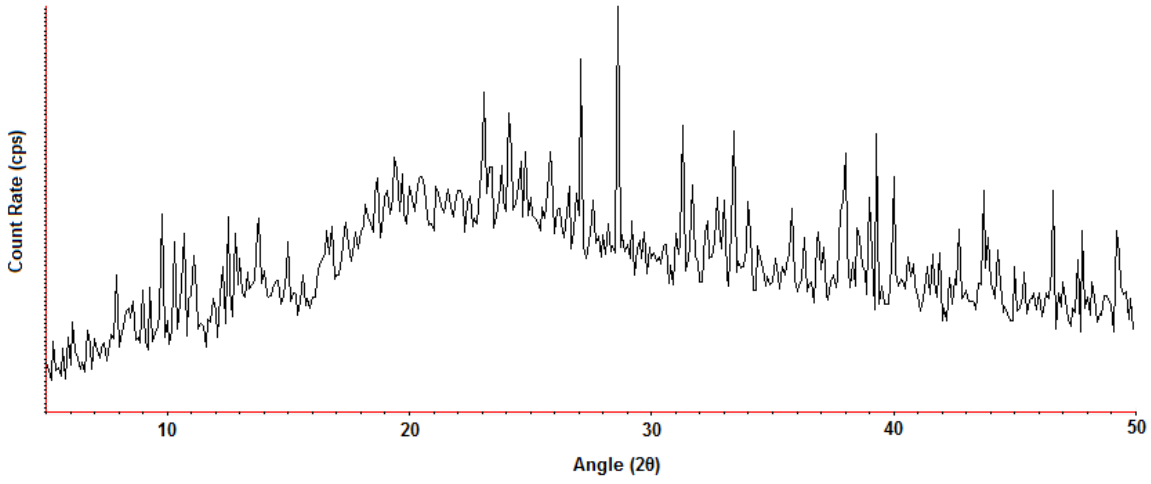

Figure 44: Wide-angle XRD pattern of as-received MCT

The solubility for MCT is better than that of unmodified β-CD. The reported solubility by Reuscher and Hirsenkorn is 0.3 g/ml water, though the solubility is said to decrease as the degree of substitution increases. Our observations also confirm the increased solubility of commercial MCT over unmodified β-CD.

Currently, no published work exists studying the threading of MCT onto a polymer. However, initial attempts at IC formation between MCT and PPG were not successful, with the reaction of the MCT with the hydroxyl groups on the polymer chain ends effectively capping off the polymer and disallowing any inclusion to take place. This behavior was confirmed by 2-dimensional ^{1}H-NMR, thus subsequent studies incorporated MCT where the reactive group had been terminated using diethylamine.

Synthesis of the Diethylamine-terminated Monochlorotrizinyl-β-CD

Monochlorotrizinyl-β-CD was dissolved in deionized water (1g per 10ml water). Diethylamine (Sigma-Aldrich) was added at a concentration of 1ml per 10ml water (molar excess). The solution was then placed in a 60° C oven for 24 hours. During this time, the diethylamine reacted with the MCT to replace the chlorine on the triazine with the diethylamine. The reaction can be expressed as:

$$\text{MCT-C-Cl} + \text{HN(CH}_3\text{)}_2 \rightarrow \text{MCT-C-N(CH}_2\text{)}_2 + \text{HCl}$$

As the reaction took place, the solution went from being clear to a progressively more golden in color. After the reaction was left for 24 hours, the water was evaporated first under atmospheric conditions then under vacuum until the sample was dry. This new material is referred to throughout the remainder of this thesis as DEAMCT.

DEAMCT Characterization

Analytical testing of DEAMCT was performed to check for the integrity of the cyclodextrin as well as the presence of diethylamine modification. XRD of the material (Figure 45 below) revealed a complete absence of any long range order. From this data, we can conclude that DEAMCT would be an appropriate material to test the effects of threading a non-crystalline host CD on a polymer chain. For comparison, Figure 46 shows the crystal structure of a traditional channel β-CD IC as well as the as-received cage β-CD crystal structure.

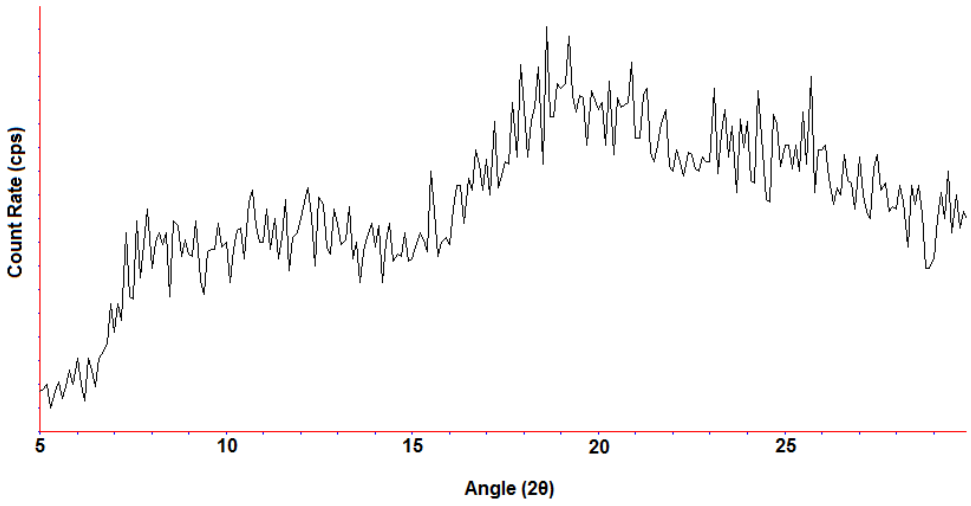

Figure 45: Wide-angle X-Ray diffraction pattern of DEAMCT

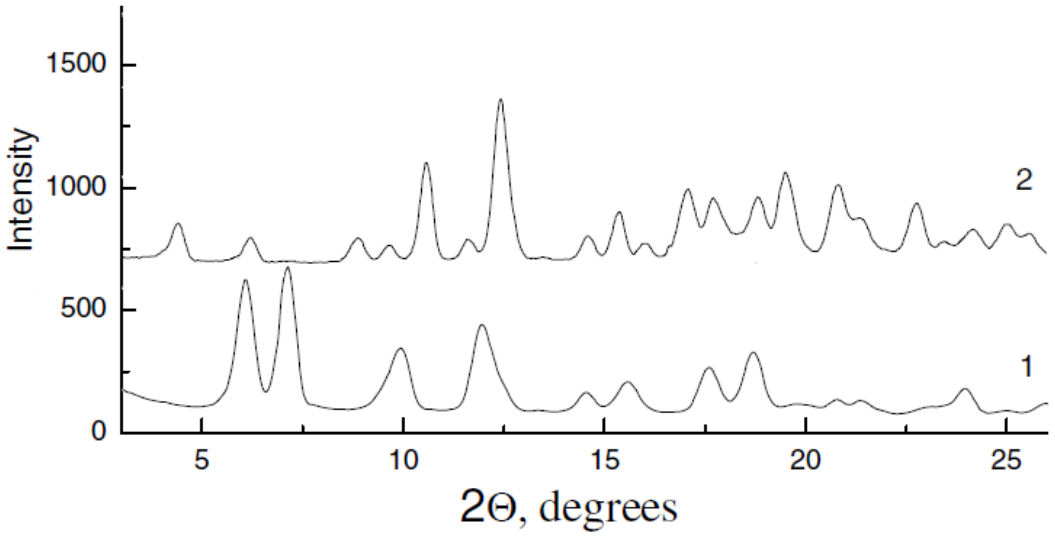

Figure 46: Example X-ray diffraction patterns of a channel PPG/β-CD IC (1) and the cage β-CD crystal structure (2)[94]

DEAMCT NMR

Figure 47 presents the 500 MHz ^{1}H NMR spectrum of DEAMCT in D_2O. DEAMCT peaks positioned between 3.5 ppm and 5.0 ppm are evident and tabulated in Table 6 below, along with those of the diethylamine terminal groups. The triazine portion of the modifier contains no protons and can therefore not be observed with proton NMR. The methyl protons of the diethylamine (DEA) modifier can be observed at 1.07, 1.12, and 1.20 ppm (all triplets). The methylene protons are visible as a quartet at 2.99 and 3.44 ppm.

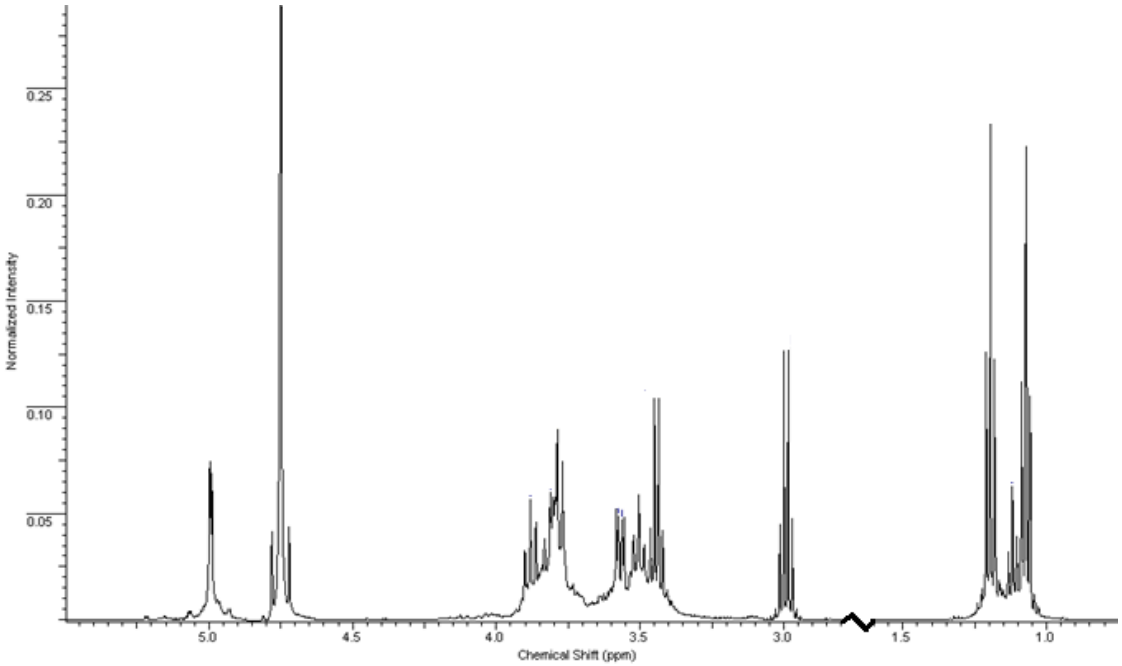

Figure 47: (Bruker 500) Proton NMR spectrum of DEAMCT in D_2O

Table 6: List of DEAMCT proton NMR peaks and their assignments

Peak (ppm)	**Proton Assignment**		**Peak (ppm)**	**Proton Assignment**
1.07	DEA methyl (a)		3.57	H2
1.12	DEA methyl (a)		3.79	H5
1.20	DEA methyl (b)		3.81	H6
2.99	DEA methylene (b)		3.88	H3
3.44	DEA methylene (a)		4.75	HDO (reference)
3.5	H4		5.0	H1

If we examine the H-H correlation by way of 2D COSY NMR, we can see that there seem to be two distinct “types” of diethylamine. We will call these two types of diethylamine type “a” and type “b.” COSY NMR allows us to examine H-H correlation through approximately 4 bonds. This particular test allows us to “connect” protons positioned on adjacent carbons. In Figure 48 below, we can see the correlation between the “a” methyl and “a” methylene protons (1.07/1.12 and 3.44 ppm respectively) and the “b” methyl and “b” methylene protons (1.20 and 2.99 ppm respectively). It is possible that not all of the excess diethylamine was removed during DEAMCT formation and the free DEA displays different peak shifts than that of the reacted DEA. Another possibility is that some of the DEA is included inside the CD cavities. However, this has not been explored.

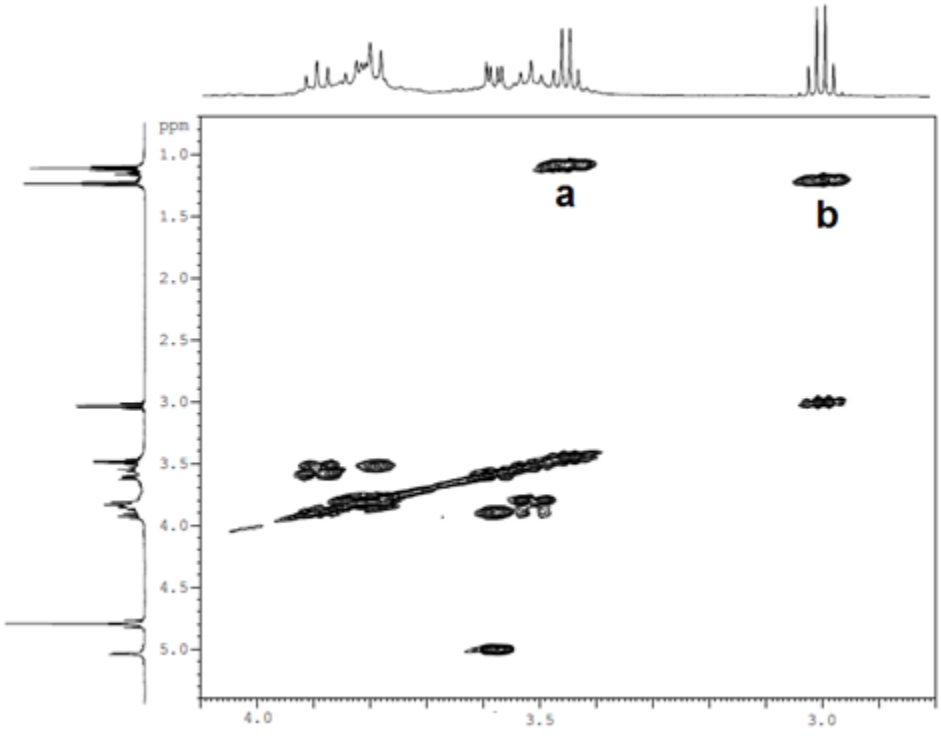

Figure 48: (Bruker 500) 2D COSY Proton NMR spectrum of DEAMCT in D_2O

If we examine the peak integration for Figure 47 (DEAMCT proton), we may be able to make an educated guess at the DEA:CD ratio as well as find a possible explanation for the two distinct types of DEA within the sample. First, let us attempt to arrive at the DEA:CD ratio. Luckily, there are two distinct peaks or peak sets that we can integrate that only correspond to one of the components: the H1 CD proton at 5.0 ppm and the set of DEA methyl protons between 0.95 and 1.35 ppm. If we integrate the H1 proton peak and define that value as 7.0 (seven total glucopyranose units in a β-CD), then we can also integrate all of the DEA methyl peaks collectively, arriving at a value of 26.7. We know that these methyl peaks represent six total protons per DEA modifier, so we arrive at a value of 4.45. Our sample contains approximately 4.45 DEA modifiers for every CD molecule. MCT-β-CD, our starting material, is reported to be substituted at a rate of 2.8 modifications per CD molecule, or approximately 63% of the stoichiometric DEA:CD ratio present in our sample.

To determine the ratio of “a” DEA to “b” DEA, we can begin by defining our methyl peak integration value at 6.0 (again, six total methyl protons for each DEA). Luckily, the “b” methylene quartet at 2.99 ppm is removed enough from the nearby peak cluster that we are able to fully integrate, arriving at a value of 1.32. This value accounts for approximately 33% of the four DEA methylene protons present in the system, suggesting then that roughly 67% of the DEA is in the “a” form while 33% is in the “b” form. Is it simple coincidence that the percentage of “a”-type DEA and the percentage of expected total DEA are so close? It may be possible that “a”-type DEA is actually the attached DEA that we expected and the “b”-type is the remaining DEA that either did not evaporate during drying or in some other way complexed or interacted with the cyclodextrin.

To test whether any peaks were simply free DEA in our solution, a small amount of DEA was added to D_2O and an NMR spectrum was collected. For the free material, 0.91 and 2.42

ppm are the chemical shifts for the methyl and methylene protons, respectively. From this information, we can likely conclude that the “b”-type DEA peaks do not belong to free DEA. Perhaps, then, these peaks belong to DEA in some other way associated with CD.

Studies of IC formation between Modified Cyclodextrin and Low Molecular Weight Polypropylene Glycol

NMR Studies of PPG/DEAMCT IC Materials

Because we may no longer be forming a fully developed channel-structured crystalline IC, we must look to a more complex and reliable method for the detection of IC formation, NMR. Polymer inclusion may lead to peak shift changes between the original materials and the IC material. Additionally, we can try to observe the previously mentioned through-space NOE effect between one or more polymer protons and CD protons. Any of these observations will be strong evidence that we have threading of the modified cyclodextrin onto the polymer chain.

PPG NMR Observations

To begin examining the NMR data for evidence of polymer inclusion, we must first begin by examining the individual components. We have already studied the 1D and 2D COSY proton NMR NMR spectra of our modified CD, DEAMCT, but we must also examine the NMR spectra for as-as-received PPG. Figure 49 is the NMR spectrum of PPG (Mw=1,000 g/mol) in D_2O. For PPG, we can observe the methyl side chain proton peaks at 1.04-1.07 ppm. The main chain backbone protons are clustered between 3.26 ppm and 3.86 ppm. The peak at 4.75 ppm represents the HDO solvent peak. If we integrate the methyl proton peak and the backbone proton peak cluster, we arrive at 3.0 and 2.99 respectively, in agreement with expected values.

Table 7 summarizes the NMR peak assignments for PPG 1,000 in D_2O.

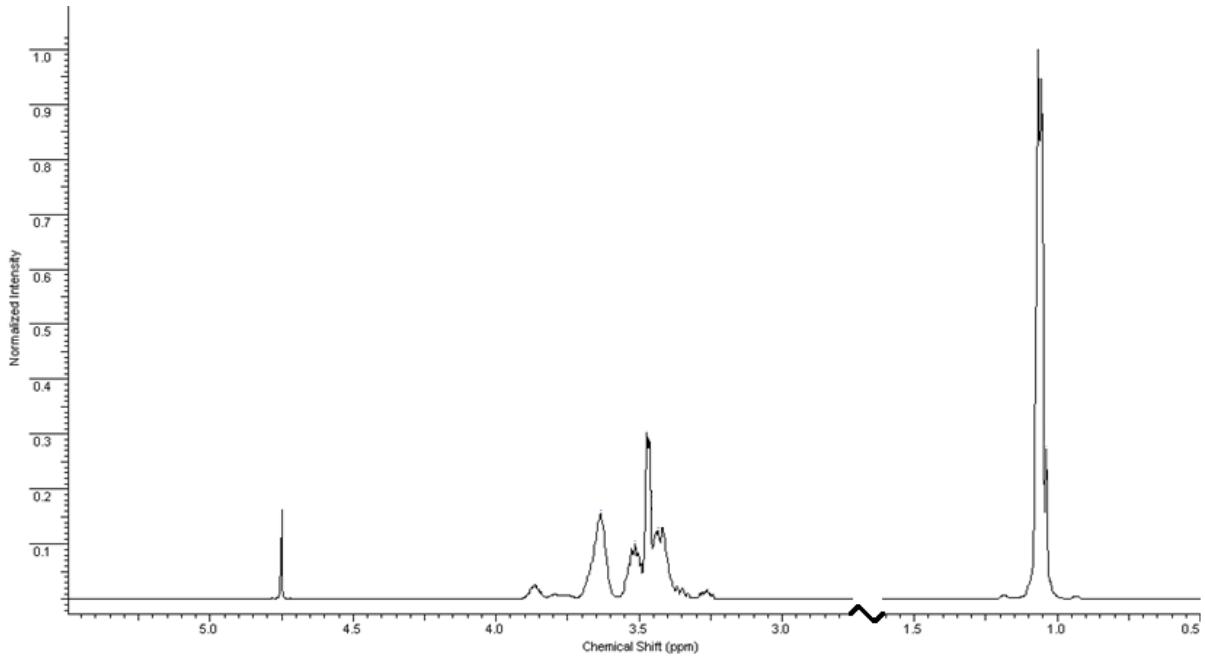

Figure 49: (Bruker 500) Proton NMR spectrum of PPG (Mw=1,000 g/mol)

Table 7: List of PPG 1,000 proton NMR peaks and their assignments

Peak (ppm)	**Proton Assignment**
1.04 - 1.07	Methyl side chains protons
3.26-3.86	Backbone protons

PP-DEAMCT IC Sample NMR Observations

We can begin looking for evidence of IC formation by comparing the peak shifts of the raw materials to that of the potential IC materials. Since there is a large amount of peak overlap, we can anticipate some difficulty in distinguishing between the two components. However, if we examine each grouping of peaks closely, we may be able to identify shifts in certain peaks after any inclusion has taken place.

IC formation at elevated temperature was used to produce samples specifically for 1D and 2D NMR analysis on the Bruker 500 NMR. One sample, 2.0%-35, was prepared by dissolving 1.0g of DEAMCT in 10ml of deionized water. 0.2 g of PPG (MW=1,000 g/mol) was added to the DEAMCT solution and the mixture was placed in a 70° C oven for three days to watch for any kind of IC-type precipitate. After this time, no filterable precipitate was formed so the water was first evaporated, then the remaining material was dried overnight in a vacuum oven.

Two other samples were prepared later and designed to have a much higher "coverage" ratio and to possibly produce separate solid and soluble components. 1.01 g of DEAMCT was dissolved in 10ml of deionized water. 0.094 g of PPG 1,000 was added to the solution and was left to stir for four days in an oil bath at 65° C. After removal from the oil bath, the sample was left to sit for 3 more days at room temperature. The precipitate was then filtered out and the precipitate and filtrate were dried overnight under vacuum. The solid component is referred to as 0.9%-75-solid and the liquid component as 0.9%-75-liquid.

If we examine the 0.8 – 1.5 ppm (methyl) region for sample 2.0%-35 (Figure 50) we can observe a shift in the PPG 1,000 methyl proton peak from 1.05/1.07 to 1.08/1.10 ppm. Looking at the 2.8 – 4.25 ppm region, we can also observe PPG methyelene proton peaks at 3.47 and 3.63 ppm shifting to 3.5 and 3.66 ppm respectively (see Figure 51). This

consistently observed shift value is therefore most likely attributed to a slight change in the HDO peak position before referencing, a phenomenon often observed with changes in temperature.

When examining regions in Figures 50 and 51, as well as the region containing the H1 proton (not shown), we can see that there are no shifts observed for the DEAMCT proton peaks. Additionally, when we examine the 1D proton NMR of the higher coverage samples, the same behavior is observed. No peak shifts are observed for the DEAMCT peaks while the whole PPG spectrum is shifted by a similar amount. Comparison of the proton NMR of 0.9%-75-solid and -liquid to the original components also demonstrated no peak shifting.

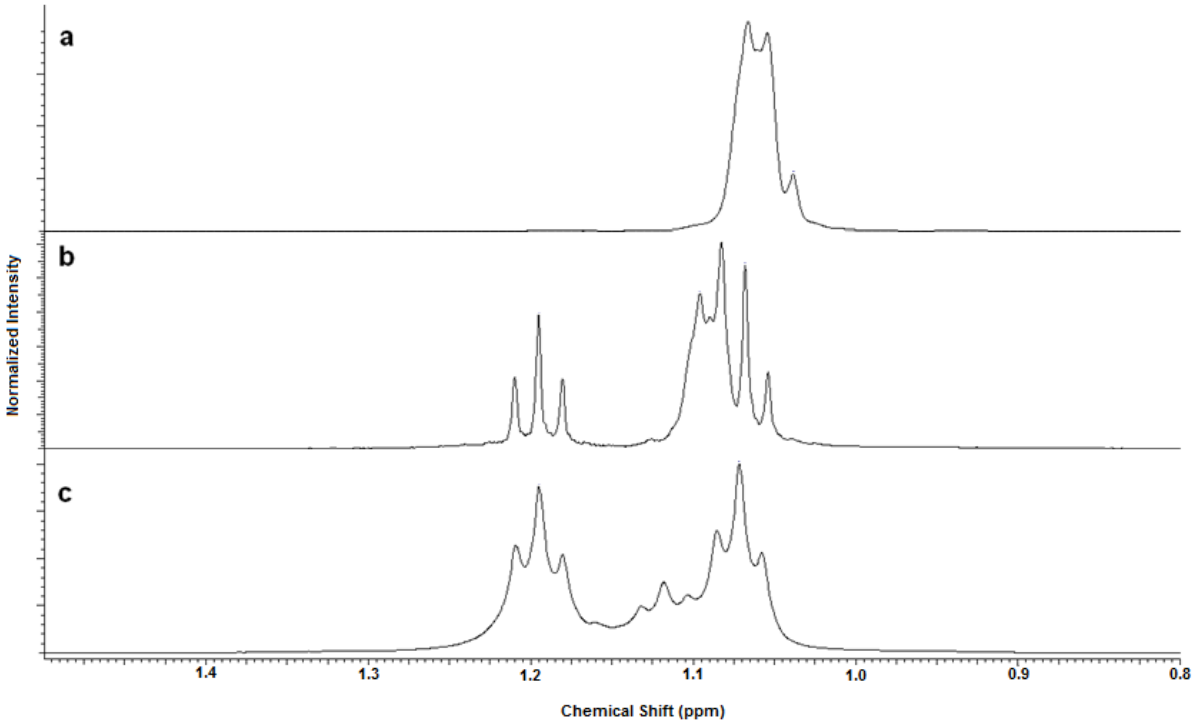

Figure 50: One-dimensional proton NMR spectra comparison between PPG (Mw=1000) (a), 2.0%-35 (b), and DEAMCT (c). [0.8-1.5 ppm]

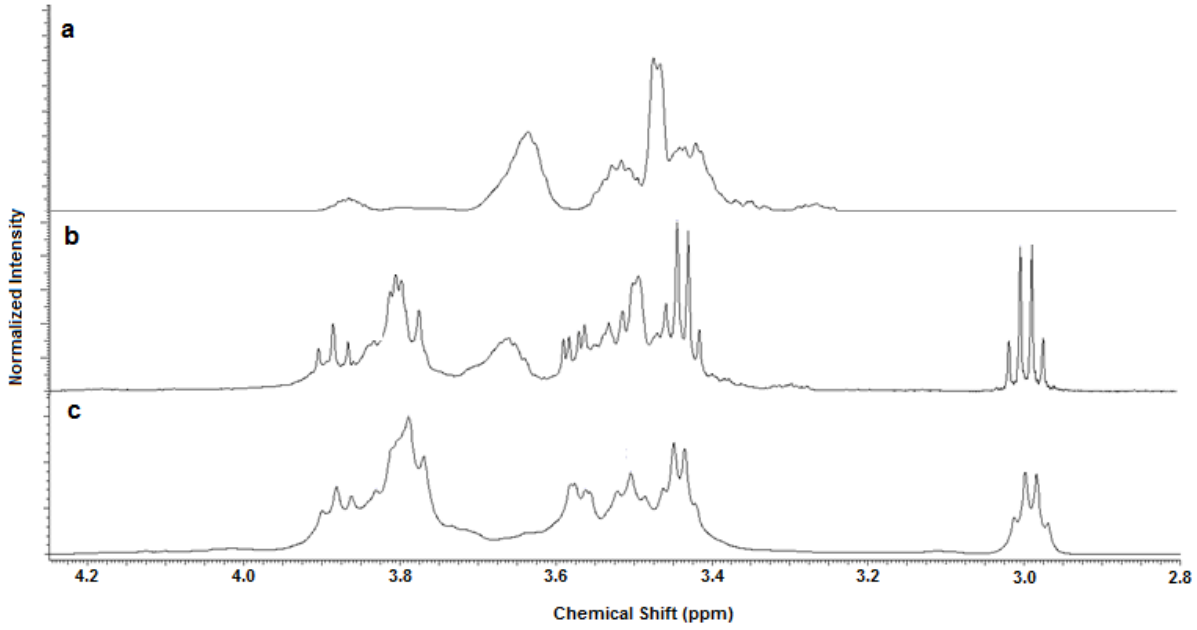

Figure 51: One-dimensional proton NMR spectra comparison between PPG (Mw=1000) (a), 2.0%-35 (b), and DEAMCT (c). [2.8 – 4.25 ppm]

We also examined the two-dimensional NMR of some of these samples to look for evidence of inclusion. If we perform certain types of NMR, we should be able to observe the previously discussed Nuclear Overhauser Effect. This through-space interaction between the cyclodextrin and polymer protons has been used previously in the literature to suggest IC formation.[41] In our particular case, we should be able to compare the COSY NMR (only through-bond interactions observed) and ROESY NMR (through-space interactions) to look for interaction between the two.

Unfortunately for our analysis, many of our peaks overlap and will thus be difficult to distinguish. However, we should be able to look for interactions between certain peaks that do stand out, such as the H1 proton and some of the PPG backbone protons. The “b” methyl protons do stand out well, but if they do actually belong to free DEA, we would not

expect to observe any interactions. We may also be able to distinguish between the PPG and DEA methyl peaks.

The most easily distinguishable DEAMCT peak and PPG main-chain peak is also the location of one of our most easily distinguished interactions. When examining the region of the H1 proton and PPG backbone peak at 3.66 ppm, we can see a very distinct cross-peak indicating some kind of interaction between these two protons. Figure 52 below highlights the region where the 3.66 PPG backbone protons would show an interaction with another proton. In spectrum d, we can see where the small cross peak appears when the DEAMCT and PPG component are both present. For comparison, this small peak is not present in the ROESY spectrum of DEAMCT only (b) or in the COSY spectrum of the IC sample (c), so we can confidently say that this is a through-space interaction between the two components.

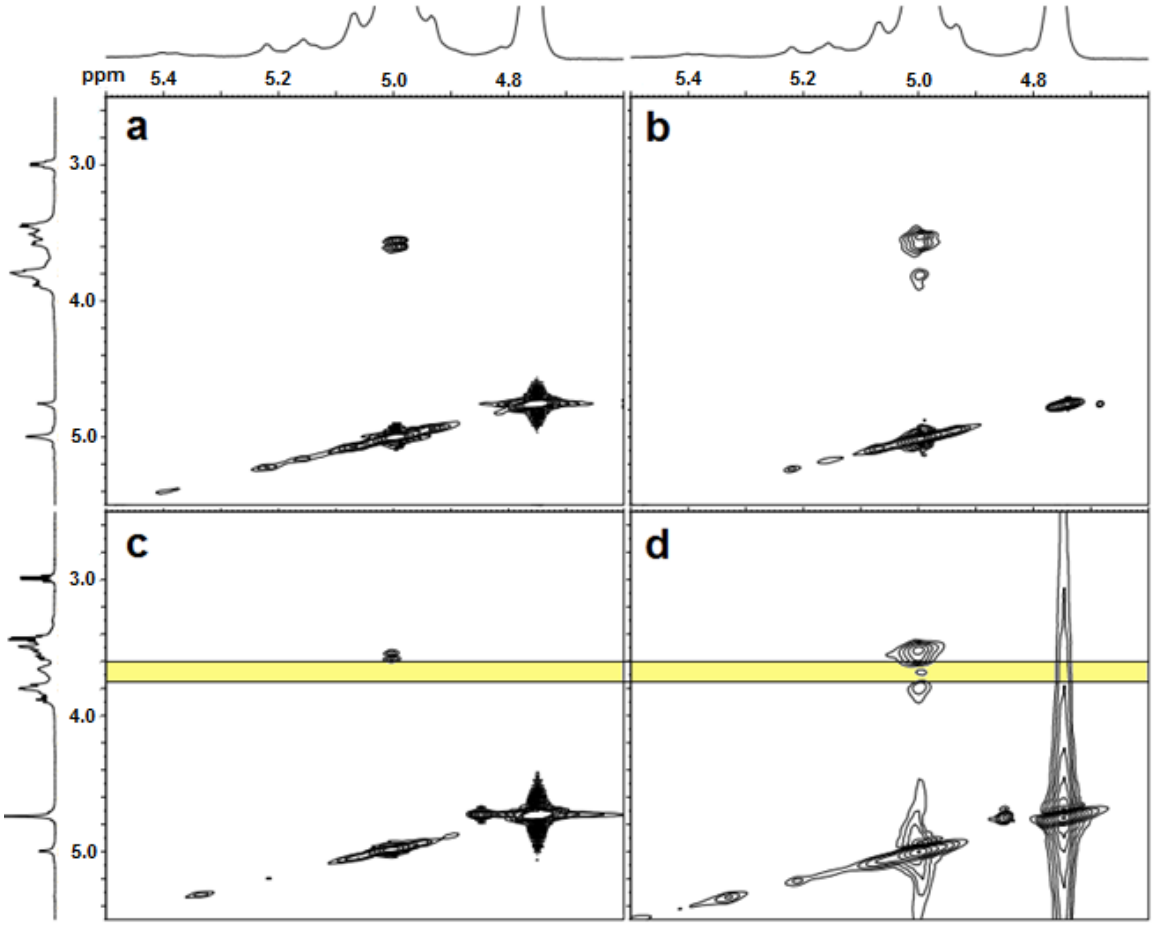

Figure 52: COSY NMR spectra of DEAMCT (a) and 2.0%-35 (c) vs. ROESY NMR spectra of DEAMCT (b) and 2.0%-35 (d) [Low Amplitude]

The above figure is a low amplitude view of the ROESY NMR signal. This low amplitude view only shows the most common H1 interaction. If we increase the amplitude enough to examine all the lesser common H1 peak shifts (caused by the random DEAMCT substitution) then we can also see the interaction of other H1 protons with the PPG backbone groups. Figure 53 below shows the higher amplitude view of the COSY and ROESY NMR spectra seen in Figure 52. We can see a second and third interaction taking place at 5.34 and 5.2 ppm. These smaller interactions help support the suggestion that we are observing real through-

space dipolar interaction instead of some testing artifact. The interaction between the H1 CD proton and the PPG backbone protons are the only observed interactions for 2.0%-35.

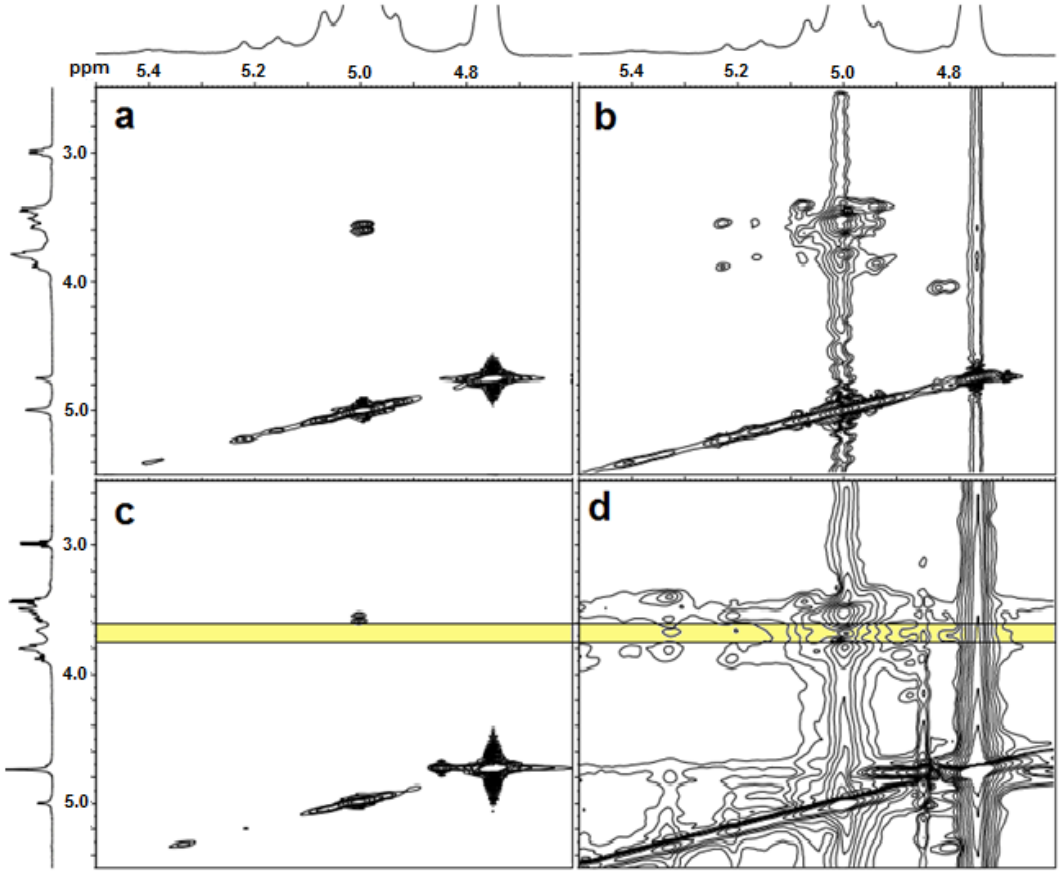

Figure 53: COSY NMR spectra of DEAMCT (a) and 2.0%-35 (c) vs. ROESY NMR spectra of DEAMCT (b) and 2.0%-35 (d) [High Amplitude]

When we examine the higher coverage samples, the same cross peak between H1 and PPG backbone protons is observed. Figure 54 and Figure 55 are the ROESY NMR spectra for 0.9%-75-solid and 0.9%-75-liquid, respectively. These and future 2D NMR spectra do not

show the comparable COSY and reference material spectra, but indicated cross-peaks have been validated to be true NOE peaks. In Figures 54 and 55, the cross peak between the H1 proton and PPG backbone protons are observed in both samples, suggesting that IC threading is present in the precipitated material as well as in the soluble portion.

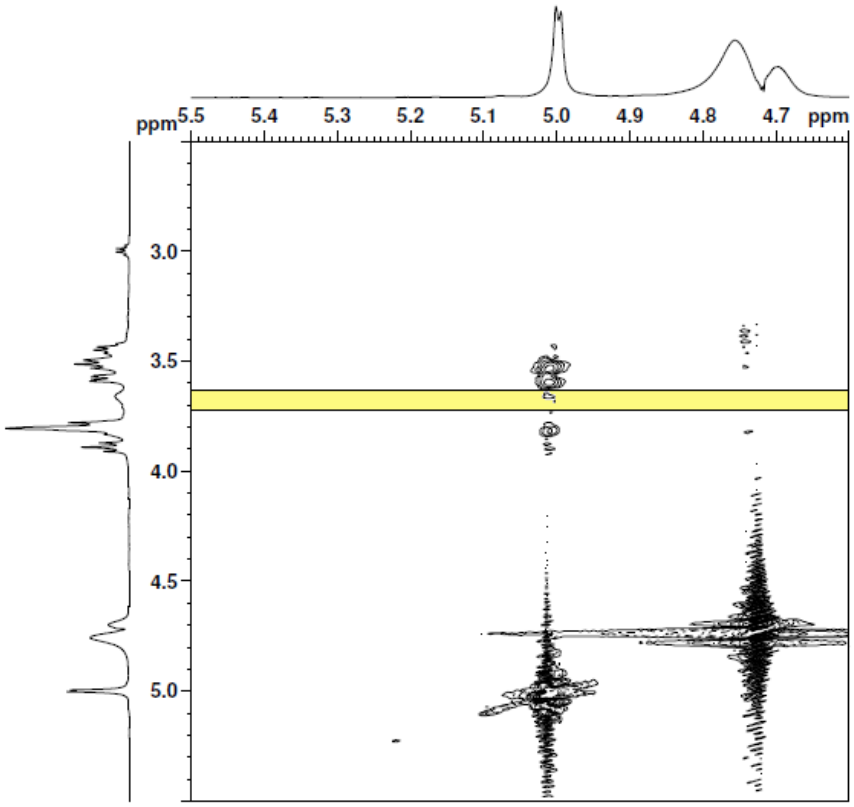

Figure 54: ROESY NMR spectrum of 0.9%-75-solid [H1 CD proton region]

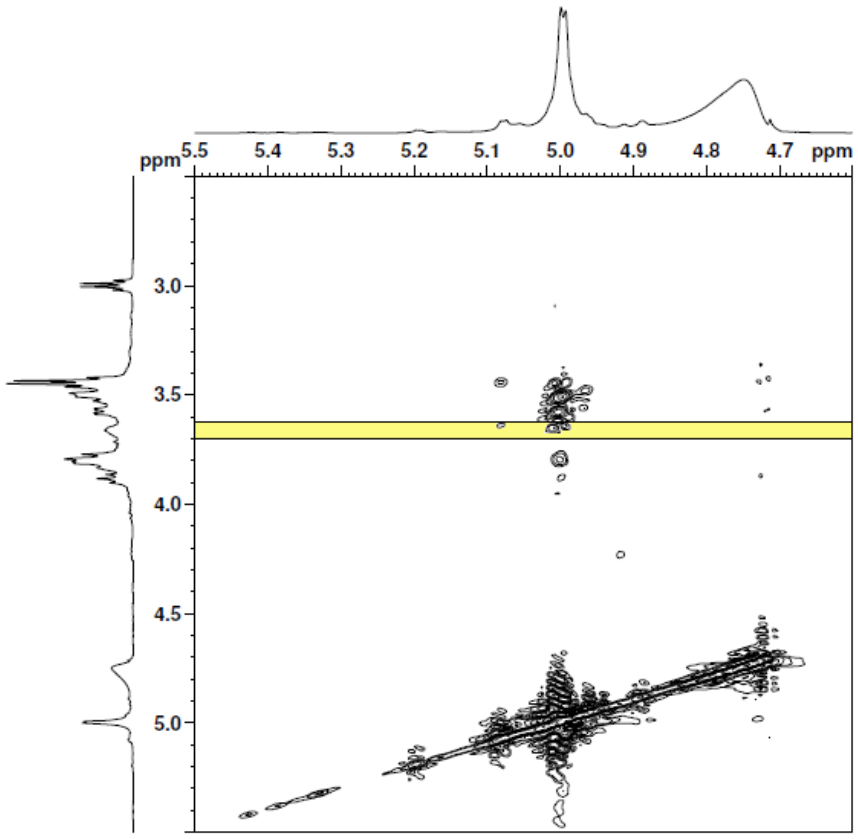

Figure 55: ROESY NMR spectrum of 0.9%-75-liquid [H1 CD proton region]

If we zoom into the region of the H2 CD proton for 0.9%-75-solid and 0.9%-75-liquid, we are able to observe a second NOE interaction with the PPG backbone protons. Figures 56 and 57 below are the ROESY spectra for both samples in the H2 region. The cross-peaks indicating interaction are designated with arrows. Interestingly, these interactions were not observed in 2.0%-35. It is possible that these interactions are weak and required the higher CD:PPG ratio for observation.

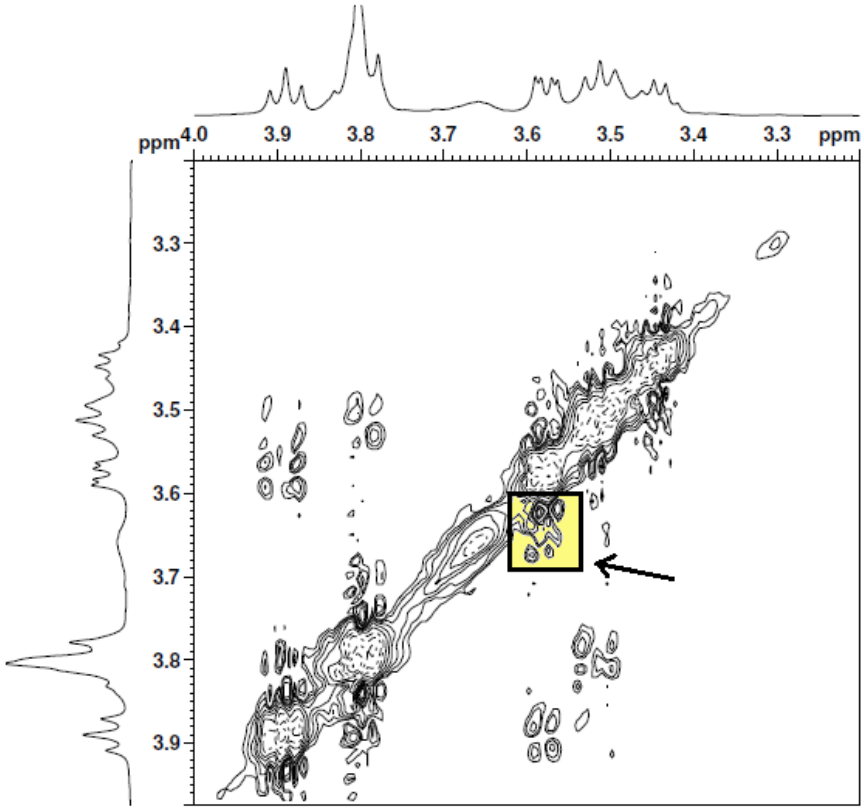

Figure 56: ROESY NMR spectrum of 0.9%-75-solid [H2 CD proton region]

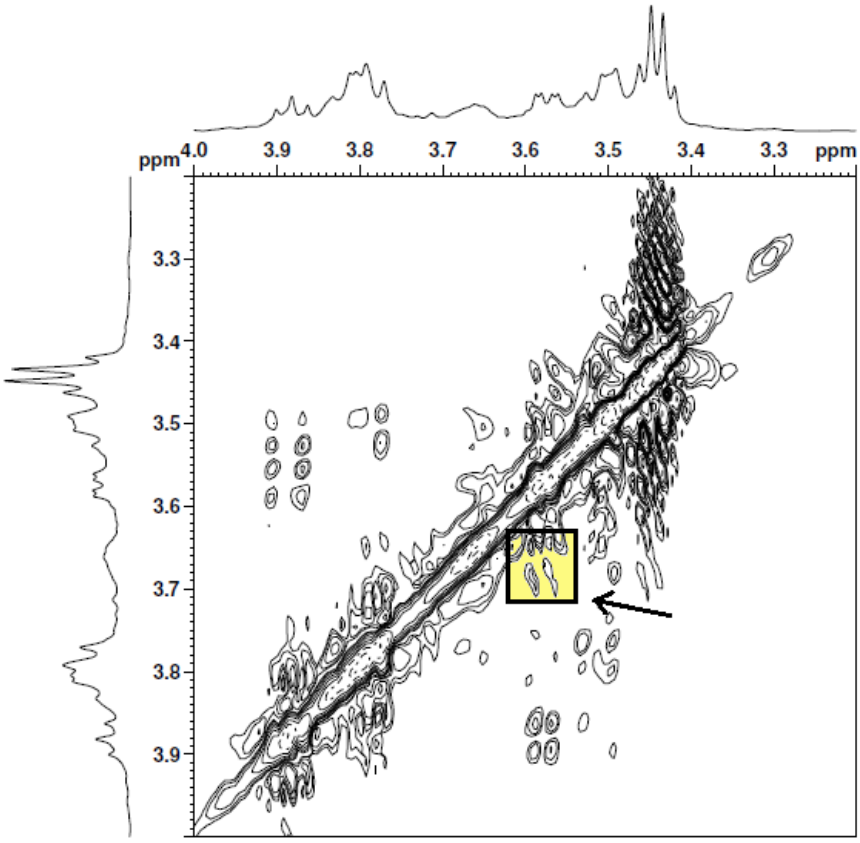

Figure 57: ROESY NMR spectrum of 0.9%-75-liquid [H2 CD proton region]

From these 2D NMR observations, we can definitely conclude that there is at least some threading taking place. The multiple interactions between the PPG backbone protons and DEAMCT H1 and H2 protons are clear evidence that some of the polymer resides in the cyclodextrin cavity.

At higher DEAMCT:PPG ratios (such as 0.9%-75-solid and 0.9%-75-liquid), both a soluble IC component and insoluble IC component are produced. It is very likely that the soluble component consists of the PPG chains with lower coverage and the solid component consists of more highly covered PPG chains. This would suggest that, even for a modified

CD, a relatively high coverage (possibly 50% or more) would result in an insoluble component. Conceptually, this makes sense if we are to assume that the precipitation of a traditional IC is perhaps caused by aggregation in general, a phenomenon that is only enhanced by the crystallizability of the unmodified CD.

No 2D NMR was performed on the precipitated high coverage samples due to insolubility in D_2O. It may be possible in future studies, however, to end-cap these higher coverage insoluble samples and look for NOE interactions in d_6-DMSO, which is a much better solvent for polymer-CD-ICs.

Our original expectation was that a prominent interaction peak would be observed between the PPG methyl peaks and some of the inward-facing protons on the DEAMCT glucopyranose repeat units (H1-H4). However, this behavior was not observed in any of our samples, suggesting that if inclusion is in fact taking place, the PPG methyl groups are not positioned inside the CD cavity in a way to produce these interactions.

One-dimensional proton NMR spectra for 1.2%-50RT-R and 3.5%-25RT-R were collected and are presented in Figure 58 and Figure 59, respectively. Similar NMR behavior to the high temperature PPG IC samples is observed. The 400 MHz NMR spectra are a little harder to distinguish, but there seems to be no discernable peak shifting in these samples. Two-dimensional NMR spectra were not collected for these samples. Because of this, we could not verify inclusion, though similar behavior in other samples suggest inclusion has most likely taken place as well for these samples.

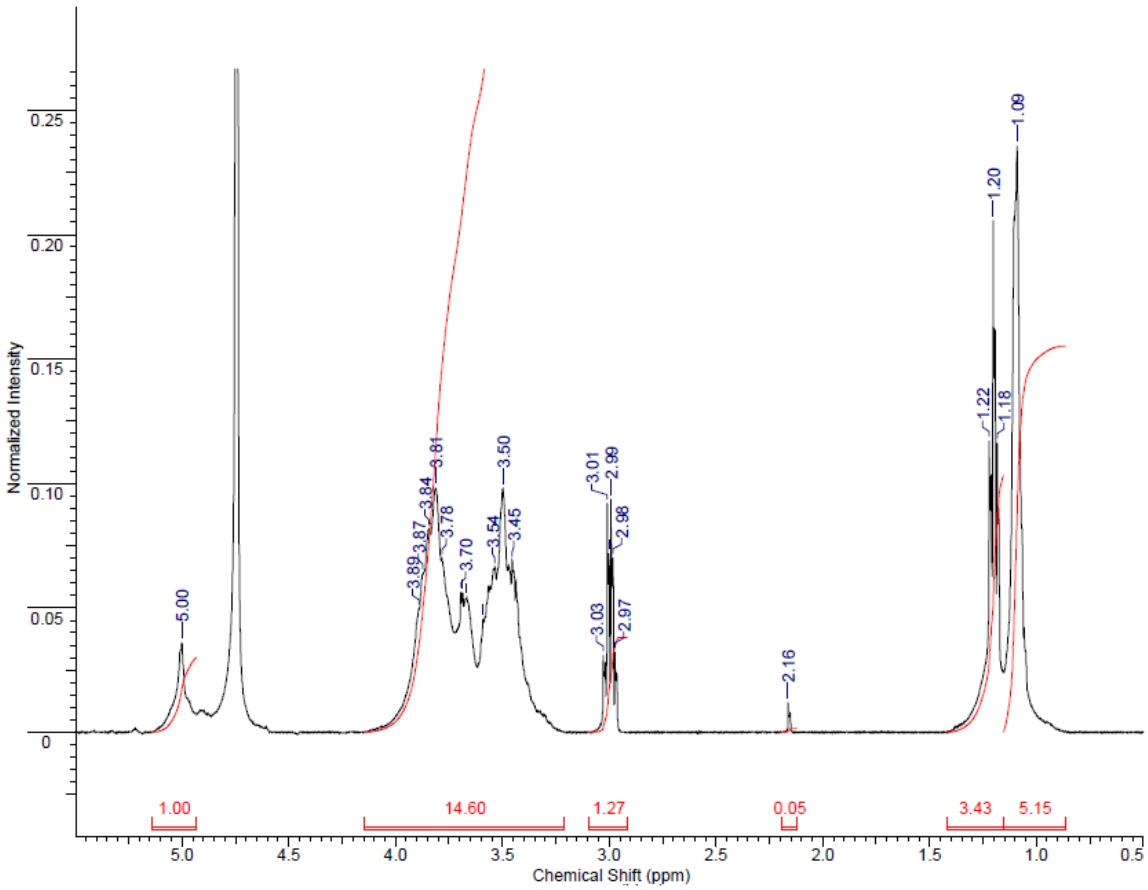

Figure 58: NMR spectrum of Sample 1.2%-50RT-R

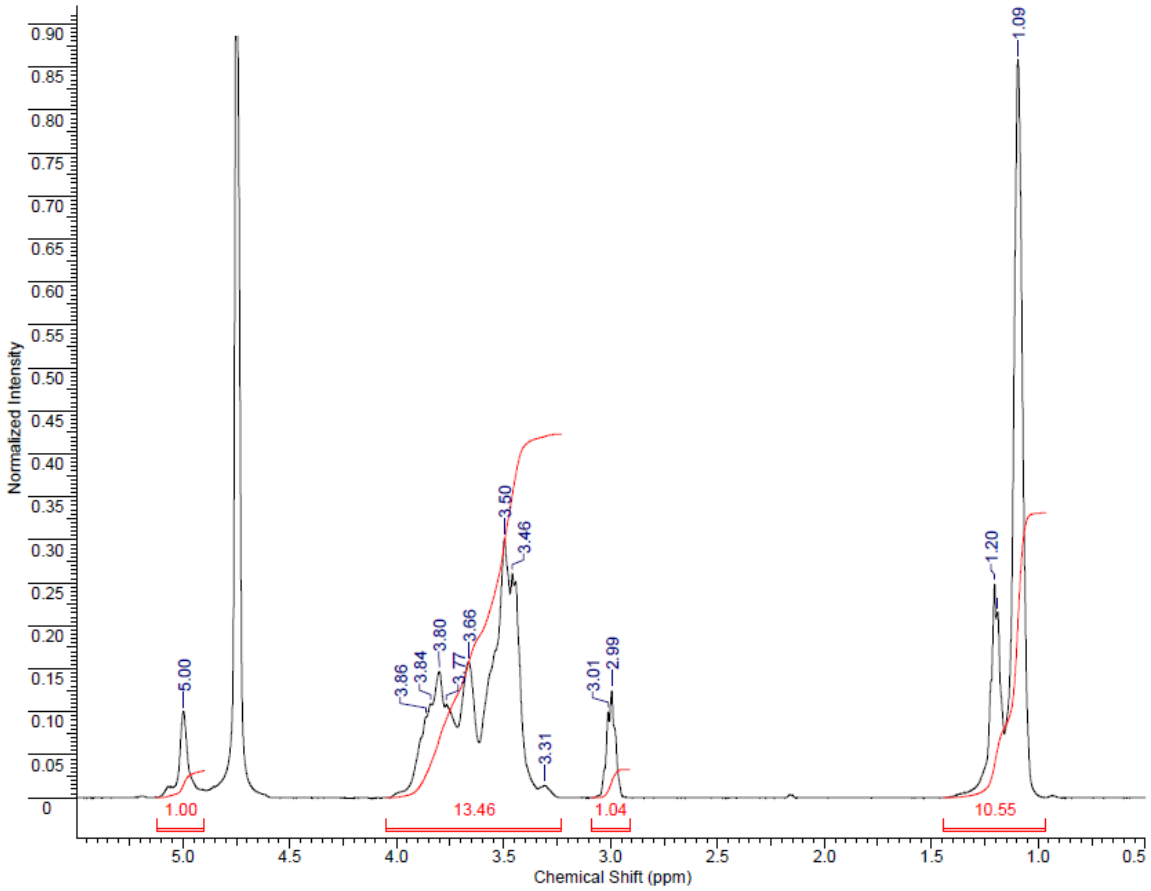

Figure 59: NMR spectrum of sample 3.5%-25RT-R

Zhao and Beckham performed studies on low-coverage, end-capped PEG/α-CD rotaxanes[95] that may help provide some insight into the solution behavior of our material. They examined the solution behavior of these materials and discovered that the IC acts like a polymer coil with a larger radius of gyration than the uncomplexed polymer. It was also observed that, without end-capping of the polymer, most or all of the α-CD's dethread upon introduction of the IC into a good solvent (DMSO). It is possible then, that while we may have polymer threading of PPG into DEAMCT in aqueous solution, introduction into D_2O may have resulted in some dethreading of the DEAMCT. This potential dethreading could

explain the relatively low intensity of the observed peak interactions. End-capping of the PPG after IC formation would be a valuable step to determine whether dethreading is taking place.

X-ray Diffraction Observations

After verifying that we do have inclusion taking place, we should observe the solid behavior of the materials. We would not expect our IC samples to exhibit long-range crystalline behavior but would expect to see this behavior in the control sample using unmodified β-CD. Figures 60 and 61 show the wide angle X-Ray diffraction patterns of a traditional PPG 1,000/β-CD IC as they compare to three of our different PPG/DEAMCT IC samples. Figure 46 demonstrated the presence of the 2θ = 12° peak can act as an indicator of channel IC formation for traditional β-CD's since this peak is not prominent in the as-received cage pattern. A largely amorphous structure is observed for our PPG/DEAMCT IC samples, but with some indication of weak long-range ordering [See Figure 61 (c)].

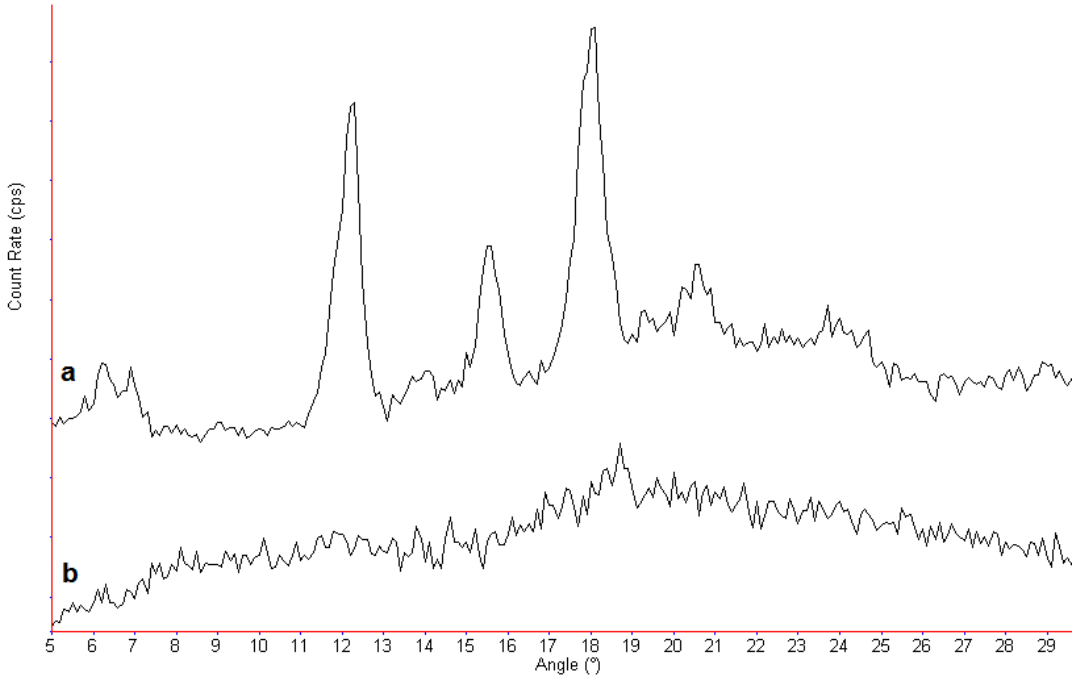

Figure 60: Wide angle XRD patterns of the control 1000 g/mol PPG/β-CD sample (a) and 2.0%-35 (b)

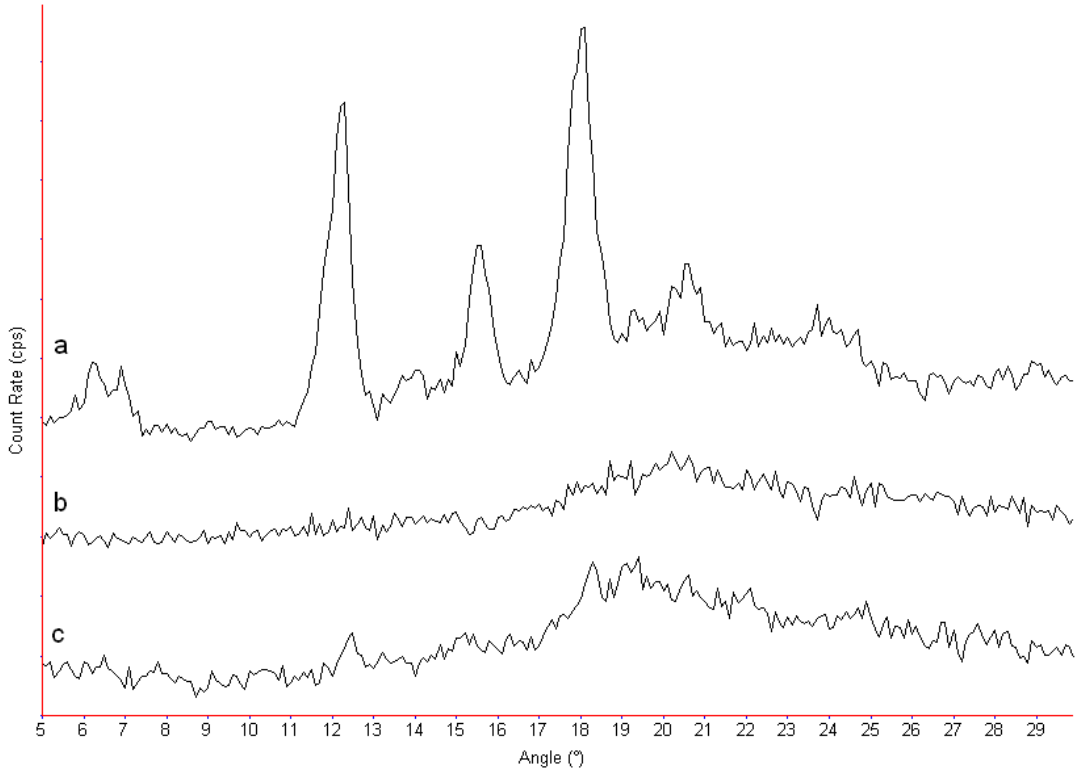

Figure 61: Wide angle XRD patterns of the control 1000 g/mol PPG/β-CD sample (a) as well as DEAMCT/PPG samples 1.2%-50RT-R (b) and 3.5%-25RT-R (c)

Effects of DEAMCT on the Solubility of PPG in Water

PPG is commonly reported as insoluble in water; however, our laboratory tests have demonstrated that PPG with a molecular weight of 2,000 g/mol can be dissolved in water at room temperature up to roughly 1 wt%. From 1 wt% to 4 wt%, the material can be dispersed in the water with increased clouding until the sample is opaque. Above 4 wt%, the PPG will generally form a second phase and be completely insoluble.

DEAMCT was added to aqueous PPG solutions at different concentrations to test whether the addition of the modified CD would increase the solubility of the PPG. The room temperature IC samples formed during these experiments became samples 1.2%-50RT-R and 3.5%-25RT-R.

For the first solubility test, enough DEAMCT was added to a 1.2 wt% aqueous PPG solution (just past the clouding point) to cover the polymer 25% initially. More DEAMCT was added later when no change was observed, enough to cover the polymer by 50%. The solution was left to stir overnight and no changes were observed in the material. The material did not "decloud," nor was there any precipitation of the PPG observed. The water was evaporated and the material was dried overnight in a vacuum oven. This sample became 1.2%-50RT-R.

A higher concentration solution of PPG (3.5 wt%) was formed and to this solution was added a 25% coverage stoichiometric amount of DEAMCT. At this high concentration of PPG, a dispersed, pearlized precipitate was formed while stirring overnight. This precipitate was suspended in solution and appeared partially dissolved. The material was unable to be filtered well, so like the low concentration sample, the water was allowed to evaporate and the material dried in a vacuum oven overnight. This sample became 3.5%-25RT-R.

A non-stoichiometric control sample containing PPG and unmodified β-CD was also prepared. This sample was prepared from the same 3.5 wt% concentration solution with a 25% coverage amount of β-CD added. A solid white precipitate was formed as expected. This material was collected and compared to the DEAMCT samples.

Contrary to our expectations, threading some small percentage of DEAMCT onto PPG did not increase the solubility of the polymer. In fact, doing so seems to decrease the solubility of the material, something that might be expected for high coverage values. It seems likely then that the crystallization of the CD may not be the only reason that traditional IC's precipitate out of solution. Perhaps the modified cyclodextrins are also able to aggregate

without crystallization. If this were the case, it would certainly be reasonable to conclude that this behavior could cause precipitation of the polymeric material.

DSC Observations

DSC scans in the region of the glass transition temperature may also give us more information regarding the interaction of the material. Figure 62 shows DSC cooling scans for various materials taken at a cooling rate 20° C per minute. We can see that the control IC sample made with unmodified β-CD has a very similar T_g to the as-received PPG. As the control IC polymer is only partially covered (≤ 25%), the T_g is visible but less prominent. We know from literature and our observations that the control sample threads the PPG and results in a crystalline IC.[96] Compared to the control sample, however, it seems that the presence of the DEAMCT acts to decrease the T_g of the PPG.

Tonelli's follow-up calculations to the work by Zhao and Beckham attempted to determine the location of the cyclodextrin molecules on the polymer chain.[80] His calculations suggested that small segregated groupings of 3-4 α- CD molecules placed randomly on the PEG chain resulted in a similar radius of gyration increase to that observed by Zhao and Beckham. If the DEAMCTs in our IC's are also dispersed along the polymer chain in small largely non-crystalline groups, then perhaps this might act to increase free volume and reduce the overall molecular entanglement of our PPG chains. This behavior would likely result in a decreased T_g.

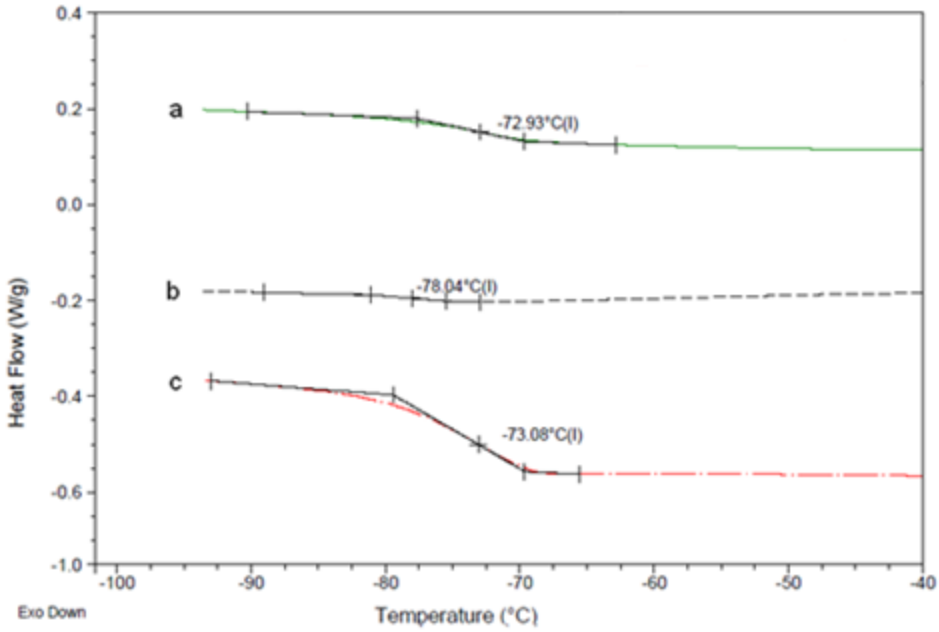

Figure 62: DSC cooling scans of the control PPG 1000/β-CD sample (a), DEAMCT/PPG sample 3.5%-25RT-R (b), and as-received PPG (MW=1000 g/mol) (c)

Studies of IC formation between Modified Cyclodextrin and PEG-PPG-PEG Triblock Copolymers

Introduction

Pluronics (BASF) are the trade name for triblock copolymers consisting of a center block of propylene glycol repeat units surrounded by two blocks of ethylene glycol repeat units. This particular type of triblock has also been given the generalized name of “polaxamer”, but here we will use Pluronic to indicate that we are using the specific type provided by BASF.

The Pluronics naming scheme is simple, yet different from the common polaxamer naming scheme. The letter designation for each Pluronic type represents the physical form of the material. Liquid Pluronics have the letter L. P stands for a soft paste form while F represents a solid Pluronic material. The numerical designation provides two more pieces of information about the material. The first digit (or two digits in a three digit number) represents the molecular weight of the hydrophobic PPG block divided by 300. The last digit indicates the rough molecular weight percentage of the PEG blocks. Figure 63 demonstrates the range of Pluronic materials available from BASF and their common forms.

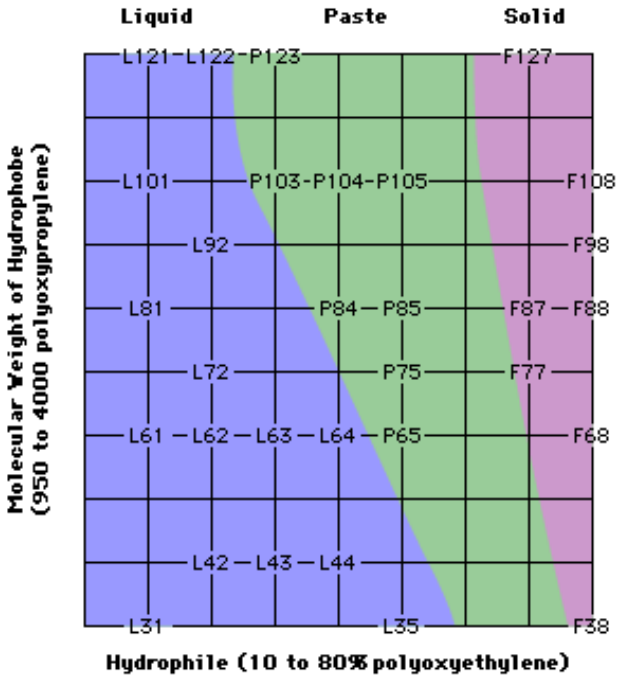

Figure 63: The Pluronics Grid, an ordered schematic of available Pluronic triblock copolymers

It was observed that the naming scheme does not necessarily correlate to exact molecular weight values. Specific molecular weight information can be obtained online and differs slightly from the values obtained using the naming scheme (which is probably generalized to make naming easier). The material data sheets provide relevant molecular weight values and, using these values, the molecular weights of the particular blocks can be calculated.

Previous study of the crystallization properties of Pluronics have shown that the PPG block remains amorphous while the PEG blocks crystallize into ordered lamellar domains.[97] For Pluronic P104, it was demonstrated that the melting of these crystalline regions begin at approximately 35° C and corresponds to multiple FTIR band shifts during this transition. Pluronics are also known to exhibit micellization behavior in aqueous solution.[97-99] As the temperature of a dilute aqueous Pluronic solution increases, the polymer chains go from individual coils to a micellar structure. For P104 in particular, this transition occurs between 20° C at a concentration of 1% w/v to 34° C at 0.01% w/v.[100]

Samples of Pluronics ranging across the entire Pluronics Grid (see Figure 63 above) were provided courtesy of BASF. The hydrophilic PEG arms allowed a higher concentration of PPG to be dissolved in water and thus potentially be complexed. It was anticipated that the complex could also potentially remain soluble in D_2O for NMR observation. It was determined that Pluronics P104 and F108 provided an optimal balance between solubility in water and demonstrated complexation behavior to that of PPG when exposed to DEAMCT in water.

NMR Studies of Pluronic/DEAMCT IC Materials

Pluronic Copolymer NMR Observations

Pluronic P104 and F108 were chosen for the Pluronic IC studies. Their NMR spectra are similar to each other and to PPG 1,000. Figures 64 and 65 are the proton NMR spectra for P104 and F108 Pluronics, respectively. The only difference between these spectra and the PPG 1,000 spectrum is a more prominent peak at 3.68 ppm corresponding to the methylene protons on the PEG blocks and the absence of the small peak at 3.93 (likely protons at the end of the PPG 1000 chains).

If we integrate the PPG methyl peak and the backbone proton peak cluster (contains both PEG and PPG backbone protons) in Figure 64, we arrive at an PEG:PPG repeat unit ratio of 1.16:1. This corresponds to a PEG block molecular weight percentage of 46.8%, only slightly higher than reported for the product.

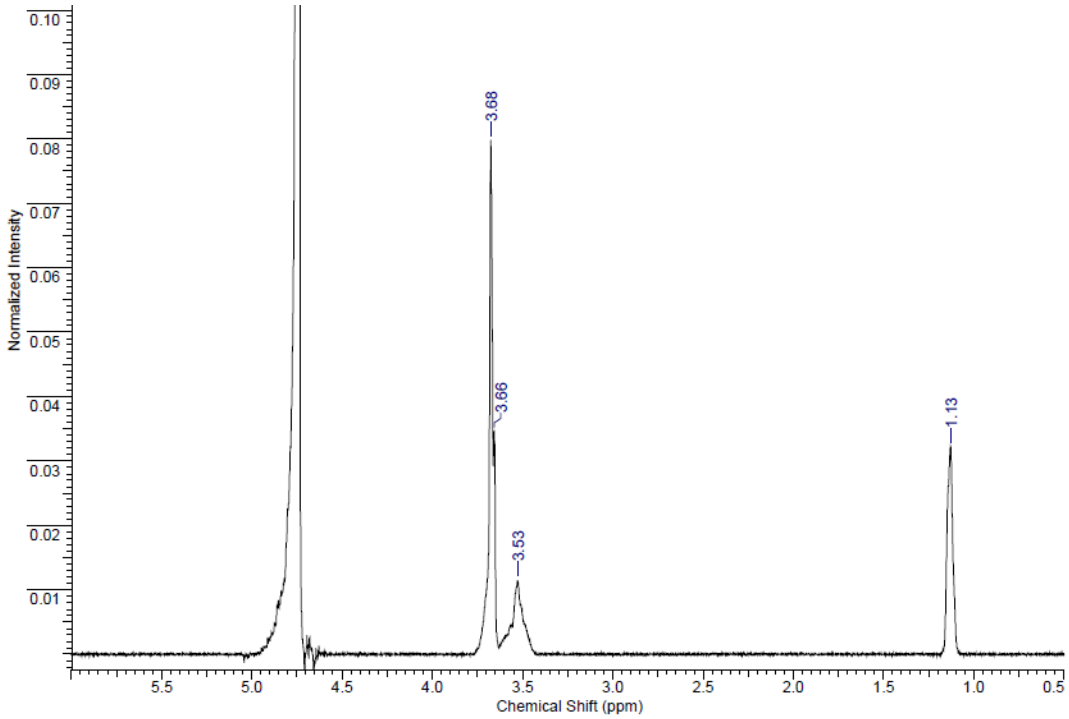

Figure 64: Mercury 400 Proton NMR spectrum of Pluronic P104

If we perform the same integration analysis for F108 (Figure 65), we arrive at an PEG:PPG repeat unit ratio of 6.36:1. This ratio corresponds to a PEG block molecular weight percentage of 82.8%, again very similar to the reported value.

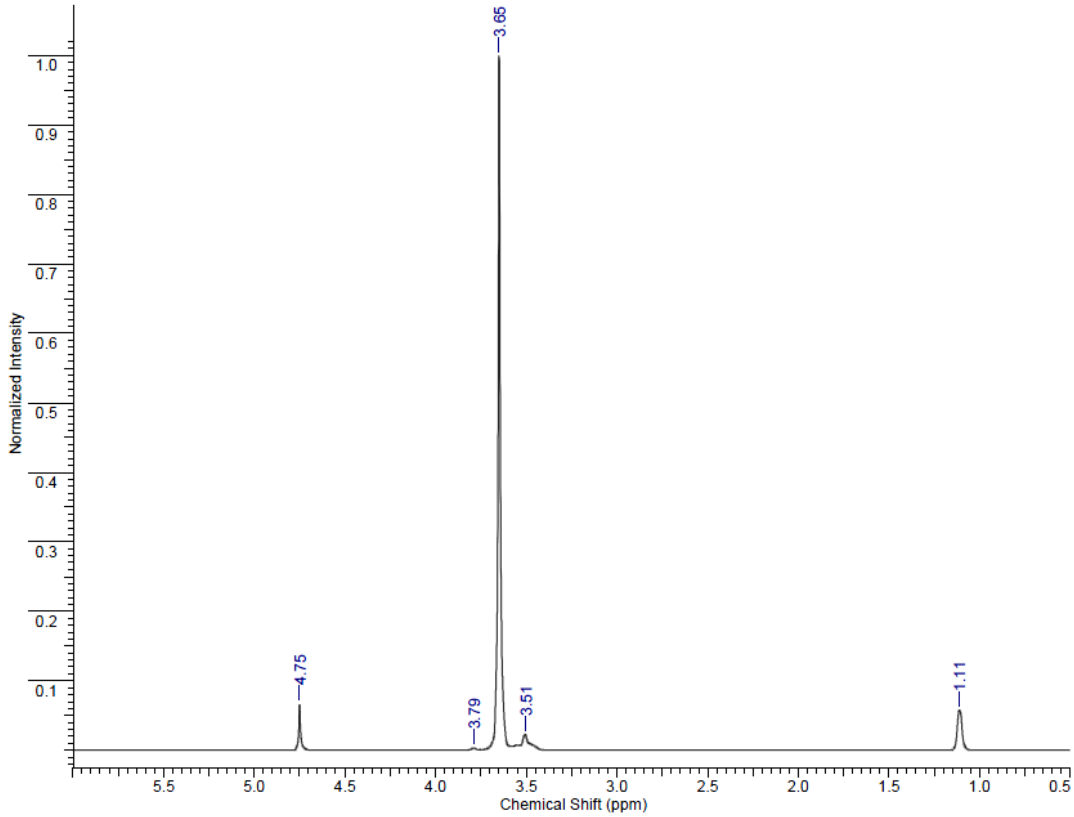

Figure 65: Bruker 500 Proton NMR spectrum of Pluronic F108

The reported PEG:PPG repeat unit ratio for P104 and F108 are 0.89:1 and 5.32:1, respectively. These values are significantly lower than the NMR-observed values, so it should be noted that our particular samples could contain longer PEG blocks than are reported for our samples even though the molecular weights roughly match.

It should also be noted that the slight difference in chemical shift values between Figures 64 and 65 can be attributed to differences in the reference peak value (HDO, 4.75 ppm), not environmental shifting. Small temperature differences between instruments are responsible for a slight discrepancy in the reference peak.

Pluronic IC Sample NMR Observations

To try and determine if there were any NMR interactions taking place between potentially covered PPG blocks and DEAMCT, IC formation was attempted for Pluronic P104 and F108. The higher ratio of PEG units to PPG units would allow for a high percentage of DEAMCT coverage on the center PPG block, while retaining D_2O solubility.

Initially, a P104/DEAMCT IC was produced by dissolving 0.25 g of Pluronic P104 in 10ml deionized water. Then, 2.53 g (approximately enough DEAMCT necessary to cover all of the PG repeat units) was added to the solution. The sample was allowed to stir for three days at room temperature, forming a white pearlized precipitate after approximately one day. After the three days, about half of the water was evaporated to encourage precipitation and the solid sample was collected by centrifugation and dried overnight under vacuum. This sample was named P2.4%-100RT-R.

While this sample did not dissolve completely in D_2O, one-dimensional proton spectra were taken on a Mercury 400 MHz NMR. In this sample, there were a few minor changes that could be observed. Figure 66 shows the stacked spectra of P2.4%-100RT-R (a), P104 (b), and DEAMCT (c). The most prominent change is the downfield shifting of the DEA methylene peak (originally at 2.86). Another less noticeable change is the appearance of a peak shoulder at 3.92 ppm. This small shoulder where there was none before may indicate possible environmental changes in the H3 proton of the DEAMCT.

Another possible conclusion to draw from the DEAMCT spectra comes from the two sharp peaks in the presence of an otherwise low resolution spectrum. Earlier in the chapter we discussed that there may possibly exist both reacted DEA and unreacted DEA in our DEAMCT NMR samples. It was also suggested that DEA may possibly incorporate into the DEAMCT and later be replaced by the polymer. The presence of sharp peaks suggests that

the material creating these peaks is able to move more freely within the solution. Small molecules often have sharper peaks in solution NMR compared to bulkier molecules like CD or polymers. Based on these observations, it is very possible that the 1.13/2.86 peaks belong to the free DEA. These values correspond to the “b” DEA peaks discussed in the original DEAMCT NMR analysis. In this particular sample, both “a” DEA peaks are spread out in a fashion similar to the rest of the cyclodextrin peaks.

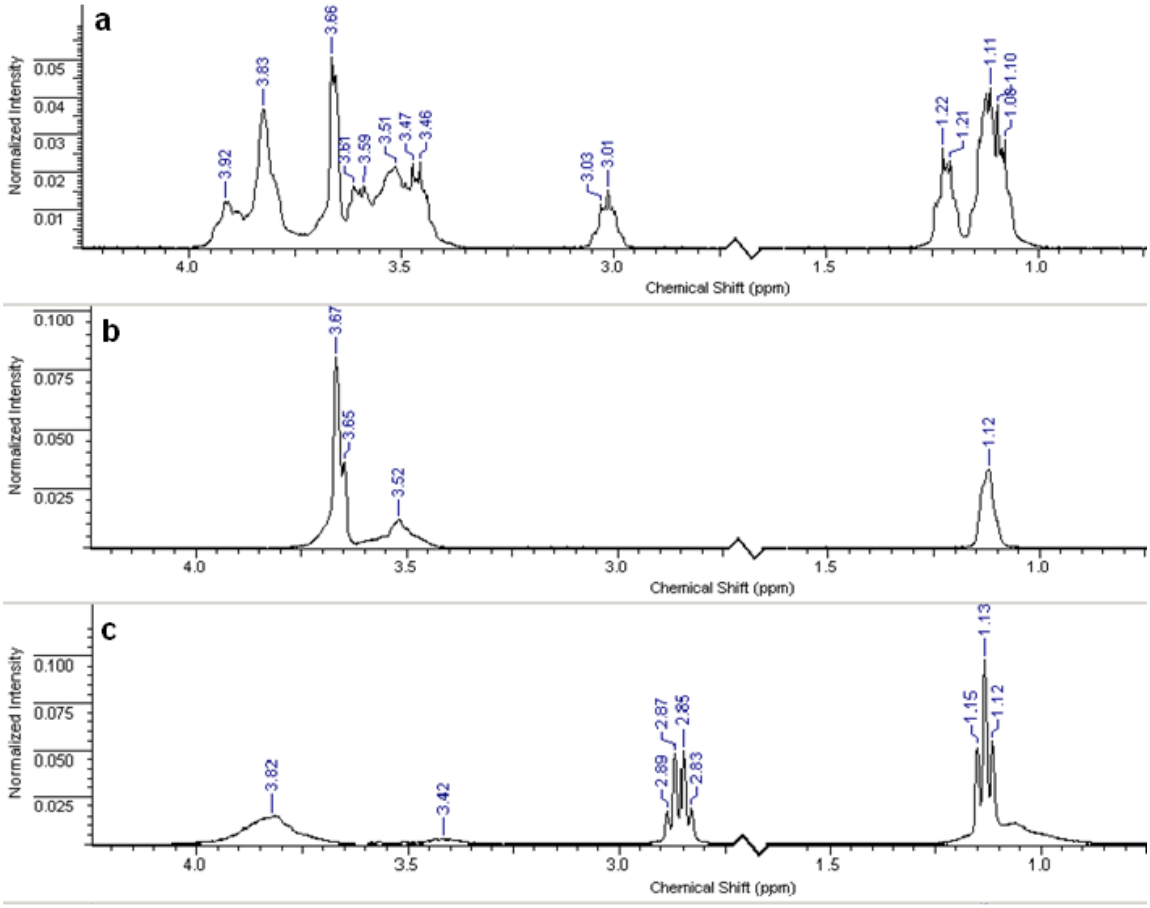

Figure 66: Mercury 400 Proton NMR spectra of P2.4%-100RT-R (a), Pluronic P104 (b), and DEAMCT (c)

A second IC sample was produced with F108. The goal was to produce a sample that was even more soluble than P2.4%-100RT-R. 1.51 grams of DEAMCT were dissolved in 15ml deionized water. 0.484 g Pluronic F108 were then dissolved into the DEAMCT solution. The solution was allowed to sit for a period of 4 days, during which time no precipitation was observed. The water was evaporated from the sample under atmospheric conditions and then the material was dried overnight under vacuum. This sample is referred to as P3.1%-105RT-R.

Figure 67 shows the stacked spectra of P3.1%-105RT-R (a), F108(b), and DEAMCT (c). The particular DEAMCT spectrum used here was collected with the Bruker 500 NMR and does not show a shift for the “b” DEA methylene peaks. It is unclear what the difference between both DEAMCT samples is or why the shift value would be different. It is possibly tied to inclusion of the DEA.

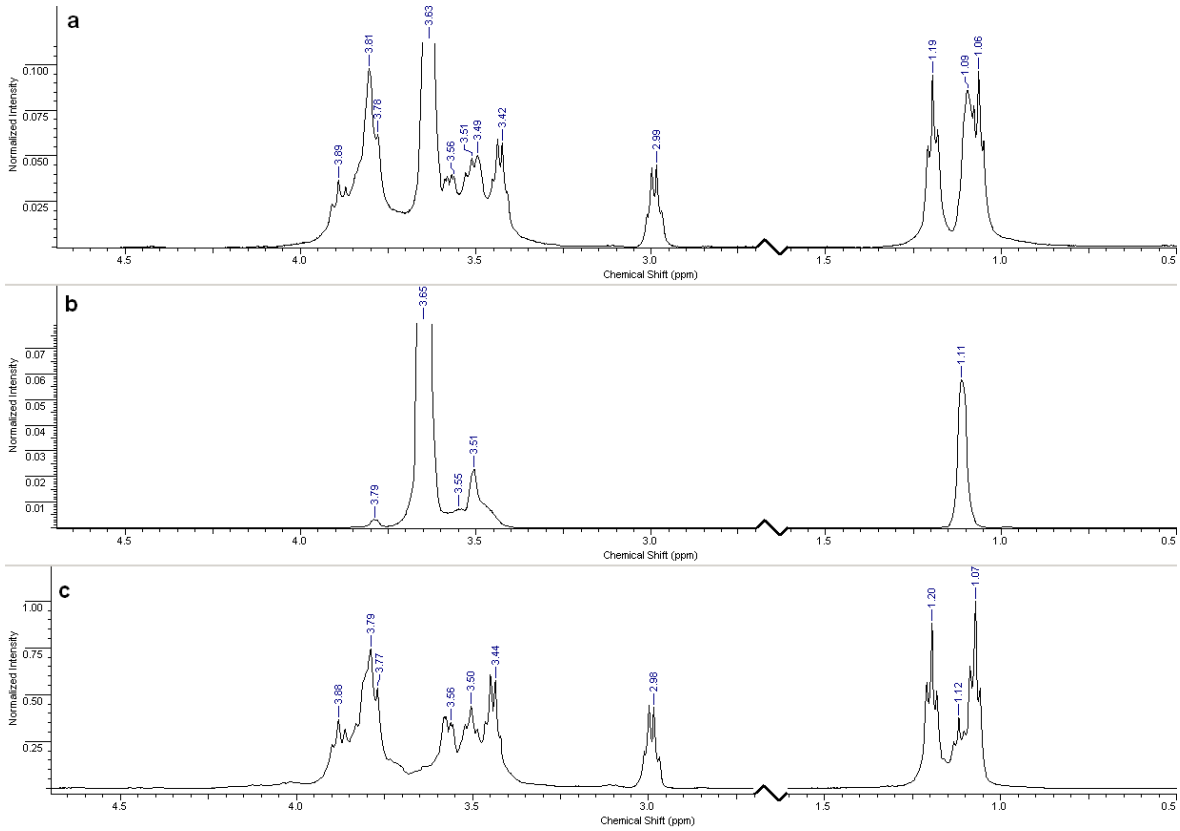

Figure 67: Bruker 500 proton NMR spectra of P3.1%-105RT-R (a), Pluronic F108 (b), and DEAMCT (c)

Two-dimensional ROESY NMR spectra were collected for P3.1%-105RT-R in the same fashion as the PPG IC samples. Figures 68 and 69 below are the spectra in the familiar H1 and H2 proton regions. Highlighted are the areas of interest where prior NOE interactions were observed for the PPG/DEAMCT IC samples. For the H1 interaction, there seems to be evidence of a small peak corresponding to backbone proton interaction in a similar fashion to the PPG IC samples. There also seems to be some activity in the H2 region. The proximity to the large PEO backbone proton peak creates a large amount of background signal, making it hard to distinguish whether the expected cross-peak is present. No other new cross-peaks indicating polymer-to-CD interactions were observed.

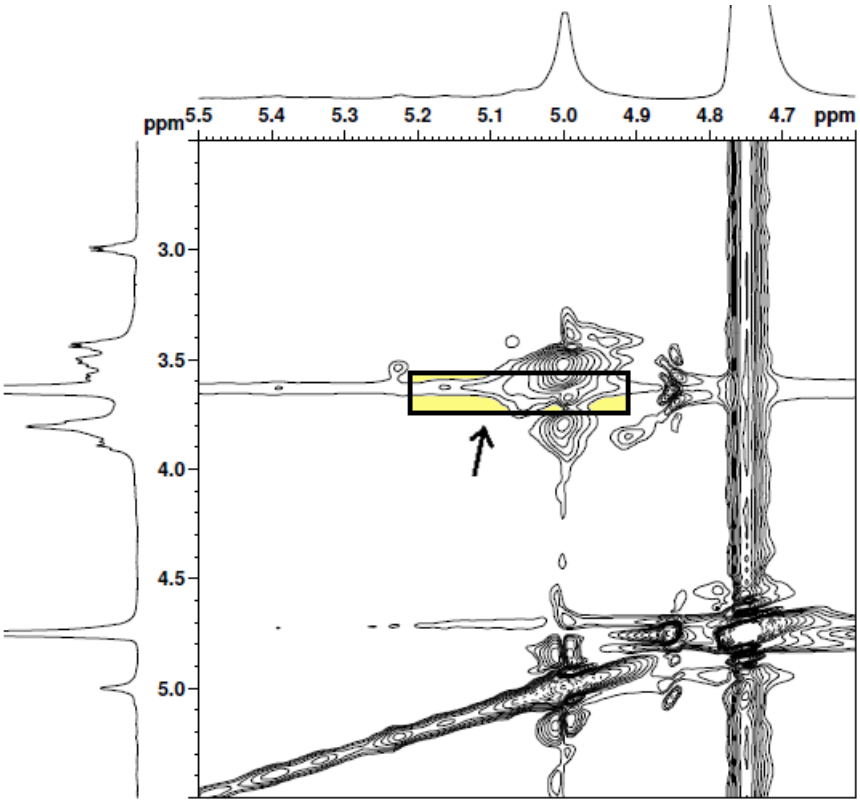

Figure 68: ROESY NMR spectrum of P3.1%-105RT-R [H1 CD proton region]

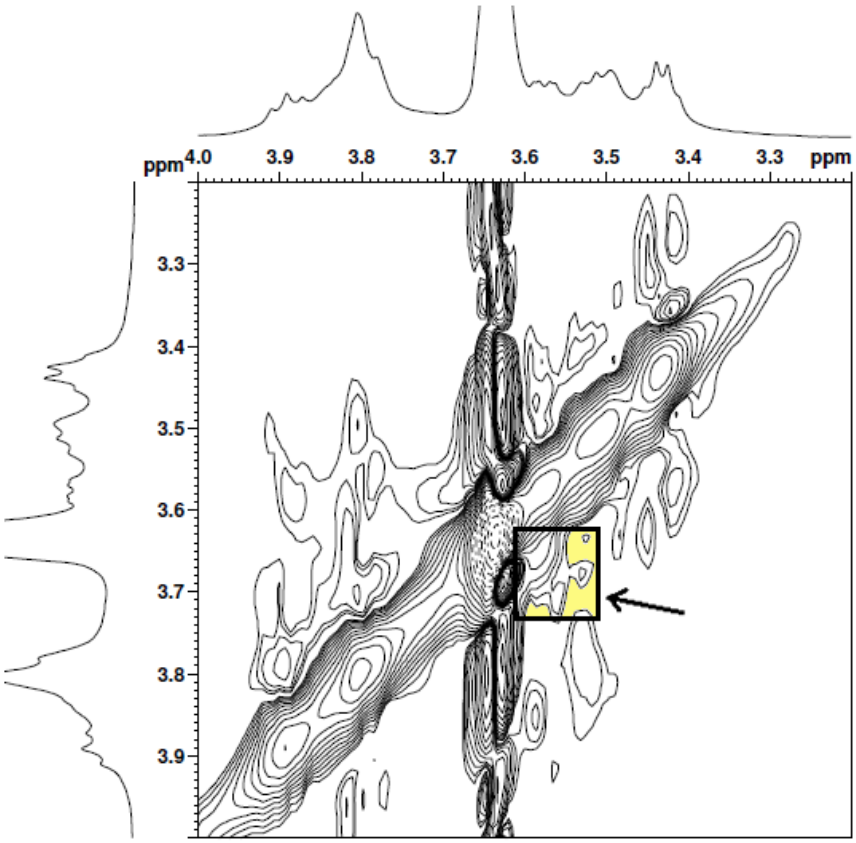

Figure 69: ROESY NMR spectrum of P3.1%-105RT-R [H2 CD proton region]

Solubility of Pluronic in Water

Solubility tests for Pluronic P104 were carried out in a similar fashion to PPG with the goal of finding out the effects of the presence of DEAMCT. Pluronic P104 (BASF) has a reported solubility of ">10%." This information was confirmed as solutions of 5 wt% and 10wt% P104 in water were completely dissolved. DEAMCT was added to these solutions at a 15% coverage stoichiometric ratio. The DEAMCT was able to completely dissolve and the samples were stirred over a period of several days. A pearlized precipitate began forming

after roughly one hour for the 10% sample and quickly resulted in an opaque suspension. The 5% solution also formed the same precipitate, but took a period of 24 hours to reach the same level of precipitation that the 10% solution only took a few hours to reach.

This partially soluble precipitate is presumably an IC between the PPG section of the Pluronic triblock and the DEAMCT. The solubility characteristics of this precipitate remained constant even at a temperature of 80° C. A 10 wt% solution containing only the Pluronic was held at 80°C (above the critical micellization temperature) to examine whether the pearlized precipitate was due to a disruption of the micelle structure; however, only a thickening of the material was observed (presumably from the micellization of the polymer chains). No precipitation or opacity similar to that of the IC samples was observed.

The precipitated 5 wt% P104/IC solution was diluted in an attempt to find a concentration at which the precipitate would completely dissolve; however at concentrations of 2.5 wt% and 1.25 wt%, the pearlized precipitate remained and would not dissolve. It seemed that even at these low concentrations and only a 15% coverage stoichiometric ratio, the CD-polymer interaction was enough to create an insoluble IC.

X-Ray Diffraction

X-ray diffraction patterns were collected for P2.4%-100RT-R, a pure PEG, and a reference IC made in a similar fashion to P2.4%-100RT-R, but with traditional β-CD, and are displayed in Figure 70. Our intention was to examine the crystalline behavior of the PEG blocks before and after complexation. It is clear that the two distinct peaks at 2θ = 19 and 23° correspond to the crystalline structure of PEG and that these two peaks are not observed in the reference β-CD- and DEAMCT-IC samples. Similar behavior was also reported recently by Tsai et al. for Pluronic-β-CD-ICs,[101] and suggests that the PEG crystallization is somehow

inhibited as a result of the IC formation process. It can also be observed that the reference β-CD- and DEAMCT-IC diffraction patterns are very similar, though the reference IC (P104-β-CD-IC) seems slightly more ordered (as determined by their slightly better resolved and more prominent peaks).

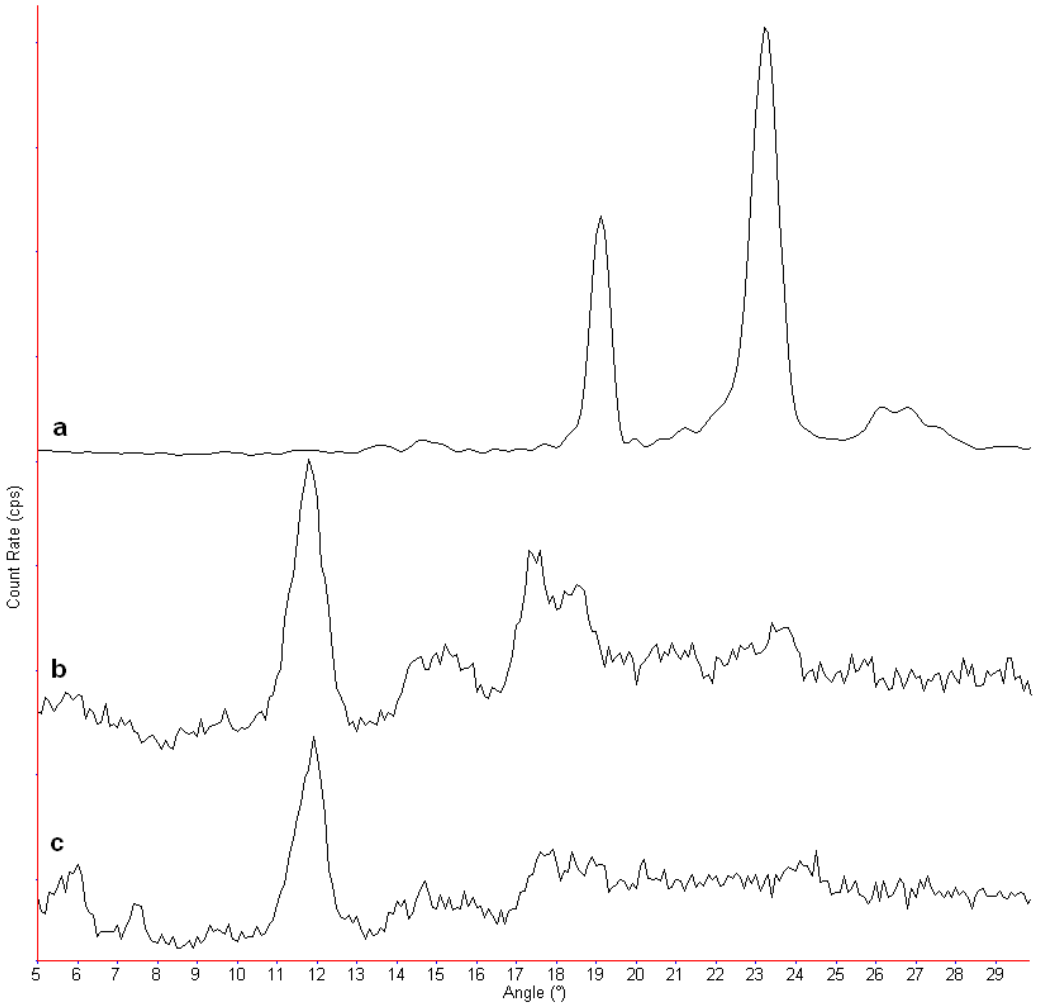

Figure 70: XRD patterns of a 2000 Mw PEG (a), a reference P104-β-CD IC (b) and P2.4%-100RT-R (c)

Since P2.4%-100RT-R should contain close to 100% covered PPG blocks, we would expect to observe a forced proximity of the DEAMCT molecules, which would likely result in diffraction behavior similar to the IC channel structure, at least along the polymer chain direction. In this regard, the diffraction peak at 2θ ~ 6°, which corresponds to the close packing of adjacent pairs of CDs threading the same chain, is noticeably stronger in the DEAMCT-IC, while the peaks at 2θ ~ 12°, which corresponds to the height of a single CD, are closely similar in magnitude for both ICs. This might imply that the rather bulky diethylaminotriazinyl substituents are predominantly attached to one rim or edge of the DEAMCT, thereby permitting the close approach between the unsubstituted rims of pairs of DEAMCT. Similar pairing is not observed in the control Pluronic-β-CD-IC because both rims are unsubstituted and permit H:T, T;T, and H:T threading and packing on the PPG blocks.

The diethylaminotriazinyl substituents could also potentially interfere with and possibly eliminate the ordered packing of DEAMCT-threaded Pluronics in the lateral directions. Perhaps this is the explanation for the suppression of peaks at 2θ = 14-16 and 17-19°, which reflect this lateral packing and are observed to be much more prominent in the control Pluronic-IC made with unmodified β-CD.

Possibly more important is the comparison of the X-ray diffraction seen for the Pluronic P2.4%-100RT-R- (Figure 70) and for the PPG-DEAMCT-ICs (Figures 60 and 61). While the PPG-ICs with DEAMCT appear largely amorphous, the Pluronic-ICs with DEAMCT are clearly crystalline. Both PPG-DEAMCT (high coverage) and Pluronic-DEAMCT-ICs show scattering from single threaded DEAMCTs, as reflected by the peak at 2θ ~ 12° , while only the Pluronic-DEAMCT-ICs show a peak at 2θ ~ 6°, corresponding to an adjacent pair of DEAMCTs threaded on the same PPG chain.[80] Similar behavior was also observed by Tsai et al. for Pluronic-β-CD-ICs.[101] This means that DEAMCTs threaded lightly over PPG homopolymer do not tend to aggregate, not even in pairs, while they do when threaded tightly over the Pluronic PPG blocks. Also note in Figure 70 the peaks at 14° < 2θ < 25°,

which correspond to lateral scattering from CDs threaded on adjacent included polymer chains, appear for Pluronic-ICs formed with both DEAMCT and β-CD hosts, but are less pronounced for the Pluronic-DEAMCT-IC. Again, the lateral packing of adjacently threaded PPG blocks is likely more difficult for DEAMCT, with each containing ~ 3 bulky diethylaminotriazinyl groups on average.

DSC

DSC scans were taken of the P104 IC sample, P2.4%-100RT-R. Initial scans were in the temperature range of both the crystallization of the PEG blocks and the glass transition of the PPG block; however, it was quickly observed that the coverage of the PPG block by the modified CD acted to suppress the T_g. Future scans were only performed to measure the changes in the PEG melting and crystallization.

Figure 71 shows the heating and cooling scans of the P2.4%-100RT-R as well as the as-received Pluronic P104 and a reference P104 IC produced with traditional β-CD. The crystallization of pure P104 can be observed quite clearly, although in both the reference traditional IC and the modified IC, the crystallization of the PEG blocks are completely suppressed.

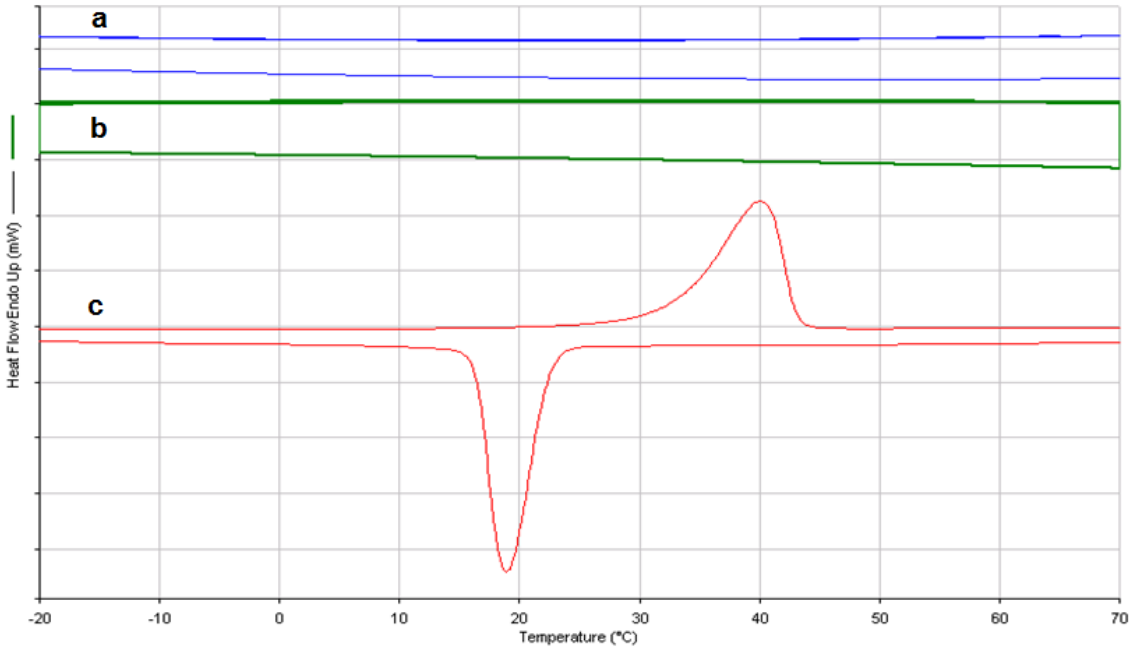

Figure 71: DSC heating and cooling scans of a reference P104-β-CD IC (a), P2.4%-100RT-R (b), and as-received P104 (c)

This absence of a PEG block crystallization peak supports the observed diffraction data. It is clear that the PEG blocks do not exist in a crystalline state after inclusion. Coverage of the PEG block by the CDs is unlikely as β-CD has shown no propensity to form an IC with PEG. The most likely explanation for this phenomenon is that the CDs threaded on the PPG blocks somehow allow the PEG segments to disperse, drastically reducing the crystallinity. It has been demonstrated that PEG and PPG are not normally miscible[102], so the threading of the PPG must act to compatibilize these two materials.

This is surprising for the crystalline reference IC. One would expect that for a traditional IC with larger β-CD crystalline regions, the PEG blocks would not be able to disperse enough to suppress their crystallization. If this does take place, however, then PEG dispersion should be theoretically easier for a modified CD IC with little lateral packing. Perhaps if this is taking

place, modified CD could act as a compatibilizer between hydrophilic and hydrophobic polymers.

Conclusions

ROESY 2D NMR offers compelling evidence that DEAMCT is able to interact with the Pluronic copolymers and PPG at high and relatively low coverage concentrations. Repeated evidence of through-space interaction between the cyclodextrin H1 and H2 protons and polymer backbone protons suggest that inclusion of this material is possible. The largely disrupted crystallinity of PPG/DEAMCT ICs, due to their extensive modification, does not necessarily prevent polymer threading.

X-ray diffraction patterns of low coverage samples demonstrate a lack of crystallinity, while high coverage samples begin to show crystalline order, suggesting that at high coverage concentrations, the DEAMCT molecules begin to order. In the Pluronic IC samples, PEG block crystallinity was inhibited upon complexation, suggesting that the threading of the hydrophobic PPG block by the outwardly hydrophilic CDs may act to compatibilize the threaded PPG and unthreaded PEG blocks. Even though neat DEAMCT does not crystallize, the Pluronic/DEAMCT ICs do, but with a packing of DEAMCTs along each threaded PPG block and between their threaded PPG blocks that is distinct from those in Pluronic ICs formed with unmodified β-CD.

The observed solubility behavior was not as expected. Upon complexation of DEAMCT and Pluronic, a pearlized partially-soluble precipitate was formed and could not be redissolved with the addition of more solvent (water). Solubility of PPG alone was also reduced upon complexation. The addition of the modified cyclodextrin seems to decrease the polymer solubility, suggesting that crystallization of traditional IC's is not the only factor responsible

for IC insolubility. Perhaps limiting CD coverage to a lower percentage would prevent the polymer from precipitating out of solution.

DSC studies of the PPG/DEAMCT ICs demonstrate a slight reduction in the T_g of the material, similar to the behavior observed in a co-dissolved and precipitated well-dispersed physical mixture of PPG and non-threading α-CD. This suggests that the DEAMCT molecules are likely well-dispersed along the polymer chain rather than grouped together.

While many specific expected behaviors for these non-crystalline IC's were not observed, we were able to demonstrate the ability for non-crystalline modified cyclodextrin to thread onto a PPG polymer chain and at sufficiently high coverage to form crystalline ICs. This fact is a proof-of-concept that non-crystalline modified cyclodextrins do not lose their ability to thread and that a novel type of IC with unique properties may be formed.

Harada demonstrated that the specific pairing of low molecular weight PPG (M_w = 1000 g/mol) with β-CD readily formed an IC.[103] This, along with the commercial availability of MCT, governed our decision on the particular polymer pairings studied. Harada observed that as the molecular weight of the PPG is increased, the yield of the IC formation process is drastically reduced. A decrease from 98% yield to 30% yield in going from a molecular weight of 1000 g/mol to 4000 g/mol was also observed. What this suggests is that PPG would be a poor candidate for studies of modified CD and higher molecular weight polymers. As PPG is one of the few polymers to include inside β-CD, it is logical to try a modified α- or γ-CD if the goal of future work were to include the study of more stable IC's containing higher molecular weight polymer guests.

Taking into consideration the potential inadequacies of our particular PPG/modified β-CD pairing, we can make some suggestions about future work to further our understanding of the behavior of polymer complexes formed with non-crystalline CD.

Future Work

Because we have shown that the threading of DEAMCT onto PPG and Pluronic triblock copolymer is possible, it would be valuable to further study the behavior of these IC's both in the solid state and in solution. Viscosity measurements would likely prove valuable, especially when compared to a solution of PPG and a non-threading CD such as α-CD. Melt rheology and other IC physical property measurements should be of interest as well. We may even be able to observe a reduction or elimination of the shape-memory behavior often found in non-stoichiometric IC's when using a non-crystalline modified CD.

Because DEAMCT dethreading may be taking place in aqueous solution, end-capping the polymer chains after IC formation may be advantageous. These materials could then be studied, revealing whether or not dethreading occurs and has an effect on the IC behavior. The solution (and possibly solid-state) behavior of these end-capped rotaxanes would likely differ from the uncapped IC's if dethreading is taking place. End-capping would also allow for the study of these materials in a better NMR solvent, such as d_6-DMSO.

In future studies of the formation and properties of non-crystalline modified CD IC's, it is likely that a transition from the modified β-CD pairing to a modified α- or γ-CD would allow for the formation of IC's with higher molecular weight polymers in higher yield. While the present work offers strong evidence that we are able to thread these modified cyclodextrins onto polymer chains, many of the property differences were unexpected and perplexing.

Higher molecular weight polymers are generally more stable and allow for less CD dethreading than low molecular weight polymers. The chemical pathways leading to the triazine-modified β-CD are well defined by Reuscher and Hirsenkorn and could likely be applied to an α- or γ-CD, allowing for the inclusion of a larger molecular weight polymer into similarly modified cyclodextrin.[86]

A larger molecular weight polymer would also allow for finer control of the coverage stoichiometry. The effects of increasingly higher polymer coverage on polymer coil size, solubility, and thermal transition behavior could be examined in greater detail. It is generally assumed that the crystallinity of the traditional CD's is responsible for the insolubility of a polymer IC; however, our work suggests that threading without crystallization may also create an IC with low solubility.

Other techniques useful for studying the polymer chain size in solution, such as dynamic light scattering, would be worth exploring on both our current and future systems. While SEC studies can be affected by polarity and filtering and are limited to particular solvents, dynamic light scattering would allow for the study of the solution behavior in a more direct way. This information may also provide further insight into grouping or dispersion of the CD's threaded on the polymer chain. There is more to understand regarding the grouping of non-crystalline CD's at high coverages and how this grouping is similar to traditional CD crystalline behavior.

A variety of questions remain unanswered and new questions will undoubtedly arise as a result of future study of polymer/non-crystalline modified CD IC's. Multiple research pathways exist that will allow for the answering of these questions and a deeper understanding of the complex interactions existing between polymers and cyclodextrins in both traditional and non-crystalline inclusion complexes.

References

(1) Villiers, A. *Cr. Hebd. Acad. Sci.* **1891**, *112*, 536.

(2) Schardinger, F. *Wein. Klin. Wochenschi* **1904**, *17*, 207.

(3) Schardinger, F. *Zentalblatt. Bakte. 2* **1905**, *14*, 722.

(4) Schardinger, F. *Zentalblatt. Bakte. 2* **1911**, *29*, 188.

(5) Pringsheim, H. *Chemistry of the Saccharides*; McGraw-Hill: New York, 1932.

(6) Walton, R. *A Comprehensive Survey of Starch Chemistry*; Chemical Catalog Company: New York, 1928.

(7) Freudenberg, K.; Rapp, W. *Ber. Dtsch. Chem. Ges. 2* **1936**, *69*, 2041-2045.

(8) Freudenberg, K.; Boppel, H.; Meyer-Delius, M. *Naturwissenschaften* **1938**, *26*, 123-124.

(9) Freudenberg, K.; Meyer-Delius, M. *Ber. Dtsch. Chem. Ges. 2* **1938**, *71*, 1596-1600.

(10) Freudenberg, K.; Blomqvist, G.; Ewald, L.; Soff, K. *Ber. Dtsch. Chem. Ges. 1* **1936**, *69*, 1258-1266.

(11) Freudenberg, K.; Cramer, F. *Z Naturforsch. B* **1948**, *3*, 464-464.

(12) French, D. *Adv. Carbohyd. Chem.* **1957**, *12*, 189-280.

(13) Cramer, F. *Einschlussverbindungen*; Springer: (Berlin), 1964.

(14) Szejtli, J. *Chem. Rev.* **1998**, *98*, 1743-1754.

(15) Cacialli, F.; Wilson, J. S.; Michels, J. J.; Daniel, C.; Silva, C.; Friend, R. H.; Severin, N.; Samorì, P.; Rabe, J. P.; O'Connell, M. J.; Taylor, P. N.; Anderson, H. L. *Nat. Mater.* **2002**, *1*, 160-164.

(16) Del Valle, E. *Process. Biochem.* **2004**, *39*, 1033.

(17) Linert, W.; Margl, P.; Renz, F. *Chem. Phys.* **1992**, *161*, 327-338.

(18) Saenger, W.; Steiner, T. *Acta Crystallogr. A* **1998**, *54*, 798-805.

(19) Rusa, C. C.; Bullions, T. A.; Fox, J.; Porbeni, F. E.; Wang, X.; Tonelli, A. E. *Langmuir* **2002**, *18*, 10016-10023.

(20) Giordano, F.; Novak, C.; Moyano, J. R. *Thermochim. Acta* **2001**, *380*, 123-151.

(21) Nakai, Y.; Yamamoto, K.; Terada, K.; Kajiyama, A.; Sasaki, I. *Chem. Pharm. Bull.* **1986**, *34*, 2178-2182.

(22) Endo, T.; Nagase, H.; Ueda, H.; Kobayashi, S.; Nagai, T. *Chem. Pharm. Bull.* **1997**, *45*, 532-536.

(23) Schneider, H.; Hacket, F.; Rudiger, V.; Ikeda, H. *Chem. Rev.* **1998**, *98*, 1755-1786.

(24) Rusa, C. C.; Bridges, C.; Ha, S.; Tonelli, A. E. *Macromolecules* **2005**, *38*, 5640-5646.

(25) Uyar, T.; El-Shafei, A.; Wang, X.; Hacaloglu, J.; Tonelli, A. *J. Incl. Phenom. Macro.* **2006**, *55*, 109-121.

(26) Suzuki, M.; Tsutsui, M.; Ohmori, H. *Carbohyd. Res.* **1994**, *261*, 223-230.

(27) Rusa, C.; Rusa, M.; Peet, J.; Uyar, T.; Fox, J.; Hunt, M.; Wang, X.; Balik, C.; Tonelli, A. *J. Incl. Phenom. Macro.* **2006**, *55*, 185-192.

(28) Wei, M.; Tonelli, A. E. *Macromolecules* **2001**, *34*, 4061-4065.

(29) Martínez, G.; Gómez, M. A.; Villar-Rodil, S.; Garrido, L.; Tonelli, A. E.; Balik, C. M. *J. Polym. Sci. Pol. Chem.* **2007**, *45*, 2503-2513.

(30) Rusa, C. C.; Shuai, X.; Shin, I. D.; Bullions, T. A.; Wei, M.; Porbeni, F. E.; Lu, J.; Huang, L.; Fox, J.; Tonelli, A. E. *J. Polym. Environ.* **2004**, *12*, 157-163.

(31) Uekama, K.; Hirayama, F.; Irie, T. *Chem. Rev.* **1998**, *98*, 2045-2076.

(32) Li, J.; Yan, D.; Jiang, X.; Chen, Q. *Polymer* **2002**, *43*, 2625-2629.

(33) Kawasaki, J.; Satou, D.; Takagaki, T.; Nemoto, T.; Kawaguchi, A. *Polymer* **2007**, *48*, 1127-1138.

(34) Lu, J.; Mirau, P.; Tonelli, A. *Prog. Polym. Sci.* **2002**, *27*, 357-401.

(35) Zhao, T.; Beckham, H. W. *Macromolecules* **2003**, *36*, 9859-9865.

(36) Kildemark, N.; Larsen, K.; Zimmerman, W. *J. Inclus. Phenom. Mol.* **1996**, *25*, 89-92.

(37) Mentzafos, D.; Mavridis, I. M.; Le Bas, G.; Tsoucaris, G. *Acta. Crystallogr. B Struct. Sci.* **1991**, *47*, 746-757.

(38) Hunt, M. The Role of Water in the Formation and Structure of Oligomer/Alpha-Cyclodextrin Inclusion Complexes **2007**.

(39) Bullions, T. A.; Wei, M.; Porbeni, F. E.; Gerber, M. J.; Peet, J.; Balik, M.; White, J. L.; Tonelli, A. E. *J. Polym. Sci. B Polym. Phys.* **2002**, *40*, 992-1012.

(40) Schneider, H.; Hacket, F.; Rudiger, V.; Ikeda, H. *Chem. Rev.* **1998**, *98*, 1755-1786.

(41) Uyar, T.; Gracz, H.; Rusa, M.; Shin, I.; Elshafei, A.; Tonelli, A. *Polymer* **2006**, *47*, 6948-6955.

(42) Hedges, A. *Chem. Rev.* **1998**, *9*, 2035.

(43) Becheri, A.; Lo Nostro, P.; Ninham, B. W.; Baglioni, P. *J. Phys. Chem. B* **2003**, *107*, 3979-3987.

(44) Peet, J.; Rusa, C. C.; Hunt, M. A.; Tonelli, A. E.; Balik, C. M. *Macromolecules* **2005**, *38*, 537-541.

(45) Hu, J.; Tao, Z.; Li, S.; Liu, B. *J. Mater. Sci.* **2005**, *40*, 6057-6061.

(46) Uyar, T.; Rusa, C.; Hunt, M.; Aslan, E.; Hacaloglu, J.; Tonelli, A. *Polymer* **2005**.

(47) Karaky, K.; Reynaud, S.; Billon, L.; François, J.; Chreim, Y. *J. Polym. Sci. A Polym. Chem.* **2005**, *43*, 5186-5194.

(48) Miura, Y.; Narumi, A.; Matsuya, S.; Satoh, T.; Duan, Q.; Kaga, H.; Kakuchi, T. *J. Polym. Sci. A Polym. Chem.* **2005**, *43*, 4271-4279.

(49) Rusa, C. C.; Tonelli, A. E. *Macromolecules* **2000**, *33*, 1813-1818.

(50) Rusa, C. C.; Luca, C.; Tonelli, A. E. *Macromolecules* **2001**, *34*, 1318-1322.

(51) Xue, J.; Jia, Z.; Jiang, X.; Wang, Y.; Chen, L.; Zhou, L.; He, P.; Zhu, X.; Yan, D. *Macromolecules* **2006**, *39*, 8905-8907.

(52) He, Y.; Inoue, Y. *Biomacromolecules* **2003**, *4*, 1865-1867.

(53) He, Y.; Inoue, Y. *J. Polym. Sci. B Polym. Phys.* **2004**, *42*, 3461-3469.

(54) Liu, Y.; Fan, X. *Biomaterials* **2005**, *26*, 6367.

(55) Savarino, P. *Dyes Pigments* **2004**, *60*, 223-232.

(56) Cireli, A.; Yurdakul, B. *J. Appl. Polym. Sci.* **2006**, *100*, 208-218.

(57) Okumura, Y.; Ito, K. *Adv. Mater.* **2001**, *13*, 485-487.

(58) Zhao, C.; Domon, Y.; Okumura, Y.; Okabe, S.; Shibayama, M.; Ito, K. *J. Phys. - Condens. Mat.* **2005**, *17*, S2841-S2846.

(59) Buchanan, F. *Degradation rate of bioresorbable materials : prediction and evaluation*; CRC Press; Woodhead: Cambridge, 2008.

(60) Chiellini, E. *Environmentally compatible food packaging*; CRC press; Woodhead: Boca Raton, 2008.

(61) Wei, M.; Shuai, X.; Tonelli, A. E. *Biomacromolecules* **2003**, *4*, 783-792.

(62) Luo, H.; Liu, Y.; Yu, Z.; Zhang, S.; Li, B. *Biomacromolecules* **2008**, *9*, 2573-2577.

(63) Luo, H.; Fan, M.; Yu, Z.; Meng, X.; Li, B.; Zhang, S. *Macromol. Chem. Phys.* **2009**, *210*, 669-676.

(64) Middleton, J. C.; Tipton, A. J. *Biomaterials* **2000**, *21*, 2335-2346.

(65) Mano, J. F.; Sousa, R. A.; Boesel, L. F.; Neves, N. M.; Reis, R. L. *Compos. Sci. Technol.* **2004**, *64*, 789-817.

(66) Daniels, A. U.; Chang, M. K. O.; Andriano, K. P.; Heller, J. *J. Appl. Biomater.* **1990**, *1*, 57-78.

(67) Shin, K.; Dong, T.; He, Y.; Taguchi, Y.; Oishi, A.; Nishida, H.; Inoue, Y. *Macromol. Biosci.* **2004**, *4*, 1075-1083.

(68) Shin, K.; Dong, T.; He, Y.; Inoue, Y. *J. Poly. Sci. B Poly. Phys.* **2005**, *43*, 1433-1440.

(69) Dong, T.; Mori, T.; Pan, P.; Kai, W.; Zhu, B.; Inoue, Y. *J. Appl. Polym. Sci.* **2009**, *112*, 2351-2357.

(70) Dong, T.; He, Y.; Zhu, B.; Shin, K.; Inoue, Y. *Macromolecules* **2005**, *38*, 7736-7744.

(71) Dong, T.; Kai, W.; Pan, P.; Cao, A.; Inoue, Y. *Macromolecules* **2007**, *40*, 7244-7251.

(72) Ong, C.; Price, F. *J. Polym. Sci. Polym. Symp.* **1978**, *63*, 45.

(73) Tonelli, A. E. *J. Polym. Sci. B Polym. Phys.* **2009**, *47*, 1543-1553.

(74) Mohan, A.; Joyner, X.; Kotek, R.; Tonelli, A. *Macromolecules* **2009**, *42*, 8983-8991.

(75) Dealy, J. M.; Wissbrun, K. F. *Melt Rheology and its Role in Plastics Processing: Theory and Applications*; Van Nostrand Reinhold: New York, 1990.

(76) Bittiger, H.; Marchessault, R. H.; Niegisch, W. D. *Acta Crystallogr. B Struct. Crystallogr. Cryst. Chem.* **1970**, *26*, 1923-1927.

(77) Vedula, J.; Tonelli, A. E. *J. Polym. Sci. B Polym. Phys.* **2007**, *45*, 735-746.

(78) Shuai, X.; Porbeni, F.; Wei, M.; Bullions, T.; Tonelli, A. *Macromolecules* **2002**, *35*, 2401-2405.

(79) Girardeau, T. E.; Zhao, T.; Leisen, J.; Beckham, H. W.; Bucknall, D. G. *Macromolecules* **2005**, 38, 2261-2270.

(80) Tonelli, A. E. *Macromolecules* **2008**, *41*, 4058-4060.

(81) Eastburn, S. D.; Tao, B. Y. *Biotechnol. Adv.* **1994**, *12*, 325-339.

(82) Bettinetti, G.; Melani, F.; Monnanni, R.; Giordano, F. *J. Pharm. Sci.* **1991**, *80*, 1162-1170.

(83) Szente, L.; Szejtli, J. *Adv. Drug Deliver. Rev.* **1999**, *36*, 17-28.

(84) Yang, J.; Jung, B.; Suh DH *Polymer* **2001**, *42*, 8349-8354.

(85) Harada, A.; Okada, M. *Polym. J.* **1999**, *31*, 1095-1098.

(86) Reuscher, H.; Hirsenkorn, R. *J. Inclus. Phenom. Mol.* **1996**, *25*, 191-196.

(87) Rehmann, L.; Yoshii, H.; Furuta, T. *Starch - Stärke* **2003**, *55*, 313-318.

(88) Hebeish, A.; Higazy, A.; Al Shafei, A.; Sharaf, S. *Polym. - Plast. Technol.* **2006**, *45*, 1163-1173.

(89) Kistamah, N.; Carr, C. M.; Rosunee, S. *J. Mater. Sci.* **2006**, *41*, 2195-2200.

(90) de Bergamasco, R.; Zanin, G.; de Moraes, F. *J. Incl. Phenom. Macro.* **2007**, *57*, 75-78.

(91) Phan, T. N. T.; Bacquet, M.; Morcellet, M. *J. Incl. Phenom. Macro.* **2000**, *38*, 345-359.

(92) Furuta, T.; Kusuya, Y.; Neoh, T.; Rehmann, L.; Beak, S.; Yoshii, H. *J. Incl. Phenom. Macro.* **2006**, *56*, 107-111.

(93) Hara, K.; Mikuni, M.; Hara, K.; Hashimoto, H. *J. Incl. Phenom. Macro.* **2002**, *44*, 241-245.

(94) Panova, I.; Matuchina, E.; Topchieva, I. *Polym. Bull.***2007**, 58, 737-746.

(95) Zhao, T.; Beckham, H. W. *Macromolecules* **2003**, *36*, 9859-9865.

(96) Harada, A. *Carbohyd. Polym.* **1997**, *34*, 183-188.

(97) Su, Y.; Wang, J.; Liu, H. *J. Colloid Interf. Sci.* **2002**, *251*, 417-423.

(98) Nolan, S. L.; Phillips, R. J.; Cotts, P. M.; Dungan, S. R. *J. Colloid Interf. Sci.* **1997**, *191*, 291-302.

(99) Joseph, J.; Dreiss, C. A.; Cosgrove, T.; Pedersen, J. S. *Langmuir* **2007**, *23*, 460-466.

(100) Alexandridis, P.; Nivaggioli, T.; Hatton, T. A. *Langmuir* **1995**, *11*, 1468-1476.

(101) Tsai, C.; Zhang, W.; Wang, C.; Van Horn, R. M.; Graham, M. J.; Huang, J.; Chen, Y.; Guo, M.; Cheng, S. Z. D. *J. Chem. Phys.* **2010**, *132*, 204903.

(102) Venkatramanan, K.; Arumugam, V.; Predeep, P.; Prasanth, S.; Prasad, A. S. In *AIP Conference Proceedings*; Kollam (Kerala), 2008; pp. 235-240.

(103) Harada, A.; Okada, M.; Li, J.; Kamachi, M. *Macromolecules* **1995**, *28*, 8406-8411.

(104) Hunt, M.; Rusa, C.; Tonelli, A.; Balik, C. *Carbohyd. Res.* **2005**, *340*, 1631-1637.

Appendix

Non-stoichiometric PMMA IC's

Summaries of certain aspects of the non-stoichiometric PMMA IC project not directly pertaining to behavioral observations are noted here. This information includes attempted observation of IC formation by XRD, DSC, and NMR.

IC Formation Measurements

The solution and solid state PMMA IC formation was monitored using solution proton NMR and X-Ray diffraction techniques. The goal of these experiments was to determine whether or not inclusion of PMMA into γ-CD was observable via either method, and to determine the structures of these IC's. These tests were not performed for our triblock copolymer sample.

Solid state IC formation between PMMA and γ-CD at 105˚C was probed by X-Ray diffraction. Figure 72 is the progression of XRD patterns from the initial pattern to 18 days. A slow transition from the cage crystal structure (as defined by peaks at 12.4, 15.2, 16.5, and 18.8°[38]) can be observed. At 4 hours, the cage crystal structure seems to have been mostly disrupted, and as we progress to 20 and 44 hours, the formation of strong peaks at 2θ= 16.3and 17.1°C can be observed. Unexpectedly, there is a distinct absence of the characteristic channel γ-CD diffraction peak at 2θ = 7.5°, corresponding to the 200 plane of the channel γ-CD crystal structure.[104] The absence of a strong channel CD peak may indicate that while the PMMA is acting to disrupt the cage crystalline structure, the formation of a long range channel crystalline structure has yet to occur.

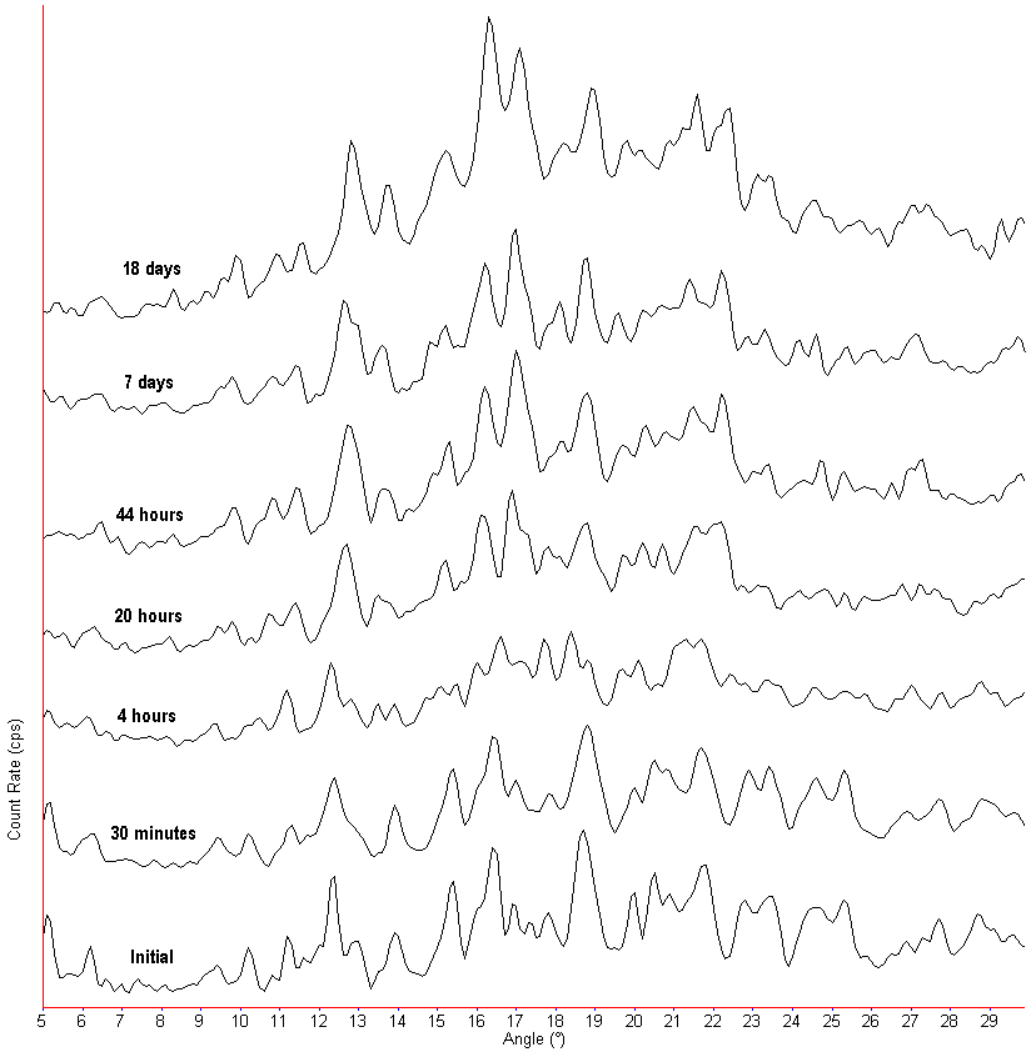

Figure 72: XRD patterns of a physical mixture of PMMA and γ-CD taken after various time intervals

To determine if the changing diffraction behavior of our samples was the result of an inclusion process, a physical mixture of PMMA and α-CD was prepared in a similar fashion. XRD patterns were collected for this material at increasing times to determine whether there was a deviation from the initial diffraction pattern (shown in Figure 73). In the α-CD mixture, the only change was a small increase in the relative peak size at $2\theta = 20.5^{\circ}$. No

disruption of the initial cage pattern was ever observed. This supports the observation that the threading of the PMMA chains into the γ-CD is likely the cause for the diffraction pattern changes in Figure 72.

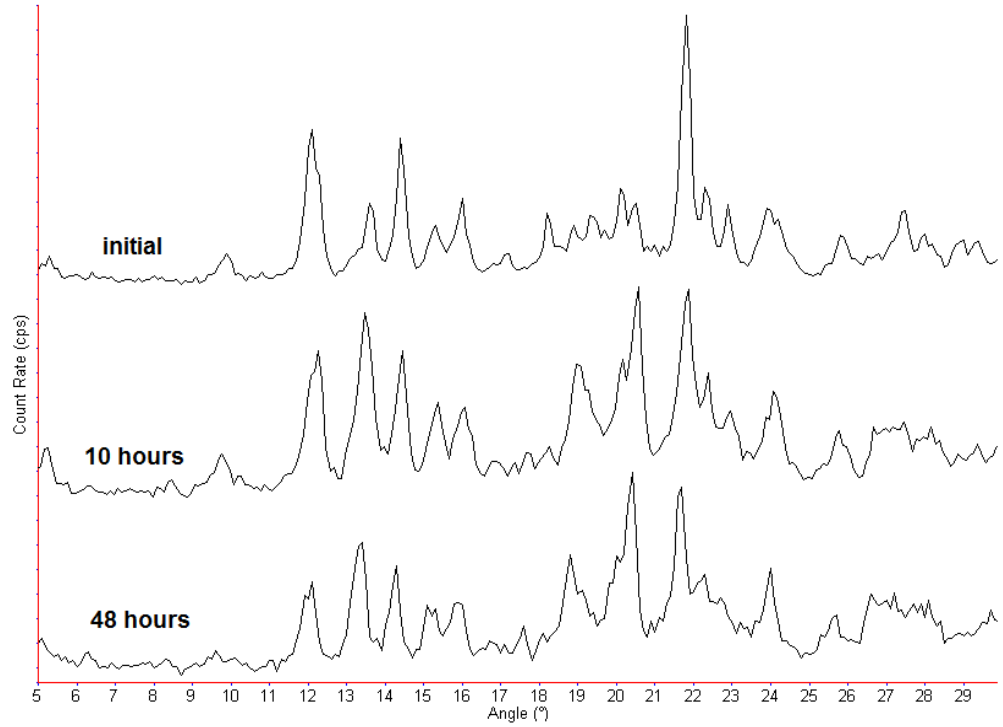

Figure 73: XRD patterns of a physical mixture of PMMA and α-CD taken after various time intervals

PMMA/γ-CD and PMMA/α-CD physical mixtures were made and examined under repeated DSC runs at increased heating times and monitored for a change in the T_g. The as-received PMMA was also subjected to this heating profile and compared to the physical mixtures. The samples undergo 5 heating/cooling cycles and are allowed to anneal after each heating step for 2, 2, 5, and 10 minutes at 130˚C and 15 minutes at 150˚C before one final heating. Figure 74 contains the stacked DSC thermograms for each of the three samples. Each

heating step for a particular sample is shown one on top of another without any vertical or horizontal translation. It is evident from the fact that all heating steps superimpose perfectly that there is no change in the DSC thermogram between each heating for all three samples, suggesting that no solid state inclusion has taken place within this time frame. It is also interesting to point out that it seems the introduction of CD particles into the bulk PMMA has the effect of increasing Tg slightly. This behavior is observed in both physical mixtures, suggesting this behavior is only tied to the mixing of both components.

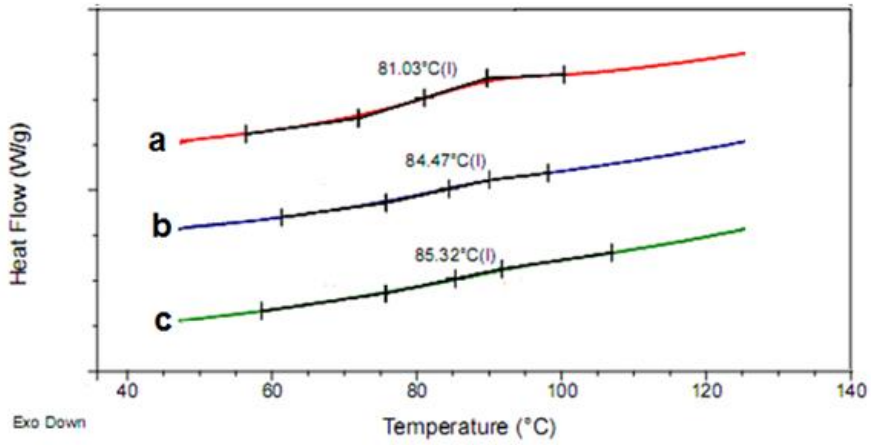

Figure 74: Multiple superimposed DSC heating steps for as-received PMMA (a), a PMMA/α-CD physical mixture (b), and a PMMA/γ-CD physical mixture (c) allowed to anneal for extended times in situ

Proton NMR spectra were collected for mixtures of PMMA and γ-CD in d_8-dioxane. The PMMA is soluble in the dioxane while the CD remains insoluble. It was expected that if inclusion were to take place, we would begin to see a reduction of the PMMA peaks and an increase in the water peak (complexing PMMA would drive the water out of the CD cavity and into the dioxane). Figure 75 shows the NMR results for this mixture at various times

over the course of a month. While the integration is not included in the Figure, it is clear the water peak increases over time relative to the solvent peak and shifts slightly downfield. The initial water:dioxane peak ratio is 0.23:1 while the final ratio after a month of exposure is 0.95:1, a significant increase.

While the initial PMMA concentration is relatively low, the integration of these peaks demonstrates that there is no change in PMMA concentration in the studied time frame. From this, we can determine that the PMMA is likely not including inside the insoluble CD. It is possible that the dioxane is including inside the CD cavities, driving the increase in water concentration. This would explain the observed behavior.

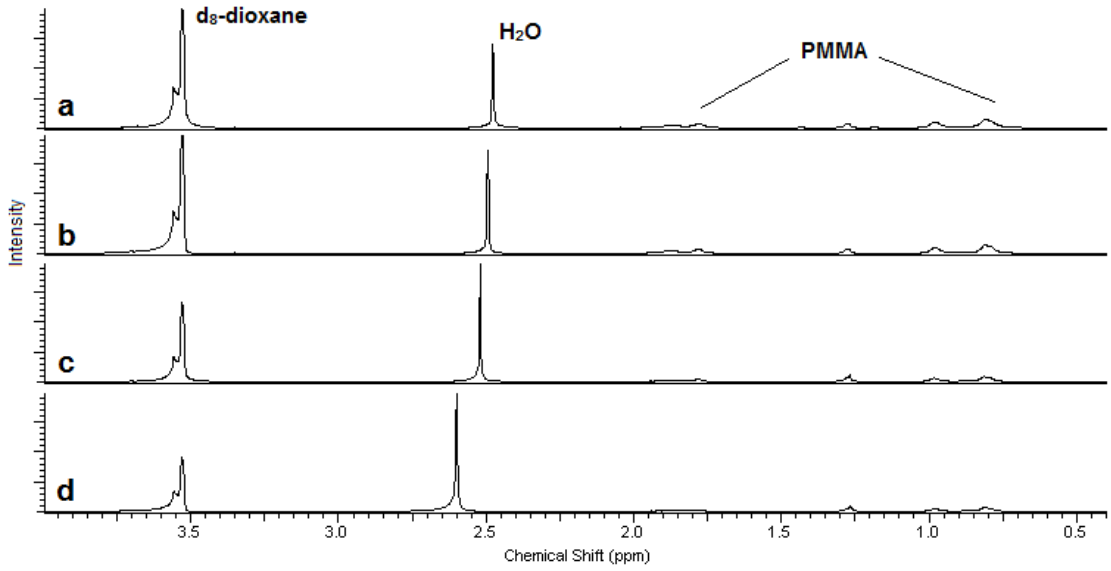

Figure 75: NMR spectra of a PMMA (soluble) and γ-CD (insoluble) mixture initially (a) and after 20 hours (b), 8 days (c), and 1 month (d) [solvent: d_8-dioxane]

Heterogeneity of PMMA NS-IC Samples

As mentioned in Chapter 3, the non-stoichiometric PMMA IC's displayed extremely heterogeneous behavior. Obtaining multiple samples from the same batch of IC yielded strikingly different DSC thermograms, presumably due to a drastic difference in the amount of uncovered polymer and the presence of non-complexed cyclodextrin. Figure 76 below demonstrates the variety of different DSC behaviors observed when sampling the same batch of IC. One particular behavior to note is the variability of the same sample before and after heating above the Tg. Runs d and e in Figure 76 are the first and second run of the *same* sample, respectively. What this suggests is that the measured glass transitions change not only among various samplings of the same IC batch, but also among the same samples depending on the thermal history. This behavior makes it difficult to narrow down the exact relationship between CD coverage and glass transition behavior, but it is worth noting the presence of an observable T_g significantly higher than that of the as-received PMMA. This suggests that it is at least *possible* to create a chain restricted environment in a PMMA NS-IC resulting in an increased T_g.

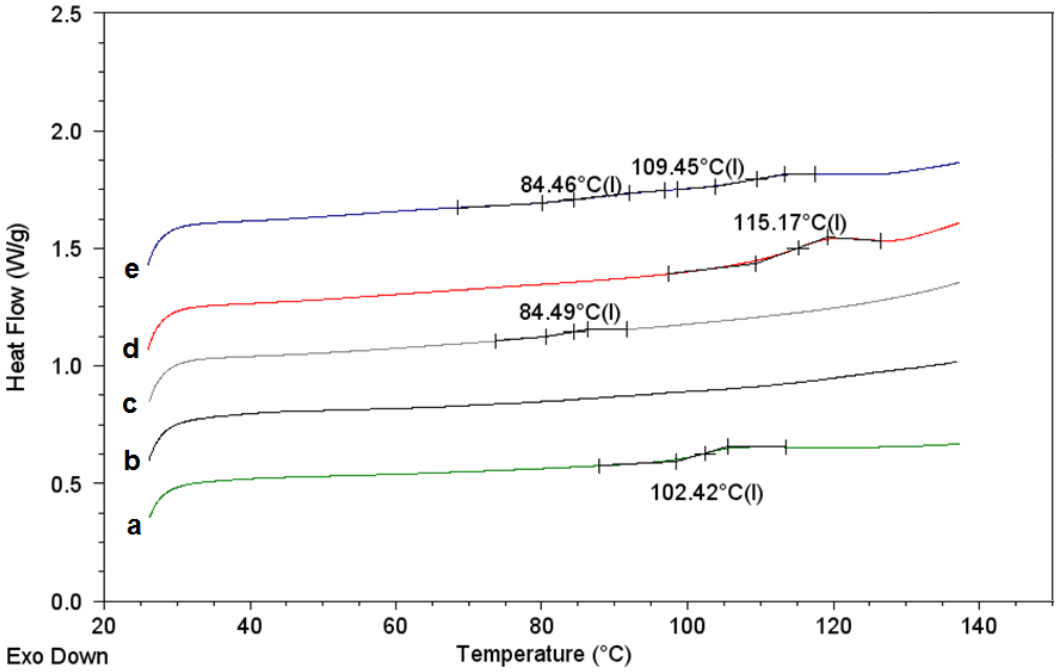

Figure 76: Multiple DSC samples obtained from the same batch of 80% coverage PMMA/γ-CD NS-IC (a, b, c, and d) as well as two repeated runs of the same sample (d and e)